universität wien

DISSERTATION

Titel der Dissertation

A study on the export apparatus of the *Salmonella typhimurium* type III secretion system

Verfasserin

Mag. Lisa Königsmaier

angestrebter akademischer Grad

Doktorin der Naturwissenschaften (Dr.rer.nat.)

Wien, im Juli 2011

Studienkennzahl lt. Studienblatt:	A 091490
Dissertationsgebiet lt. Studienblatt:	Doktoratsstudium der Naturwissenschaften, Molekularbiologie
Betreuerin / Betreuer:	Dr. Thomas C. Marlovits

CONTENTS

I ABSTRACT

I Abstract

The type III secretion system is a bacterial molecular machine essential for infection of eukaryotic cells. Employed by bacteria like *Salmonella* it is responsible for causing a variety of diseases, ranging from common food poisoning to typhoid fever. The most characteristic feature of the type III secretion system is its central core structure, the needle complex, a molecular syringe embedded in the bacterial membrane. It is composed of a base (made up by the InvG, PrgH, and PrgK proteins) which itself is traversed by a ~20-30 Å-wide conduit formed by a central inner rod (PrgJ) and a needle filament (PrgI), which allows for passage of secreted proteins. Previous studies have shown that the assembly of the needle complex occurs in a step wise manner, in which the base substructure is assembled first, followed by the formation of the inner rod and needle substructures. The assembly of the last two substructures requires a secretion competent base and the export apparatus, a group of highly conserved membrane proteins (InvA, SpaP, SpaQ, SpaR, and SpaS). Although all components of the export apparatus are essential for type III secretion, it is unknown how they assemble, if they are associated with the needle complex, where they are localized and if they fulfill a common function. This study shows that the export apparatus proteins are associated with the needle complex. It furthermore gives insights into the function of the export apparatus proteins and their role in building a secretion competent base structure by using cryo-EM and single particle analysis. Last but not least we present relevant tools and techniques for future localization studies of export apparatus proteins.

II ZUSAMMENFASSUNG

II Zusammenfassung

Das von Salmonellen exprimierte Typ-III-Sekretionssystem ist essentiell für das Eindringen der Bakterien in eukaryotische Zellen und daher auch für die Entstehung von Krankheiten wie Gastroenteritis bis hin zu lebensbedrohendem Typhus.

Das zentrale Strukturelement des Typ-III-Sekretionssystems ist der Nadelkomplex. Er ist in die Bakterienmembran eingebettet und fungiert als molekulare Spritze, die bakterielle Proteine direkt in die Zelle des Wirtes transportiert. Der Nadelkomplex besteht aus einer Basis (aufgebaut durch die Proteinen InvG, PrgH, and PrgK), die von einem ~28 Å-weiten Kanal durchdrungen ist der durch den inneren Rod (PrgJ) und das Nadelfilament (PrgI) geformt wird. Der Kanal dient als Verbindung zur eukaryotischen Zelle und wird als Durchgang für sekretierte Proteine genützt.

Frühere Studien haben gezeigt, dass der Nadelkomplex schrittweise assembliert wird: Zunächst werden die Substrukturen der Basis aufgebaut, gefolgt vom ‚inneren Rod' und dem Nadelfilament. Der Aufbau der letzten beiden Komponenten benötigt eine sekretionskompetente Basis. Für die Sekretionskompetenz sind neben den strukturellen Hauptkomponenten auch die Exportapparatproteine, eine Gruppe von hoch konservierten Membranproteinen (InvA, SpaP, SpaQ, SpaR, and SpaS) essentiell.

Es ist bisher unklar, wie diese Proteine ihre Funktion erfüllen: Ob sie zum Beispiel als Komplex in der bakteriellen Membran vorliegen, ob sie in direkt mit dem Nadelkomplex assoziiert oder gar Teil desselben sind. Die vorliegende Arbeit zeigt, dass die Exportappartusproteine mit dem Nadelkomplex assoziiert sind und liefert unter Zuhilfenahme der Cryo-Elektronenmikroskopie erste Erkenntnisse über die Funktion der Exportapparatproteine im Bezug auf Nadelkomplexaufbau und -struktur. Mit dem Bereitstellen von verschiedenen Methoden und bakteriellen Stämmen ebnet diese Arbeit darüber hinaus den Weg für zukünftige strukturelle Studien der Exportapparatproteine.

III INTRODUCTION

III Introduction

1. The type III secretion system

Bacterial membranes are physical barriers defining intracellular and extracellular space as well as surrounding cellular compartments. They are dynamic structures and allow for intra- as well as intercellular transport of molecules between different cellular compartments.
The majority of bacterial protein traffic across membranes and membrane protein insertion is mediated by the Sec-translocase, a membrane protein complex composed of SecYEG and the ATPase SecA (Driessen and Nouwen 2008). Proteins targeted for secretion are recognized by the Sec-translocase through a specific amino-terminal (N-terminal) signal sequence (Heijne 1990). Membrane protein insertion on the other hand is triggered by recognition of the protein's hydrophobic patches via the translocase (Heijne 2011).

The Sec-translocase is also employed to build up membrane embedded multiprotein complexes which have been developed for intercellular trafficking needed for DNA and protein translocation. Gram-negative bacteria provide at least six different membrane delivery systems (Type I - Type VI secretion system) spanning inner and outer membrane (Abdallah et al. 2007) (see Fig. 1). Moreover, in *Mycobacterium tuberculosis*, a Gram-positive bacterium, the type VII secretion system has been identified, needed for bacterial pathogenesis (Abdallah et al. 2007, Bitter et al. 2009). Type III - type VI secretion systems act specifically upon contact with prokaryotic or eukaryotic cells to transfer DNA or protein effectors in order to exploit the target cell (Hayes et al. 2010). One of these systems, the type III secretion system (T3SS) is used by various Gram-negative bacteria (e.g.: enteropathogenic and enterohemorrhagic *E.coli* (EPEC, EHEC, *Salmonella, Shigella, Yersinia)* to contact human tissue like the intestinal mucosa, rearrange host cell morphology and eventually invade the cells (McGhie et al. 2009). These pathogens can cause a variety of diseases ranging from common food poisoning and minor intestinal diseases to typhoid fever or even the plague (Coburn et al. 2007).

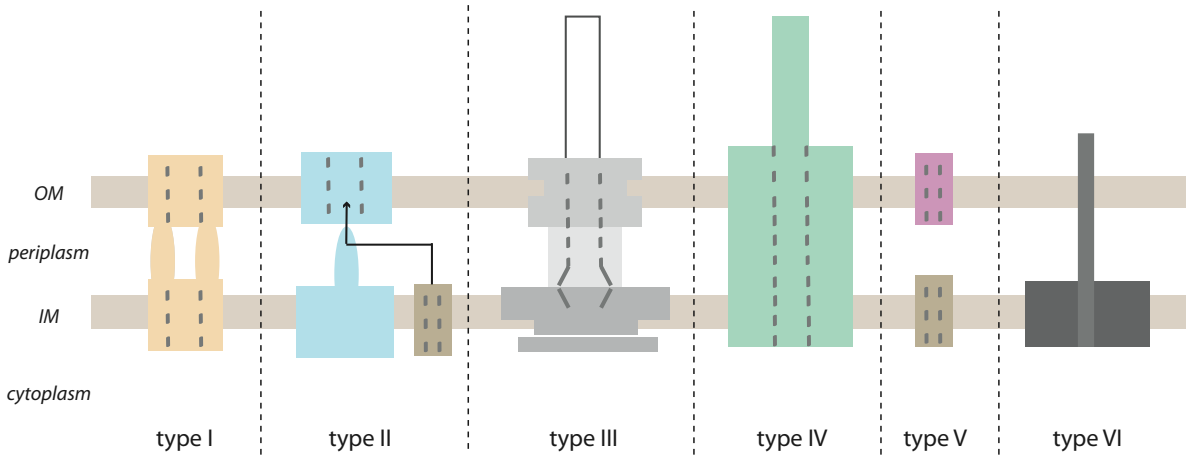

Figure 1. Transportsystems across inner and outer membrane of Gram-negative bacteria (type I - type VI secretion system). The **type I secretion system** is formed by an ATPase binding cassette, a membrane-fusion protein and an outer membrane pore and is used to transport e.g. *E. coli* α-haemolysin (Gentschev et al. 2002); the two-step **type II system** uses the Sec-translocase to mediate translocation of substrates like the *Klebsiella oxytoca* pullulanase across the inner membrane (IM), the outer membrane (OM) is traversed via the secreton, a conserved OM pore (Sandkvist 2001). **The type III secretion machinery** is characterized by the core structure the needle complex, a cylindrical structure with a protuding needle filament on top, composed of several rings embedded in OM and IM, being able to transport effector proteins into host cells (Marlovits et al. 2004). Like the type III, also the **type IV secretion system** delivers substrates (DNA and proteins) into host cells, getting in contact via a pilus like structure at the bacterial surface (Hamilton et al. 2005). The **type V system** is suggested to use a two-step mechanism, using the Sec-system to cross the IM and a β-barrel translocator domain (autotransporter) to span the OM (Mazar et al. 2007). One of its functions is to mediate growth-inhibition in *E. coli* (Hayes et al. 2010). **The type VI secretion system** is assumed to act independently from the Sec-system, and is required for the secretion of certain virulence factors in *Vibrio cholerae* and *Pseudomonas aeruginosa* (Hayes et al. 2010). Figure adapted from Abdallah et al. 2007.

The T3SS is located at the surface of the bacteria, where it acts as passage for effector proteins which are directly transported into the host cell. These effectors interfere with the host cell cytoskeleton causing membrane rearrangement by manipulation of actin polymerization leading to bacterial internalization (Haraga et al. 2008).

The major families of T3SS linked to diseases in humans and animals are the Ysc-family (e.g. *Yersinia spp*, *Pseudomonas aeruginosa*), the Inv-Mxi-Spa family (e.g. *Salmonella enterica* pathogenicity island I, *Shigella spp*) and, the Ssa-Esc family (e.g. *Salmonella enterica* pathogenicity island II, EPEC, EHEC) (Troisfontaines et al. 2005). The core components of the different family members are mainly conserved, whereas the effectors are highly specialized due to specific adaptations of the bacteria to different environments (Broems et al. 2003). Conserved proteins are also found in the flagellar core structures, which is needed for bacterial motility, suggesting an evolutionary relationship between the flagellum and other T3SS (Troisfontaines et al. 2005, Erhardt et al. 2010).

1.2. The T3SS in the center of infection

Salmonella infection of eukaryotic host cells is mainly characterized by two phases. Phase I, the invasion of epithelial cells, is mediated by the expression of T3SS associated proteins of Salmonella pathogenicity island I (SPI-1) (Fig. 2) (McGhie et al. 2009). In the beginning of phase II, SPI-1 and Salmonella pathogenicity island II (SPI-2) contribute effectors to hijack macrophages establishing Salmonella containing vacuoles (SCV) for intracellular survival leading to systemic infection of the human body (Hansen-Wester and Hensel 2001). However, some effectors are also located outside of SPI-1 and SPI-2 playing a role in the invasion process (Wood et al. 1996, Wood et al. 1998, McGhie et al. 2009).

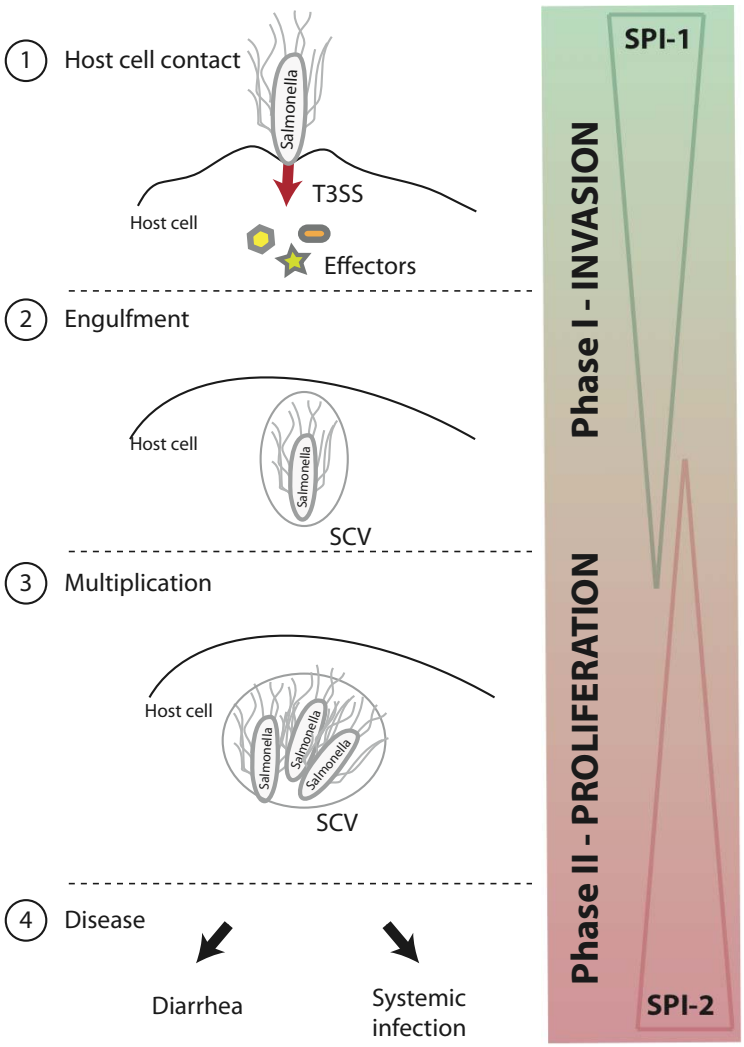

Figure 2. *Salmonella* invasion scheme. (1) *Salmonella* gets in contact with host cells, the uptake is triggered via SPI-1 T3S of effector proteins into host cell. **(2)** The entry and establishment of Salmonella containing vacuoles (SCV) is maintained by both pathogenicity islands (McGhie et al. 2009), whereas **(3)** multiplication and **(4)** further infection is mediated via the SPI-2 T3SS.

1.3. The SPI-1 T3SS

To compose a molecular machinery such as the SPI-1 T3SS, different functions have to be exerted in a temporal and spatial context (an overview of the SPI-1 gene cluster is given in Fig. 3A).

The T3SS assembly is therefore a highly regulated process and stands primarily under the control of a group of transcription factors (HilA, HilD, InvF, SprA and SprB), navigating expression of SPI-1 genes (Lucas and Lee 2000). With HilA as the central regulator in this hierarchy, it engages the expression of the structural components of the T3SS core also termed needle complex (NC). The NC is the connecting element between bacteria and host and serves as a molecular syringe mediating translocation of effectors from the bacterial into the eukaryotic cytoplasm (Fig. 3B). The NC is embedded in the outer and inner bacterial membrane mainly composed of two substructures, the needle and the base, which is subdivided into outer rings (ORs), neck, inner ring 1 (IR1) and inner ring 2 (IR2) (Marlovits et al. 2004). A section through the NC reveals three more features of its intricate design: the cup, facing the basal side of the NC, the socket anchoring the inner rod, which itself is connected to the needle (Marlovits et al. 2006).

Over the last decade various approaches elucidated the positions of almost all structural proteins of the NC, which enabled us to assign the proteins to their corresponding NC substructure (Fig. 3B): IR1 and IR2 are built up by PrgH and PrgK, InvG composes the OR and neck, PrgJ makes up the inner rod and PrgI forms the needle filament (Schraidt et al. 2010). As it was shown in *Salmonella*, PrgH and PrgK do not participate in cup and socket, thus it remains unclear which proteins build up this region. It has been speculated, that a group of conserved inner membrane proteins, SpaP, SpaQ, SpaR, SpaS and InvA (export apparatus proteins) could form cup and socket, as they are indispensable for substrate secretion via the T3SS (Minamino and Macnab 2000, Sukhan et al. 2001).

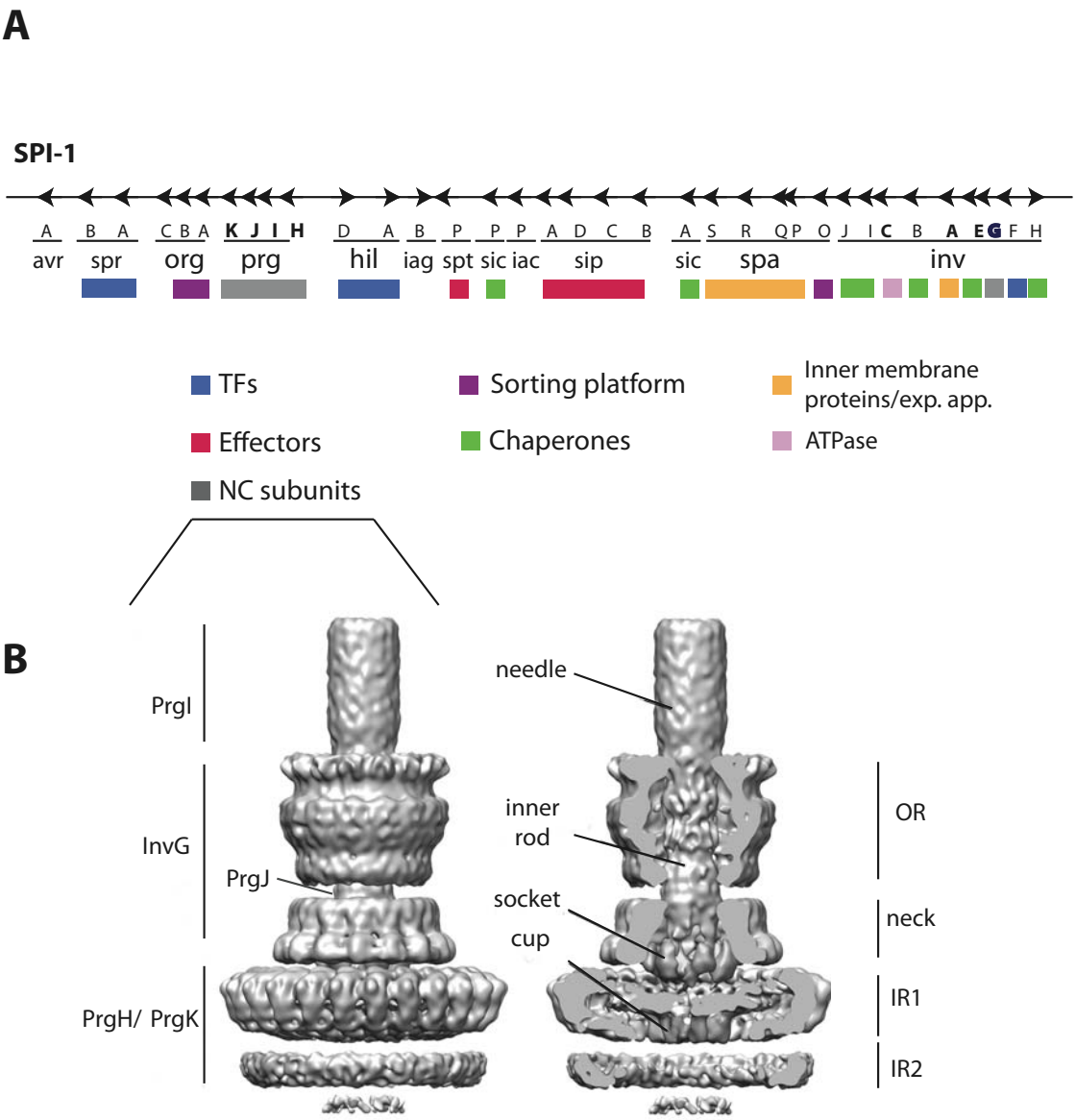

Figure 3. Overview of Salmonella pathogenicity island 1 and NC structure. (A) Salmonella pathogenicity island 1 (SPI-1) contains T3SS related proteins such as transcription factors (TFs: SprA/B, HilA/D, InvF), effector proteins (effectors: SptP, SipA/B/C/D), proteins of the sorting platform (SpaO/OrgA/B), chaperones (SicA/P, InvB/E/H/I/J), inner membrane proteins/export apparatus proteins (SpaP/Q/R/S, InvA), and the NC subunits (PrgH/I/J/K, InvG). **(B)** The needle complex (NC) can be divided into several substructures which are composed of certain proteins: needle (PrgI), inner rod (PrgJ), outer rings (OR) and neck (InvG), inner ring 1 (IR1) and inner ring 2 (IR2) (PrgH/PrgK), cup and socket (no proteins assigned). Figure adapted from Schraidt and Marlovits 2011, EMDB: 1875.

Besides the NC itself representing the connecting device bridging several membranes, the SPI-1 T3S machinery employs many more proteins to gain full functionality. A hallmark of type III secretion in *Salmonella* is the transport of early, middle and late substrates (Fig. 4). PrgJ and PrgI are the early substrates, secreted as components of the inner rod and the needle filament. As soon as these structures are fully assembled the NC undergoes a reprogramming phase, which involves changing of the substrates from needle and rod proteins to translocon and effector proteins (Galan and Wolf-Watz 2006). The substrate specificity switch results first in secretion of the middle substrates, tip protein SipD and the translocases SipB and SipC, which form a complex at the distal end of the needle filament called the translocon. This complex is supposed to act as a pore within the eukaryotic membrane preparing for the effector proteins (late substrates) to be delivered (Mueller et al. 2008). Effectors, amongst which are SipA, SipC and SopE act in concert and cause a characteristic effect called membrane ruffling, triggering bacterial uptake and SCV formation. Assisting chaperones, such as SicA and SicP sequester substrates in a secretion competent state, while the ATPase InvC provides energy for effector unfolding prior to translocation (Akeda and Galan 2005, Izore et al. 2011). A previously described substructure of the T3SS, the so called sorting platform SpaO/OrgA/OrgB (Lara-Tejero et al. 2011), was suggested to build the interface between NC and the proteins present in the cytoplasm, orchestrating the hierarchy of substrate transport.

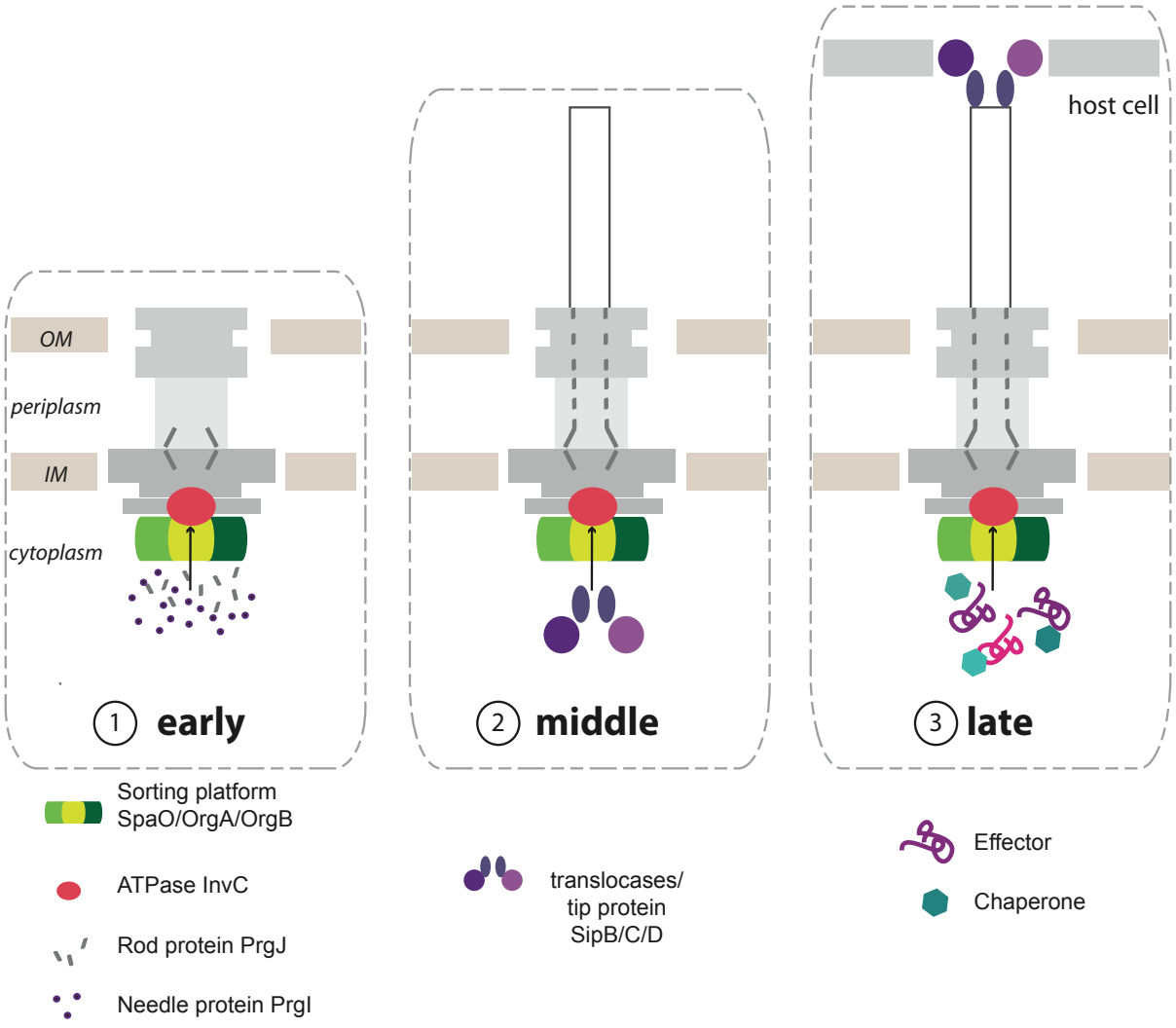

Figure 4. Schematic presentation of T3SS substructures and different states during secretion. **(1)** In the early phase PrgJ and PrgI are translocated building up inner rod and needle filament, **(2)** then the tip protein SipD and the translocases SipB/C are secreted, which form the translocon at the needle tip. **(3)** The effector proteins serve as the late substrates during T3S (adapted from Lara-Tejero et al. 2011).

1.4. Substructures of the NC

The following chapter addresses the various substructures of the NC (translocon, needle filament, outer rings, inner rings, inner rod, export apparatus, ATPase, sorting platform) starting from the extracellular space moving downwards (table of T3SS homologs in appendix).

1.4.1. The translocon

Three proteins, the hydrophobic translocases SipB, SipC and the hydrophilic tip protein SipD are needed to form the translocation pore at the distal end of the needle filament, enabling effector proteins to enter eukaryotic host cells (Mueller et al. 2008). The tip is supposed to act as connecting element between the needle and the membrane inserted translocation pore, and is required for correct assembly of the latter (Broz et al. 2007, Lara-Tejero and Galan 2009).

Scanning transmission electron microscopy revealed a first glimpse of the needle tip structures of *Yersinia* and *Shigella* (Broz et al. 2007, Mueller et al. 2008). Atomic structures of other tip proteins, *Burgholderia* BipD (Erskine et al. 2006), EPEC EspA (Yip et al. 2005), *Shigella* IpaD (Johnson et al. 2007) and *Yersinia* LcrV (Derewenda et al. 2004) were solved and modeling suggested mainly homo-pentamers as needle tip structures, except in the case of *Shigella* IpaB, which forms a hetero-pentamer with IpaD (Worrall et al. 2011). For the translocation pore itself, however, no structural information has been reported as of today.

1.4.2. The needle filament

The external needle filament is a hollow tube constructed out of many copies of a single protein PrgI (9 kDa), ~50nm long and 7nm wide with an inner channel that is typically ~2.5nm in diameter. Up to now several atomic structures of truncated needle monomers were solved - *Salmonella typhimurium* PrgI (Wang et al. 2007), *Shigella flexneri* MxiH (Deane et al. 2006), *Burkholderia pseudomallei* BsaL (Zhang et al. 2006) and EM maps of the assembled needle negative stain map from Shigella at 16 A (Cordes et al. 2003) and a cryo EM map from *Salmonella* at 18 A (Galkin et al. 2010) were generated.

The *Shigella* needle filament shares an identical helical architecture (~5.6 subunits per turn, 24-A helical pitch) and inner channel diameter (~2nm) with the structure of the flagellar hook and filament although no sequence homology is given, implying an evolutionary relationship as well as further mechanistic analogies of the T3SS NC and the flagellum (Cordes et al. 2003, Deane et al. 2006). In contrast to *Shigella*, the *Salmonella* needle is characterized by ~6.3 subunits per turn, 26-A helical pitch, and it is structurally heterogeneous (Galkin et al. 2010). This structural heterogeneity might be due to conformational changes within the needle filament, supporting the idea that the needle filament might transmit information about host cell contact upon such structural changes and thereby maintaining substrate specificity during the various phases of secretion (Deane et al. 2006).

1.4.3. The outer rings

The outer rings are built up by InvG, a member of the secretin family. This family is characterized by proteins forming higher ordered ring-like structures in the outer membrane of Gram-negative bacteria, where they are required for the assembly of the type III secretion system, extrusion of filamentous phages type IV pili, and secretion by the type II secretion system (Nouwen et al. 1999, Chami et al. 2005).

The founder of this family, PulD, is essential for secretion of the amylolytic enzyme pullulanase in *Klebsiella oxytoca* and *E. coli*. PulD and the outer rings of the base substructure of the NC appear very similar when compared to each other. In both cases two rings are formed defining two separate compartments (Chami et al. 2005). The similarities also extend to regions of the neck of the NC, which connect the outer rings with the inner rings. Therefore it was thought that the outer rings and the upper parts of the neck region of the NC were formed by members of the secretin family (Nouwen et al. 1999 - pulD *Klebsiella oxytoca*, Collins et al. 2001 - PilQ *Neisseria meningitis*, Opalka et al. 2003 - pIV multimer filamentous phage, Hodkinson et al. 2009, Spreter et al. 2009). In fact, the homologous InvG reaches far down into the periplasm of the *Salmonella* NC, with the N-terminus facing the IR1 (Schraidt et al. 2010) (Fig. 5A). In combination with additional experimental data it was shown that the outer rings harbor 15 InvG subunits (Fig. 5B), which stands in contrast to previously assumed 12-14 secretin subunits for the *Shigella* NC (Spreter et al. 2009). The 15-subunit model of the *Salmonella* NC was furthermore refined by docking the available structure of the N-terminal domain of the InvG homolog EscC into the generated cryo-EM structure yielding a near-atomic model of the NC neck region (Schraidt and Marlovits 2011).

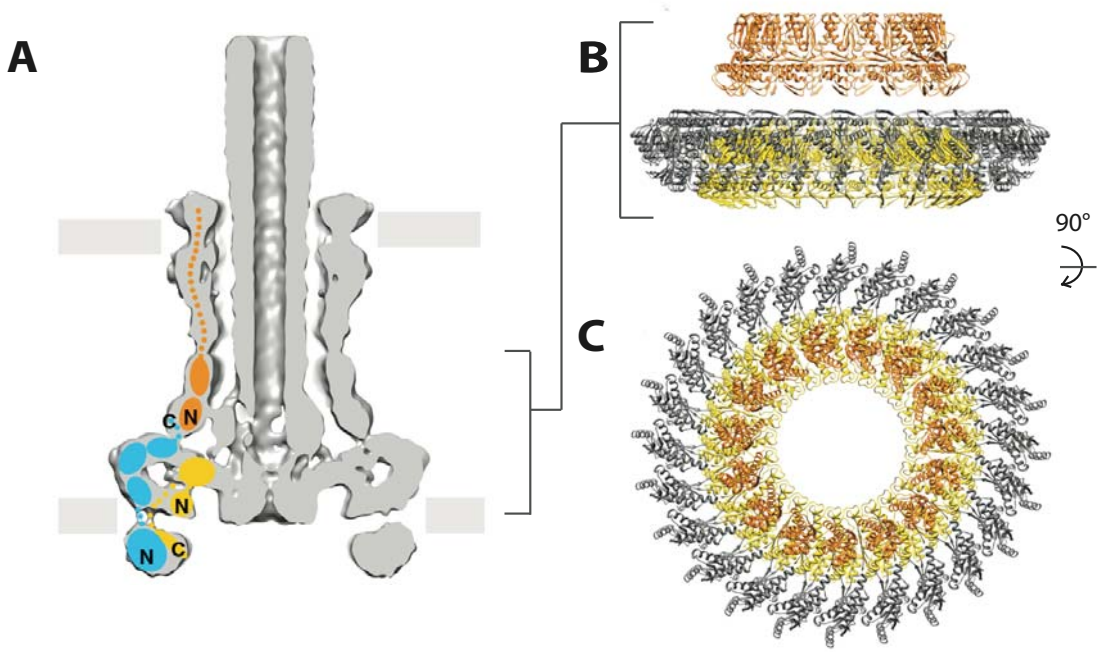

Figure 5. Topology and atomic model of the InvG, PrgH/PrgK rings. (A) InvG builds up outer rings and neck region with the N-terminus facing downwards. PrgH and PrgK compose the inner rings. PrgH C-terminus is positioned closely to the InvG N-terminus, whereas PrgH N-termins and PrgK N- and C-terminus are in proximity to each other facing downwards and to the inside of the rings, respectively. **(B)** Side views of the atomic model of InvG (15, orange), PrgH (24, grey) and PrgK (24, yellow) organized as rings. **(C)** Top views of the atomic model of InvG, PrgH and PrgK. Figures adapted from Brunner 2009 and Schraidt and Marlovits 2011, EMDB: 1875.

1.4.4. The inner rod

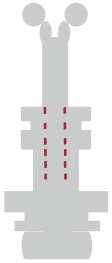

The inner rod is anchored to the socket at the center of the base. In *Salmonella* the protein PrgJ was described to form the inner rod, which traverses the entire length of the base (Marlovits et al. 2004). The authors showed that the ratio of inner rod protein to needle protein determines the length of the needle (Marlovits et al. 2006). This finding suggests that the formation of the inner rod, not the maturation of the needle structure, is the critical event triggering substrate specificity switching from needle protein to effector proteins. Besides the PrgI and PrgJ ratio, the protein InvJ plays a very important role during the reprogramming phase. Strains lacking InvJ produce extremely long needles whereas effector secretion is blocked (Collazo and Galan 1996). As they do not form a stable socket structure it was proposed that InvJ works as a stabilizer for this region within the NC base (Marlovits et al. 2006).

1.4.5. The inner rings

The lower part of the NC base is embedded in the inner membrane. This region is characterized by two particular ring structures, inner ring 1 (IR1) bordering the periplasm and inner ring 2 (IR2) facing the cytoplasm. It was suggested that the *Salmonella* proteins PrgH and PrgK comprise these prominent NC substructures due to their bioinformatic structure prediction: PrgH consists of two soluble domains of similar size divided by a transmembrane domain, whereas PrgK contains an amino-terminal (N-terminal) lipidation site and a carboxy-terminal (C-terminal) transmembrane domain. Ring-building motifs found in the atomic structures of the periplasmic PrgH domain and the PrgK homolog EscJ supported this hypothesis. Docking of these structures in previously generated lower resolution EM-maps resulted in different mutually incompatible locations for PrgH and PrgK (Yip et al. 2005, Hodgkinson et al. 2009, Spreter et al. 2009). Labeling experiments in combination with cryo-EM and cross linking analysis made it eventually possible to determine the exact location of C- and N-termini of PrgH and PrgK (Schraidt et al. 2010) (Fig. 5A). Moreover, selective disassembly of inner and outer rings facilitated the determination of the absolute stoichiometry of PrgH:PrgK:InvG = 24:24:15 within the NC resulting in a near atomic model of *Salmonella* IR1 and OR/neck region (Fig. 5B). Taken together, this model presents the PrgH C-terminus adjacent to the InvG N-terminus and PrgH N-terminus and PrgK C-terminus in proximity to each other facing the cytoplasmic side of the base. Therefore these regions of PrgH and PrgK might also interact with cytoplasmic components of the T3SS system during the secretion process as suggested for the *Shigella* homologs MxiG and MxiJ (Morita-Ishihara et al. 2006) or the Yersinia homologs YscD and YscJ (Diepold et al. 2010).

1.4.6. The export apparatus proteins

Bioinformatic predictions together with genetic analysis of the *Salmonella* T3S-involved proteins have revealed several highly conserved inner membrane proteins, including SpaP, SpaQ, SpaR, SpaS and InvA (Collazo and Galan 1996, Sukhan et al. 2001). The flagellar homologs (FliP, FliQ, FliR, FlhB, FlhA) were first shown to be essential for secretion and this encouraged the emerging hypothesis that they might be located within the basal body placed in near proximity to the cytoplasmic T3S proteins, in order to allow for substrate secretion (Fan et al. 1997, Minamino and Macnab 2000, Sukhan et al. 2001). Therefore the inner membrane proteins were collectively called export apparatus or export apparatus proteins (Jones and MacNab 1990).

Out of these five proteins, InvA and SpaS contain large cytoplasmic C-terminal domains, which were shown to interact with cytoplasmic T3S proteins such as the ATPase (Zhu et al. 2002).

InvA is the largest member of the inner membrane export apparatus. It contains a conserved ~35 kDa N-terminal integral membrane domain connected via a 20-30 residue linker to a more variable 40 kDa C-terminal soluble domain (Warrall et al. 2010) (Fig. 6A).

Interaction studies have shown that the C-terminus of flagellar InvA homolog FlhA directly binds to cytosolic T3S-proteins including the ATPase FliI (InvC), FliJ (InvI), the C-terminus of FlhB (SpaS) and FliH (OrgB) (Zhu et al. 2002, Minamino and Namba 2008). Moreover, FlhA from the Gram-positive bacterium *Bacillus subtilis* has been identified to interact with chaperone/filament and chaperone/filament-cap complexes and *Chlamydia* FlhA was found to interact with the C-terminus of FliF (PrgK), one of the inner membrane ring-building proteins (Bange et al. 2010, Stone et al. 2010). The crystal structure of InvA-CT revealed a ring-building motif found in other T3SS proteins suggesting oligomerization of InvA; the motif

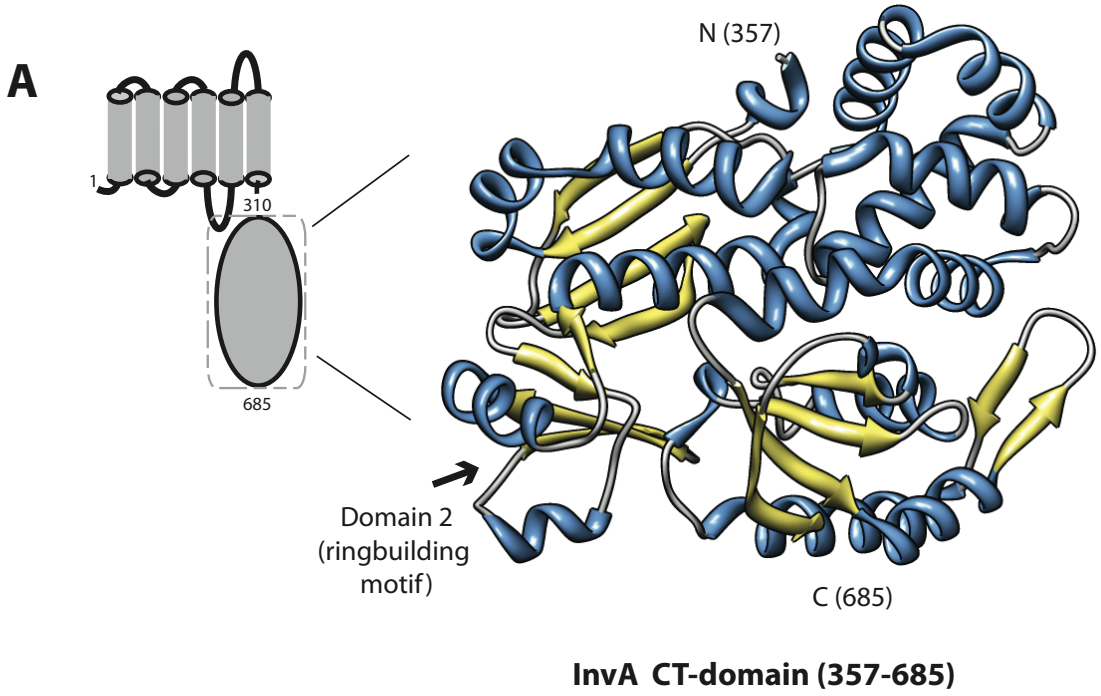

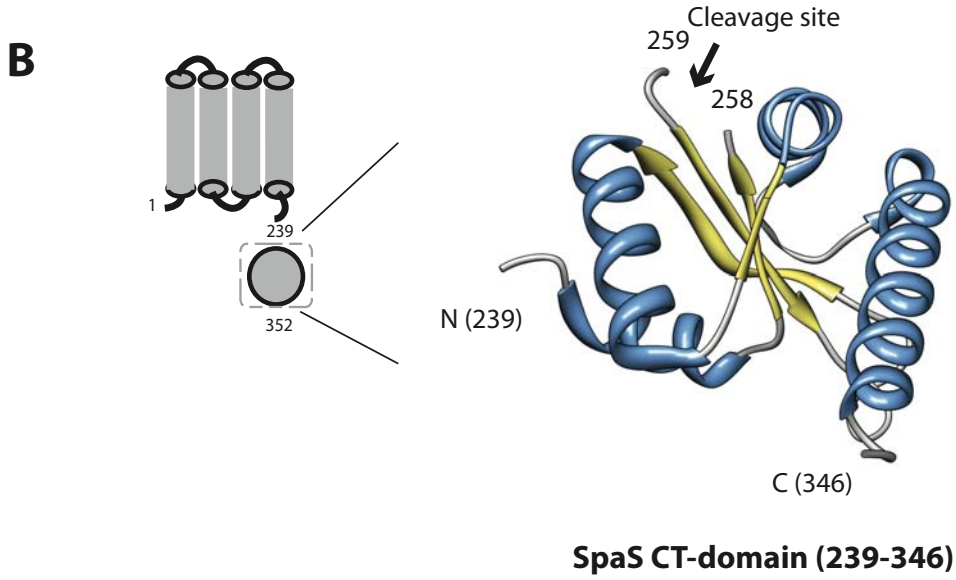

Figure 6. Atomic structures of InvA and SpaS CT-domains. (A) InvA is predicted to have 6 transmembrane domains and a large cytoplasmic CT-domain. A crystal structure is available from residue 357-695. Domain 2 harbors the ringbuilding motif, suggesting oligomerization of InvA. **(B)** SpaS consists of 4 transmembrane regions and a cytoplasmic CT-domain undergoing auto-cleavage at position 258 within the conserved NPTH motif, indicated with an arrow on the top of the atomic structure (residue 239-346 displayed).

may also play a role in peripheral membrane association (comparison with rhomboid from *P. aeruginosa*) (Lilic et al. 2010, Worral et al. 2010). Thus, it has been suggested that InvA/ FlhA forms a docking platform for the soluble T3S-components before subsequent substrate secretion (Saijo-Hamano et al. 2010).

Besides InvA, SpaS also contains a cytoplasmic C-terminal region and is characterized by two major domains: a 200 amino acid N-terminal domain associated with the inner membrane ring and a 100 amino acid C-terminal domain, which undergoes auto-cleavage and mediates a switch in the secretion substrate profile of the T3SS (Zarivach et al. 2008) (Fig. 6B). This phenomenon was first described for the flagellar SpaS homolog FlhB (Minamino and McNab et al. 2000), which conciliates the switching of export specificity from rod- and hook-type substrates to filament-type substrates during flagellar morphogenesis. FlhB-CT was furthermore shown to interact with FlhA-CT (InvA homolog), FliI (ATPase, InvC homolog) and FliH (InvI homolog), sustaining the idea of export apparatus proteins being located at the basal body and consequently being involved in substrate secretion (Zhu et al. 2002, VanArnam et al. 2004, Minamino and Namba 2008).

FlhB homologs like *Salmonella* SpaS, *Shigella* Spa40 and *Yersinia* YscU have also been shown to undergo auto-cleavage at the same conserved NPTH-motif to induce the substrate switch from needle filament to effector protein secretion **(**Zarivach et al. 2008, Riordan et al. 2008, Botteaux et al. 2010).

1.4.7. The ATPase

The ATPase InvC is essential for secretion of substrates via the *Salmonella* T3SS. Its main function is substrate recognition, chaperone release and unfolding of secreted substrates in an ATP-dependent manner (Galan and Wolf-Watz 2006). From a structural point of view it shares characteristics with the AAA+ ATPases degradation machineries (Kenniston et al. 2003). Both ATPases organize in hexameric rings and are able to recognize certain patterns at the N-terminus of substrates. Another similarity is found in the primary amino acid sequence of InvC and the beta-subunit of the F0F1-ATPases (Gauthier and Finlay 2003, Akeda and Galan 2005). The crystal structures of the EPEC EscN gave first insights into the catalytic core of a homologous ATPase, yet revealing main structural differences to the F0F1-ATPase (Zarivach et al. 2007).

How the ATPase InvC engages with substrates is still unknown, but the answer to that question could provide fundamental information about the secretion process via the T3SS.

1.4.8. The sorting platform

The larger portion of T3S-associated proteins are located within the cytoplasm among which are effector proteins and their cognate chaperones as well as the ATPase and the sorting platform proteins. They are interacting among themselves and/or with the membrane anchored secretion channel in order to establish hierarchical transport of secreted proteins as it is shown in Figure 4 (Gonzalez-Pedrajo et al. 2006, Erhardt et al. 2010, Lara-Tejero et al. 2011).

The sorting platform as such has been defined only recently (Lara-Tejero et al. 2011) as a high molecular weight complex. It is composed of three proteins, SpaO, OrgA and OrgB, which associate with the NC, export apparatus and translocases SipB, SipC and SipD but also form a complex independently in absence of all these proteins. Additional experiments made clear that the SpaO/OrgA/OrgB complex acts as a sorting platform for proteins translocated by the T3SS. SpaO/OrgA/OrgB seem to have a different affinity for the transported proteins and thus assure translocase transport before effector protein secretion maintaining the temporal hierarchy of early, middle and late substrates.

However, the network of proteins within the cytoplasm is still not fully understood and further studies are needed to clarify the details of this complex machinery.

1.5. Assembly of the NC

Genetic analysis of *Salmonella typhimurium* NC provided information on how the assembly pathway of the NC substructures might work (Fig. 7).

The inner membrane proteins, PrgH and PrgK were suggested to be the first proteins to assemble which was supported by additional experimental evidence (Kimbrough and Miller 2000, Sukhan et al. 2001, Schraidt et al. 2010). Although the outer membrane protein InvG can form a complex on its own, as already shown for *Yersinia* YscC (Koster et al. 1997), it was much more stable in combination with PrgH and PrgK (Sukhan et al. 2001) and it was shown that PrgH and PrgK overexpression in *E. coli* results in stable, hollow ring structures (Kimbrough and Miller 2000). The authors assumed that PrgH and PrgK assist on InvG assembly and would therefore have to assemble at first in the inner membrane.

In the case of *Yersinia*, the model a so called outside-in assembly was described (Diepold et al. 2010), presenting YscC (InvG homolog, outer membrane ring) as a starting point within the assembly process of the *Yersinia* injectisome. Subsequent to the assembly of the inner membrane rings formed by YscD (PrgH) and YscJ (PrgK), the cytosolic T3S-associated proteins come into play, which is in agreement with the model of *Salmonella* T3SS assembly.

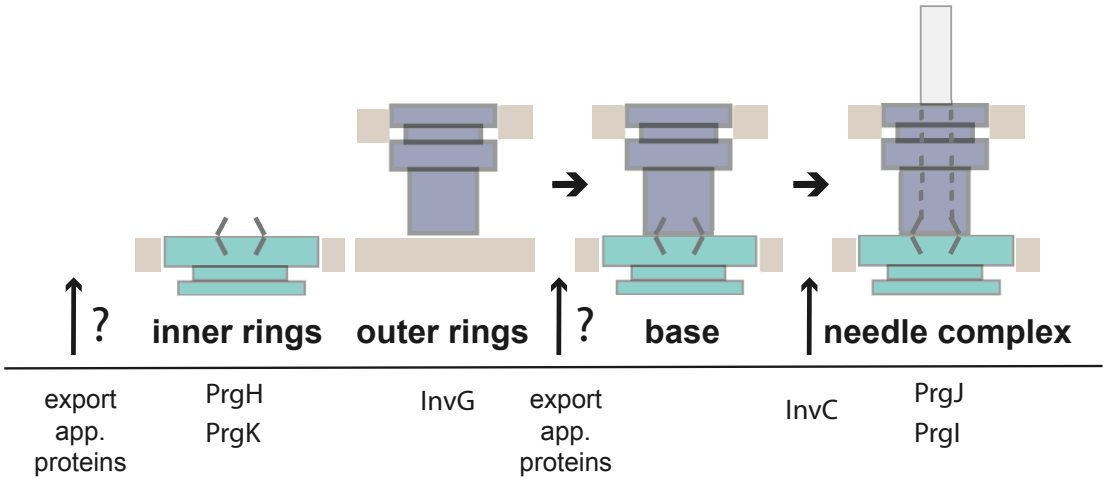

Figure 7. Model of the assembly pathway of the Salmonella NC. The base structure assembles out of inner and outer rings. Assuming that the export apparatus proteins are part of the needle complex because of their essential role for secretion, it is questionable at which timepoint during the assembly they have to be placed. (adapted from Galan and Wolf-Watz 2006).

However, the authors do not state clearly when the export apparatus proteins would join the T3SS. Taking into account that they are needed for substrate secretion, they were put at a later assembly point when the inner and outer rings are already formed. This raises the question whether the export apparatus proteins are an integral component of the NC and if so, where they are located. If they are positioned within the NC, how is it possible that these membrane proteins join the NC when the base is already assembled and the membrane is not accessible for insertion. To answer these questions, structural analysis are needed to clarify the role of the export apparatus proteins within the assembly pipeline of the NC.

1.6. Aims of this thesis

Co-fractionation of export apparatus proteins with other structural components of the T3SS has been shown for homologous systems (Fan et al. 1997, Zenk et al. 2007), but whether these membrane proteins are intrinsic structural elements of the NC or only associated with the T3SS has not been formally demonstrated. Furthermore, it is not clear when the export apparatus proteins come into play during the assembly pathway of the T3SS and/or which function they maintain during this process.

Therefore, this thesis aims at answering the following central questions:

1. Are the export apparatus proteins structurally defined within the NC structure?

2. When do they appear during NC assembly?

3. Which roles do the individual export apparatus proteins play during assembly?

4. Where are the export apparatus proteins located?

IV MATERIALS

IV. Materials

4.1. Reagents and other materials

If not stated otherwise, reagents were purchased from Sigma-Aldrich

3xFLAG peptide (in-house)
6-aminohexanoic acid
anti-FLAG M2
anti-FLAG M2 affinity gel
acetic acid
acrylamide:bisacrylamide solution (37.5:1) 30% w/v (ND)
ammonium bicarbonate (ABC)
ammonium persulfate (APS)
arabinose
BCA-protein assay (Pierce)
bis(2-hydroxyethyl)amino-tris(hydroxymethyl)methan (BIS-TRIS)
bovine serum albumin (BSA; Applichem)
Coomassie blue G-250 (Serva)
disodium hydrogen phosphate
dithiothreitol (DTT; Applichem)
dodecyl-D-maltoside (DDM; Anatrace)
ECL western blotting detection reagents (Amersham)
ECL hyperfilm (Amersham)
ethylene diamine tetraacetic acid (EDTA)
ethane
glycerol
glycine
Goat-anti-Mouse DyLight 680 (Pierce)

Goat-anti-Rabbit IgG DyLight 800 (Pierce)

Goat-anti-Mouse HRP

Goat-anti-Rabbit HRP

hen-egg lysozyme

isopropanol

lauryldimethylamine-oxide (LDAO; Anatrace)

methanol (MeOH)

magnesium chloride

PageBlue protein staining solution (Fermentas)

PageRuler pre-stained molecular weight marker (Fermentas)

phosphotungstic acid (PTA)

polyvinylidene fluoride (PVDF) Immobilon-P transfer membrane (Millipore)

potassium chloride

potassium dihydrogen phosphate

Rabbit-anti-Needle complex (produced in house)

sodium chloride

sodium dodecyl sulfate (SDS)

sucrose

Tricine

Tris(hydroxymethyl)aminomethane-HCl (Tris-HCl)

Triton X-100

Trypsin

Tween 20

4.2. Chemical solutions

Resolving gel buffer

375 mM Tris-HCl (pH 8.8)

Tris-glycine running buffer

25 mM Tris, 192 mM glycine, 0.1 % SDS (pH 8.8)

Laemmli SDS sample buffer

60 mM Tris, 100 mM DTT, 2 % SDS,

10 % glycerol, 0.005 % bromophenol blue (pH 6.8)

PBS

10 mM Na_2HPO_4, 2 mM KH_2PO_4, 137 mM NaCl, 2.7 mM KCl (pH 7.3)

PBS-T

0.1 % (vv) Tween 20 in PBS

Immunoblot blocking solution

5 % non-fat dried milk in PBS-T

Immunoblot transfer buffer

48 mM Tris, 39 mM glycine, 0.037 % SDS, 20 % MeOH

Buffer CR1

150 mM Tris, 500 mM sucrose

pH 8.0

Buffer PR2

10 mM Tris, 500 mM NaCl, 5 mM EDTA,

0.5 % LDAO or DDM

pH 8.0

Buffer FR3

10 mM Tris, 500 mM NaCl, 5 mM EDTA,

0.1 % LDAO or DDM

pH 8.0

4.3. Bacterial strains

The experiments were conducted with non-flagellated S. typhimurium strains (SJW2941 and SL1344 background respectively). They all carry the plasmid pSB3291 (AmpR) expressing the transcriptional regulator hilA under the araBAD promoter (Kubori et al. 2000): SB1922 (Δ*spaPQRS, invA*), SB2161 (Δ*invA*), SB2162 (Δ*spaP*), SB2163 (Δ*spaQ*), SB2164 (Δ*spaR*), SB2165 (Δ*spaS*), SB1769 (SpaS-N258A-FLAG), SB1906 (InvA-FLAG).

SB905 was used as wild-type control (Sukhan et al. 2001). A comprehensive overview is given in Table 1.

Name	Description	Parent strain	Reference
SB762	Wild type (SL1344, Flg-)	SL1344	Kaniga et al. 1995
SB905	Wild type (SJW2941)	SJW2941	Yamaguchi et al. 1986
SB1769	SpaSN258A-FLAG	SL1344	Wagner et al. 2010
SB2161	*invA*	SL1344	Wagner et al. 2010
SB917	*invC*	SL1344	Sukhan et al. 2001
SB2162	*spaP*	SL1344	Wagner et al. 2010
SB2163	*spaQ*	SL1344	Wagner et al. 2010
SB2164	*spaR*	SL1344	Wagner et al. 2010
SB2165	*spaS*	SL1344	Wagner et al. 2010
SB1906	InvA-FLAG	SL1344	Wagner et al. 2010
SB1922	*invA, spaPQRS*	SJW2941	Wagner et al. 2010

Table 1: *S. typhimurium* strains used in this thesis. All strains are Flg⁻.

V METHODS

V. Methods

BIOCHEMICAL METHODS

5.1. SDS-PAGE

(Sodium Dodecyl Sulfate-Polyacrylamide Gel Electrophoresis)

5.1.1. Gradient gels

Gradient PAGE 4 - 20 % was performed in a mini-gel system (Biorad). Self-cast gradient gels and buffers were prepared as specified in the LabRef Handbook (Balkwill et al. 2002). Gels were run under constant current, 40 mA per gel. Before being loaded onto the gel, samples were denatured 5 minutes at 95 °C in Laemmli SDS sample buffer. In addition a pre-stained molecular weight marker (Fermentas) was applied on the gel (see also Materials).

5.1.2. Protein detection

Protein gels were stained in PageBlue (Fermentas). Gels were washed three times in double distilled water (ddH_2O), optionally fixed in 25 % isopropanol, 10 % acetic acid, stained for one hour or over night and destained in ddH_2O, with all steps under gentle agitation.

5.2. Immunoblotting - Westernblot of SDS-PAGE

Immunoblotting was performed according to the LabRef Handbook, using a semi-dry cell (Biorad) to blot on a PVDF membrane immobilon-P (Millipore). The membrane was activated in methanol and equilibrated in transfer buffer, the gel was washed in ddH_2O and equilibrated in transfer buffer as well. The transfer was performed at a constant voltage of 13 V with the run time of 70 minutes. Transfer efficacy was confirmed by having a pre-stained molecular weight marker (Fermentas) applied on the gel.

After the transfer non-specific binding sites were blocked by immersing the membrane in blocking solution for one hour at room temperature or over night at 4 °C. The primary antibody was applied diluted in PBS-T 1 % milk for at least one hour under gentle agitation (dilutions: anti-NC: 1:10000, anti-FLAG: 1:10000). After washing thouroughly in PBS-T, the secondary HRP-coupled antibody was applied diluted in PBS-T 1% milk for 30 minutes to one hour, again under gentle agitation (anti-Rabbit: 1:10000, anti-Mouse:1:150000). After 3x 10 minutes PBS-T washes, signals were detected by applying detection reagents (Amersham) and exposing hyperfilms (Amersham) in the dark (see also Materials).

Alternatively, western blots were analyzed by the Odyssey Infrared Imaging System (Licor) (Lara-Tejero et al. 2011). In this case, immobilon-FL was the membrane of choice and the blocking was done with the Odyssey Blocking Buffer. Fluorescently labeled antibodies were diluted 1:15000 in Odyssey Blocking Buffer supplied with 0.1 % Tween and incubated for 45 minutes under gentle agitation.

5.3. Determination of protein concentration by BCA protein assay

Protein concentration of purified NC was measured by using BCA protein assay (Pierce). It is detergent compatible and therefore the method of choice for concentration determination of membrane proteins. BSA standards were prepared as suggested by the user manual in a range of 20 - 2000 µg/ml. The working reagent was mixed by adding reagent A:B in a 50:1 ratio. 2 ml working reagent and 0.1 ml sample were well mixed and incubated for 30 minutes at 37 °C. After cooling down the samples were measured at 526 nm in a spectrophotometer.

5.4. Needle complex purification

This protocol was adapted from Marlovits et al. 2006. Seed cultures were grown overnight at 37 °C in L-broth supplemented with 0.3 M NaCl and appropriate antibiotics. Cultures were diluted 1:10 in 2 L of the same medium and grown to an OD600 of 0.5 before inducing expression of hilA by adding arabinose to a concentration of 0.012 %. From here on the sample was always kept on ice or in the cold, unless otherwise stated. The cells were harvested by centrifugation at 4250 g for 12 minutes (Beckman Coulter Avanti J-26XP, rotor JLA 9.1000) and the pellets resuspended in 100 ml of buffer CR1. Outer membranes and peptidoglycan layers were disintegrated while slowly stirring on ice with 5 mM EDTA and 0.5 mg/ml hen-egg lysozyme added, for 60 minutes on ice and, subsequently 15 minutes adjusted to 37 °C. Cells were lysed by addition of LDAO (to 0.3 %) or DDM (to 0.3 %). MgCl2 and, subsequently, NaCl were added to a final concentration of 10 mM and 500 mM, respectively.

The lysate was cleared from cellular debris at 14000 g for 20 minutes (Beckman Coulter Avanti J-26XP, rotor JLA 16.250). NC and bases were sedimented by ultra-centrifugation (Sorvall Discovery 90SE, rotor Type 45 Ti, 40 krpm, 2.5 h). The pellets were gently resuspended in buffer PR2 and prepared for isopycnic density gradient centrifugation by adding CsCl to a final concentration of 26.25 % w/v. The sample was centrifuged for 14 hours or longer, in a Sorvall Discovery 90SE ultracentrifuge, rotor TH-660, at 50 krpm, 4 °C. Six to eight fractions of approximately equal volume were taken starting from the top of the tube. Each was supplemented with CsCl-free buffer FR3 and spinned at 90 krpm for 30 minutes (Sorvall RCM 150GX, rotor S100-AT4). The pellets were resuspended gently in 50 ul buffer FR3. NC bases can be expected in fraction 3, NC with intact needles in fraction 4 and 5. From two liters of SB905 culture harvested at an OD600 of 1.5 the total yield of NC with intact needles was usually about 0.5 mg to 1 mg/ml as measured by BCA-protein assay. At this point, the integrity and purity of the sample was usually verified by EM and SDS-PAGE.

5.5. Immunoprecipitation of FLAG-tagged proteins

FLAG-tagged export apparatus components (SpaS, InvA) were immunoprecipitated from solubilized membranes and purified NC using the anti-FLAG M2 affinity gel. Approximately 70 ul - 100 ul beads were transferred into a 0.7 ul tube, were washed 3x with FR3 base (without detergent) and then equilibrated 3x 10 minutes with FR3 supplied with detergent. 200 - 400 µg of solubilized membranes and 100 ul complete protease inhibitor were added to the equilibrated beads and filled up to 500 ul with FR3. The solution was kept at 4 °C and gentle agitation for 2 h. Precipitated complexes were eluted with 150 ng/ul 3X FLAG peptide (50 - 70 ul) in buffer FR3 supplemented with respective detergent and subsequently analyzed by Western blot and transmission electron microscopy.

5.6. Mass spectrometry (MS)

Sample preparation, MS, protein identification and analysis were performed by the in-house MS-facility and the respective protocols were provided by them.

5.6.1. In solution digest

Sample volume was between 70 and 100 ul with a protein content of about 0.5 mg/ml. Samples were digested over night at 37 °C following the addition of 1 µg trypsin (mass spectrometry grade; Promega) per 15 µg protein; pH was checked to be in range for high proteolytic activity. Optionally, an additional aliquot of protease was added in the morning and the sample was incubated for another 14 hours. Digestion was stopped by addition of 10 % TFA to a final concentration of 0.5 %.

5.6.2. Protein identification by LC-MS

Separation was performed on an Ultimate 3000 Dual Gradient HPLC system (ComDionex) coupled to an LTQ Orbitrap XL mass spectrometer (Thermo Fisher Scientific), equipped with a Proxeon nanospray source (Proxeon). Peptides were loaded onto a trap column (Dionex PepMap C18, 5 mm × 300 µID, 5 µparticles, 100 Å pore size) at a flow rate of 25

μmin^{-1}using 0.1% TFA as mobile phase. After 15 minutes, the trap column was switched in line with the analytical column (Dionex PepMap C18, 250 mm × 75 μID, 3 μ, 100 Å).
Peptides were eluted using a flow rate of 275nl/min, and a ternary 50 minutes gradient, respectively 105 minutes, with the following mobile phases: A (water/acetonitrile/formic acid, 95/5/0.1, v/v/v), B (water/acetonitrile/formic acid, 70/30/0.08, v/v/v), and C (water/ acetonitrile/trifluoroethanol/formic acid, 10/80/10/0.08, v/v/v/v) at 30°C. The LTQ Orbitrap XL was operated in data-dependent mode, using a full scan in the Orbitrap (m/z range 400-1800, nominal resolution of 60 000 at m/z 400, target value 1E6) followed by MS/ MS scans of the five most abundant ions in the linear ion trap. MS/MS spectra (normalized collision energy, 35%; activation value q, 0.25; activation time, 30 ms; isolation width, 3 m/z units, target value 5E4) were acquired and subsequent activation was performed on fragment ions through multistage activation. The neutral loss mass list was therefore set to -98, -49, and -32.6 m/z. Precursor ions selected for fragmentation (charge state 2 and higher) were put on a dynamic exclusion list for 180 s. Additionally, singly-charged parent ions were excluded from selection for MS/MS experiments and the monoisotopic precursor selection feature was enabled.

5.6.3. Data analysis

For peptide identification, all MS/MS spectra were searched using Mascot 2.2.04 (Matrix Science, London, UK) against the NCBI non redundant protein sequence database, using the taxonomy salmonella. The generation of dta-files for Mascot was performed using the Extract MSn program (version 4.0, Thermo Scientific). The following search parameters were used: carbamidomethylation on cysteine was set as a fixed modification, oxidation on methionine, pyro-carbamidomethylation on N-terminal cysteine, substitution of Glutamine against pyro-Glutamic Acid were set as variable modifications. Monoisotopic masses were searched within unrestricted protein masses for tryptic peptides. The peptide mass tolerance was set to ±5 ppm and the fragment mass tolerance to ±0.5 Da. The maximal number of missed cleavages was set to 2.

5.7. Electron microscopy of the needle complex

Carbon-coated CuPd grids (400 mesh hexagonal) were glow-discharged for 30 seconds. Five µI of purified NC, diluted 1:30 to 1:45 in buffer FR3, were dropped onto the grid and incubated for 30 seconds. The grid was washed and subsequently stained with 2 % PTA at neutral pH for 20 seconds. The specimen was typically observed at 52000x magnification in a Morgagni TEM (FEI) operated at 80kV. Micrographs were recorded on a 11 megapixel CCD camera using the ITEM software package (FEI).

5.8. Plunge freezing

Purified NC (5 µI of appropriate dilution, typically 1:30) was applied to glow-discharged carbon-coated CuPd grids (400 mesh hexagonal) before vitrification by plunge freezing in liquid ethane. Plunge freezing was either done manually with an in-house constructed plunge-freezer or with the Grid Plunger from Leica. For manual freezing, the sample application varied between 30 seconds to 1 minute, blotting was performed from one side, and a series of several blotting times was used (1, 2, 3 seconds). The Grid Plunger was used with following adjustments: 65 % humidity, RT, blotting time 0.8-1.2 seconds, ethane temperature -185 °C.

5.9. Cryo-electron microscopy

Low dose data, with a range of 15-25 electrons/square angstrom, was collected with a FEI Tecnai Polara at 300 kV using a Gatan Ultrascan 4000 UHS CCD camera (4k x 4k, 15 micron pixel size). Images were acquired semi-automatically, using Point to Point Acquisition, a specific in house-software (by Guenter Resch and Oliver Schraidt). After having defined areas of interest on the sample, the microscope was able to take pictures without an operator and can therefore produce a dataset of up to 500 images per night.

The data was collected at 71,949-fold magnification which corresponds to 2.08 angstrom/ pixel with under focus values ranging from 1.7 - 3.5 µm.

5.10. 2D analysis

The processing scheme is presented in Fig. 8.

First, images were normalized and the contrast transfer function (CTF) of the objective lens was corrected at micrograph level using the mean under focus value of the respective CCD-images as determined by the program CTFFIND3cite (Mindell and Grigorieff 2003).

Individual particle projections were extracted by SIGNATURE (Chen et al. 2007). The particles were combined into a dataset and processed by IMAGIC-5 (Image Science Software GmbH, Germany).

The single particle analysis was started with maximum likelihood-based classification, alignment of these classes, sorting out low quality particles, and eventually alignment of the classes to an already existing template of the NC/NC base. Multi variate statistical analysis (MSA) were used to generate classes which were subsequently used as new references for a multi reference alignment (MRA) with the particles. This process was repeated several times to orient the particles in the same way and refine the 2D classaverage.

5.11. 3D reconstruction

3D reconstruction was performed according to the protocol described in Schraidt 2010.

Briefly, the above mentioned 2D analysis was the basis for further 3D analysis, processed by IMAGIC-5 (Image Science Software GmbH, Germany).

Local projection matching (“correlation” only) of an already existing template was used in order to determine the Euler angles of each particle for the 3D reconstruction to generate a 3D map of the NC base.

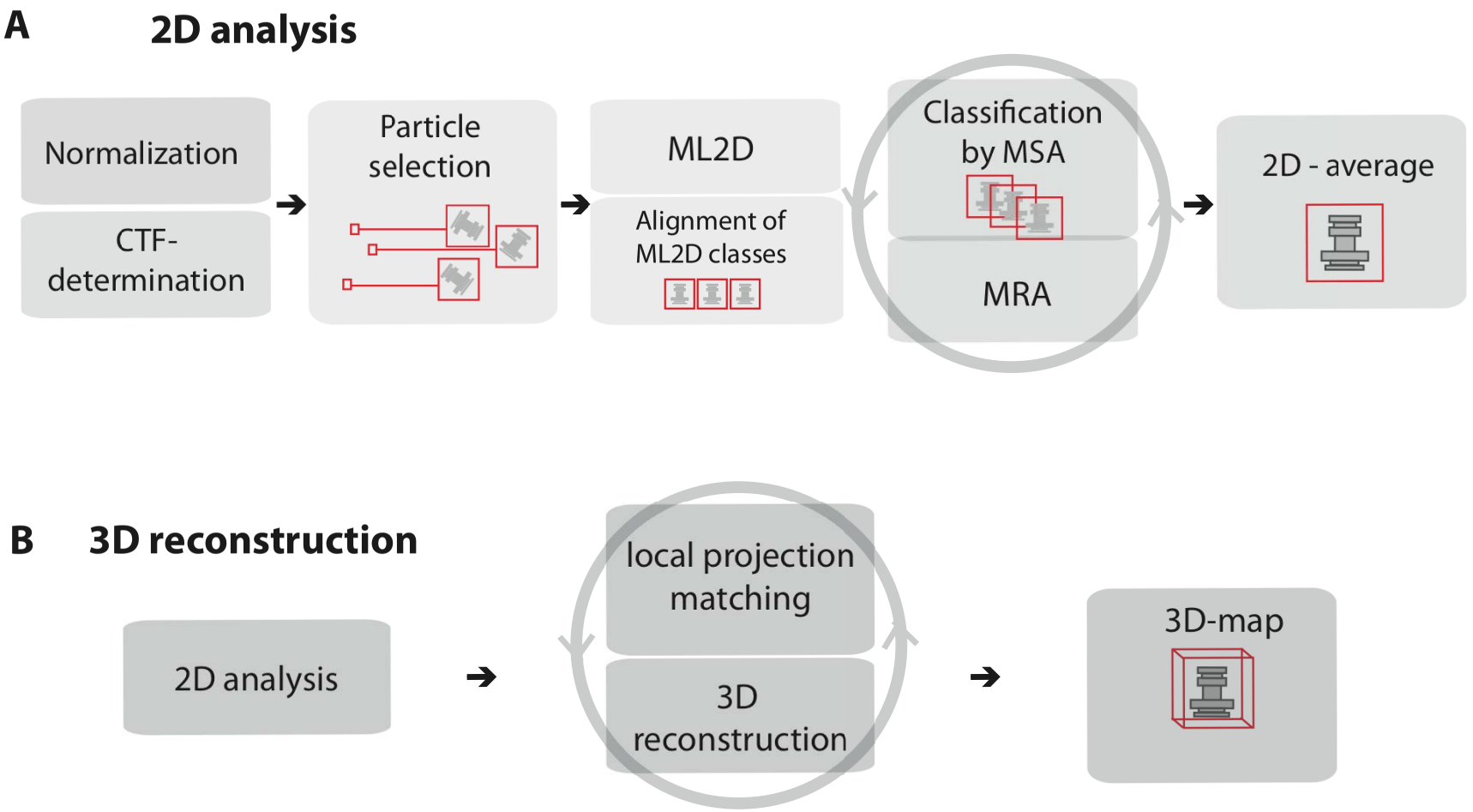

Figure 8. Overview of 2D single particle analysis and 3D reconstruction of the NC/NC base. (A) 2D analysis is started by preprocessing the images (normalization, CTF determination), then particles are selected automatically and further processed iteratively, by maximum likelihood classification (ML2D), alignment of the resulting classes, classification by MSA (multivariate statistical analysis), and MRA (multi reference alignment) leading to a 2D-average of the protein complex. **(B)** 3D reconstruction is based on the previously perfomed 2D analysis; via local projection matching to a reference the euler angles of each particle are defined, and a model can be reconstructed. Iterating this process leads to a refined and final 3D-map of the NC/NC base (see Schraidt 2010).

VI RESULTS

VI. Results

6.1. Export apparatus proteins SpaP, SpaQ, SpaR, SpaS and InvA co-fractionate with NC

The export apparatus proteins SpaP, SpaQ, SpaR, SpaS, InvA and their homologs found in the flagellum and other Gram-negative bacteria are membrane bound proteins essential for T3S functionality (Sukhan et al. 2001). Therefore they have been suggested to be physically associated to the bacterial inner membrane (Ohnishi et al. 1997). Analysis of the flagellum and the *Shigella* NC have furthermore shown co-purification of Spa homologs with other structural elements of the T3SS (Fan et al. 1997, Zenk et al. 2007). These results prompted us to test Spa and InvA protein association with the *Salmonella* NC.

NCs were purified from *S. Typhimurium* (wild type SB905) using membrane preparation, solubilization and density gradient fractionation (Schraidt et al. 2010) (Fig. 9A). The purified sample was analyzed by SDS-PAGE, and the main NC protein components InvG, PrgH, PrgK, PrgI and PrgJ were separated and visualized. The same sample was also analyzed by mass spectrometry (MS) using in-solution digest (Fig. 9B).

Peptides of the known NC components InvG, PrgH, PrgK, PrgI and PrgJ were identified; the sequence coverage of the individual proteins was as follows: 85% of InvG, 69% of PrgH, 69% of PrgK, 100% of PrgI and 75% of PrgJ. The export apparatus proteins SpaP, SpaQ, SpaR, SpaS and InvA were also detected, however fewer peptides of the individual proteins were found. The sequence coverage was 34% of SpaP, 22% of SpaQ, 5% of SpaR, 3% of SpaS and 27% of InvA. In addition to the inner membrane proteins of SPI-1, the tip protein SipD and the effector protein SipA representing members of the T3SS were found. However, the sample still contained T3SS unrelated proteins because of the properties of density gradient fractionation (major contaminant GroEL, prophages Gifsy-1, Fels-1, see also Diploma thesis of Matthias Brunner, 2009).

Taken together these results demonstrate that the membrane proteins SpaP, SpaQ, SpaR, SpaS and InvA co-fractionate with the *Salmonella* NC proteins.

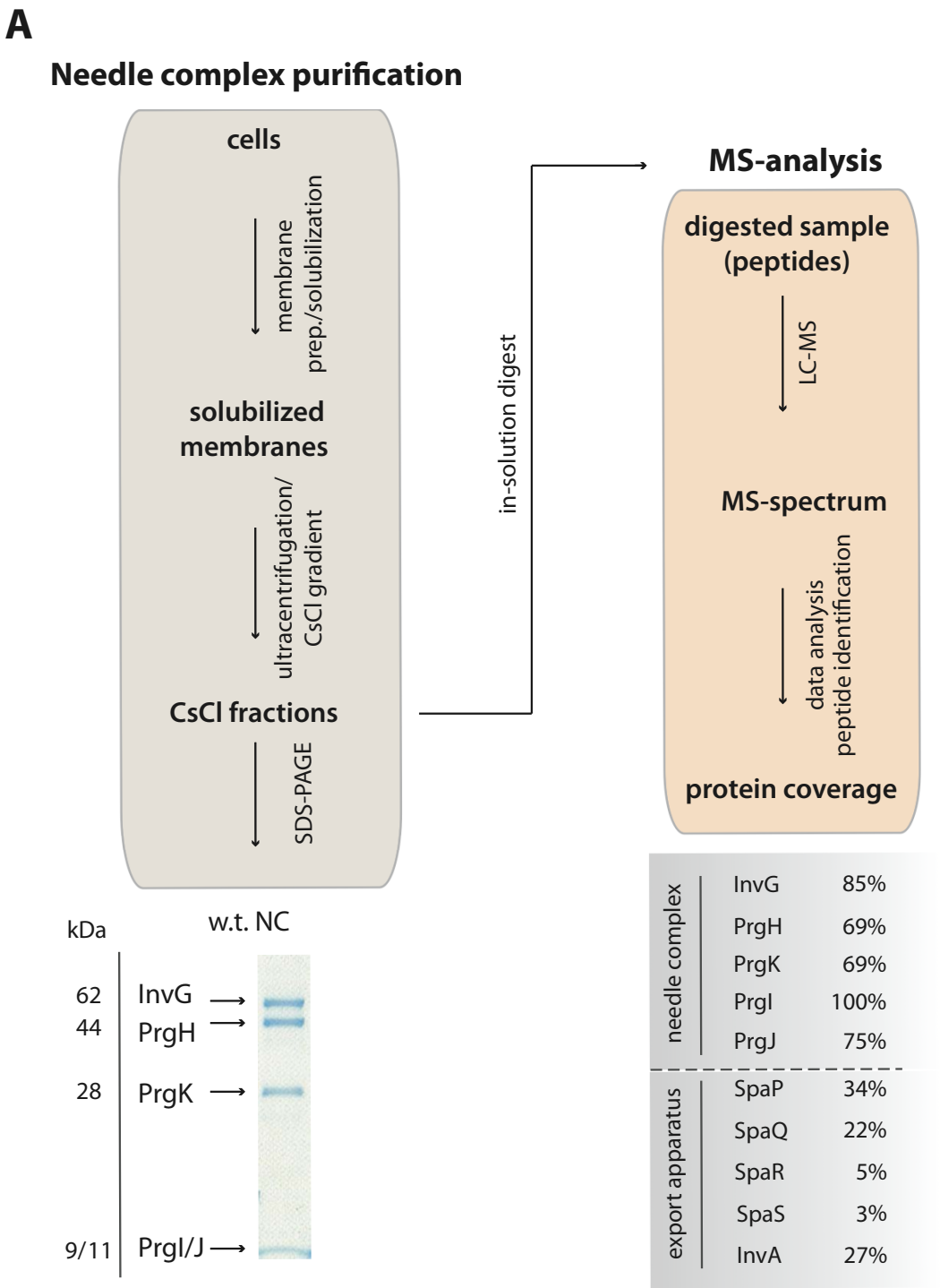

Figure 9. Export apparatus proteins co-fractionate with NC. (A) Purified NC was analyzed by SDS-PAGE and mass spectrometry analysis (MS-analysis) using in-solution digest. The experiment revealed co-fractionation of NC proteins (InvG = 62 kDa, PrgH = 44 kDa, PrgK = 28 kDa, PrgJ =11 kDa, PrgI = 9kDa) with export apparatus proteins (SpaP = 25kDa, SpaQ = 9, SpaR = 28kDa, SpaS = 40kDa, InvA = 76kDa).

B

SpaP

Sequence Coverage: 34% Unique peptides: 12

```
  1 MGNDISLIAL LAFSTLLPFI IASGTCFVKF SIVFVMVRNA LGLQQIPSNM
 51 TLNGVALLLS MFVMWPIMHD AYVYFEDEDV TFNDISSLSK HVDEGLDGYR
101 DYLIKYSDRE LVQFFENAQL KRQYGEETET VKRDKDEIEK PSIFALLPAY
151 ALSEIKSAFK IGFYLYLPFV VVDLVVSSVL LALGMMMMSP VTISTPIKLV
201 LFVALDGWTL LSKGLILQYM DIAT
```

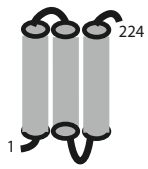

SpaQ

Sequence Coverage: 22% Unique peptides: 2

```
  1 MDDLVFAGNK ALYLVLILSG WPTIVATIIG LLVGLFQTVT QLQEQTLPFG
 51 IKLLGVCLCL FLLSGWYGEV LLSYGRQVIF LALAKG
```

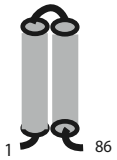

SpaR

Sequence Coverage: 5% Unique peptides: 1

```
  1 MFYALYFEIH HLVASAALGF ARVAPIFFFL PFLNSGVLSG APRNAIIILV
 51 ALGVWPHALN EAPPFLSVAM IPLVLQEAAV GVMLGCLLSW PFWVMHALGC
101 IIDNQRGATL SSSIDPANGI DTSEMANFLN MFAAVVYLQN GGLVTMVDVL
151 NKSYQLCDPM NECTPSLPPL LTFINQVAQN ALVLASPVVL VLLLSEVFLG
201 LLSRFAPQMN AFAISLTVKS GIAVLIMLLY FSPVLPDNVL RLSFQATGLS
251 SWFYERGATH VLE
```

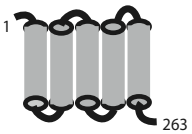

SpaS

Sequence Coverage: 3% Unique peptides: 1

```
  1 MSSNKTEKPT KKRLEDSAKK GQSFKSKDLI IACLTLGGIA YLVSYGSFNE
 51 FMGIIKIIIA DNFDQSMADY SLAVFGIGLK YLIPFMLLCL VCSALPALLQ
101 AGFVLATEAL KPNLSALNPV EGAKKLFSMR TVKDTVKTLL YLSSFVVAAI
151 ICWKKYKVEI FSQLNGNIVG IAVIWRELLL ALVLTCLACA LIVLLLDAIA
201 EYFLTMKDMK MDKEEVKREM KEQEGNPEVK SKRREVHMEI LSEQVKSDIE
251 NSRLIVANPT HITIGIYFKP ELMPIPMISV YETNQRALAV RAYAEKVGVP
301 VIVDIKLARS LFKTHRRYDL VSLEEIDEVL RLLVWLEEVE NAGKDVIQPQ
351 ENEVRH
```

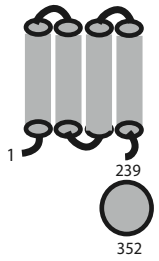

InvA

Sequence Coverage: 27% Unique Peptides: 18

```
  1 MLLSLLNSAR LRPELLILVL MVMIISMFVI PLPTYLVDFL IALNIVLAIL
 51 VFMGSFYIDR ILSFSTFPAV LLITTLFRLA LSISTSRLIL IEADAGEIIA
101 TFGQFVIGDS LAVGFVVFSI VTVVQFIVIT KGSERVAEVA ARFSLDGMPG
151 KQMSIDADLK AGIIDADAAR ERRSVLERES QLYGSFDGAM KFIKGDAIAG
201 IIIIFVNFIG GISVGMTRHG MDLSSALSTY TMLTIGDGLV AQIPALLIAI
251 SAGFIVTRVN GDSDNMGRNI MTQLLNNPFV LVVTAILTIS MGTLPGFPLP
301 VFVILSVVLS VLFYFKFREA KRSAAKPKTS KGEQPLSIEE KEGSSLGLIG
351 DLDKVSTETV PLILLVPKSR REDLEKAQLA ERLRSQFFID YGVRLPEVLL
401 RDGEGLDDNS IVLLINEIRV EQFTVYFDLM RVVNYSDEVV SFGINPTIHQ
451 QGSSQYFWVT HEEGEKLREL GYVLRNALDE LYHCLAVTLA RNVNEYFGIQ
501 ETKHMLDQLE AKFPDLLKEV LRHATVQRIS EVLQRLLSER VSVRNMKLIM
551 EALALWAPRE KDVINLVEHI RGAMARYICH KFANGGELRA VMVSAEVEDV
601 IRKGIRQTSG STFLSLDPEA SANLMDLITL KLDDLLIAHK DLVLLTSVDV
651 RRFIKKMIEG RFPDLEVLSF GEIADSKSVN VIKT
```

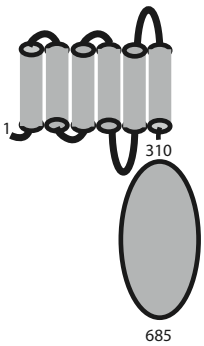

Figure 9. Export apparatus proteins co-fractionate with NC. (B) Detailed view of found peptides and their sequence coverage (shown in red) of export apparatus proteins SpaP, SpaQ, SpaR, SpaS and InvA (membrane topology adapted from Moraes et al. 2008) .

6.2. A Δ*spa Salmonella* mutant strain builds up bases and can be purified to levels comparable to wild type

Co-fractionation of Spa proteins with NC components as well as additional Blue Native-PAGE analysis from our collaborators (Wagner et al. 2010) highly suggested interaction between export apparatus and NC proteins and their potential involvement in the NC structure. Therefore a *S. Typhimurium* mutant strain lacking the inner membrane proteins (SpaP, SpaQ, SpaR, SpaS and InvA, termed Δ*spa*, SB1922) was investigated. The strain expressed InvG, PrgH, PrgK, PrgI and PrgJ at wild type (w.t.) levels as shown by immunoblotting against NC proteins (Fig. 10A).

Comparing w.t. NC with Δ*spa* mutant purification, a similar migration of NC proteins on a CsCl gradient was observed indicating that Δ*spa* built up structures similar to w.t. (Fig. 10B). The NC components were mainly found in fraction 3, at similar protein concentrations of 0.5 mg/ml - 1mg/ml measured on average. In case of the Δ*spa* mutant, PrgJ/PrgI did not co-migrate with InvG, PrgH and PrgK, indicating that they are not assembled and associated with the base to form NCs (Fig. 10C). This observation is in agreement with previous results, that the export apparatus proteins are essential to build up the inner rod and needle filament (Sukhan et al. 2001).

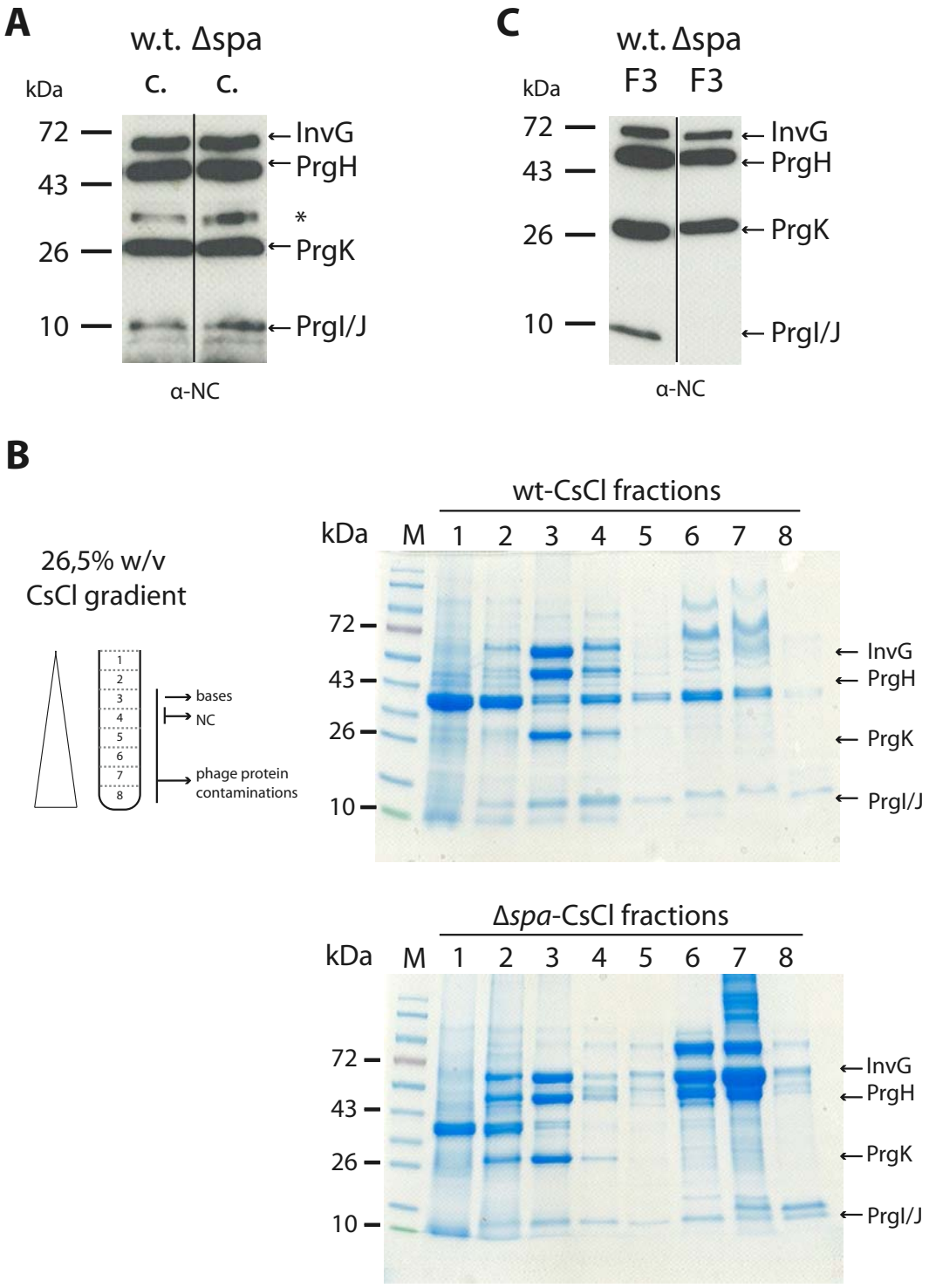

Figure 10. Comparison of NC purification from Δ*spa* to w.t. strain. (A) Δ*spa* cells express the major NC components at w.t. levels as shown by immunoblotting. InvG, PrgH, PrgK and PrgJ/I were detected using Anti-NC antibody. * Band present in w.t. and Δ*spa* cells not representing NC proteins. **(B,C)** NC proteins InvG, PrgH and PrgK are mainly found in CsCl gradient fraction 3 in w.t. and Δ*spa* NC purification; for Δ*spa,* PrgJ/I do not co-purify with the base proteins. M = marker, kDa: 10, 17, 26, 34, 55, 72, 95, 130, 230.

6.3. Structural analysis of ΔSpa bases

NC bases could be isolated from *S. Typhimurium* strains lacking export apparatus components. Thus, the next question was which role the Spa proteins play within the NC structure. Therefore negative stain electron microscopy (EM) and cryo-EM were used to investigate the mutant bases from a structural point of view.

6.3.1. Negative stain EM as a tool to investigate ΔSpa base stability

ΔSpa bases were first analyzed by negative stain EM. Negative stain is based on the application of heavy metal salts (derived from e.g. uranium or tungsten), thereby causing strong dehydration of the biological sample of interest, which can result in distortion of the observed structures (Frank and Radermacher 1992). In the case of ΔSpa, negative stain treatment caused disassembly of the bases and only the single outer and inner ring structures remained visible, while w.t. bases stayed fully intact (Fig. 11A). This result suggests that bases lacking SpaP, SpaQ, SpaR, SpaS and InvA leads to weaker interactions between PrgH/ PrgK and InvG ring structures.

6.3.2. Using Cryo-EM to investigate the structure of ΔSpa base complexes

A milder approach for visualization of macromolecular complexes such as ΔSpa bases is vitrification and subsequent cryo-EM. This technique ensures imaging of biological samples under fully hydrated, near-native conditions with minimal disturbance (Radermacher et al. 1992). Aliquots of the same samples as used for negative stain EM were vitrified and observed by cryo EM (Fig. 11B). Thus, this technique preserves the integrity of the complex and made it possible to visualize the ΔSpa bases in a fully assembled state, which was an important prerequisite for further structural analysis.

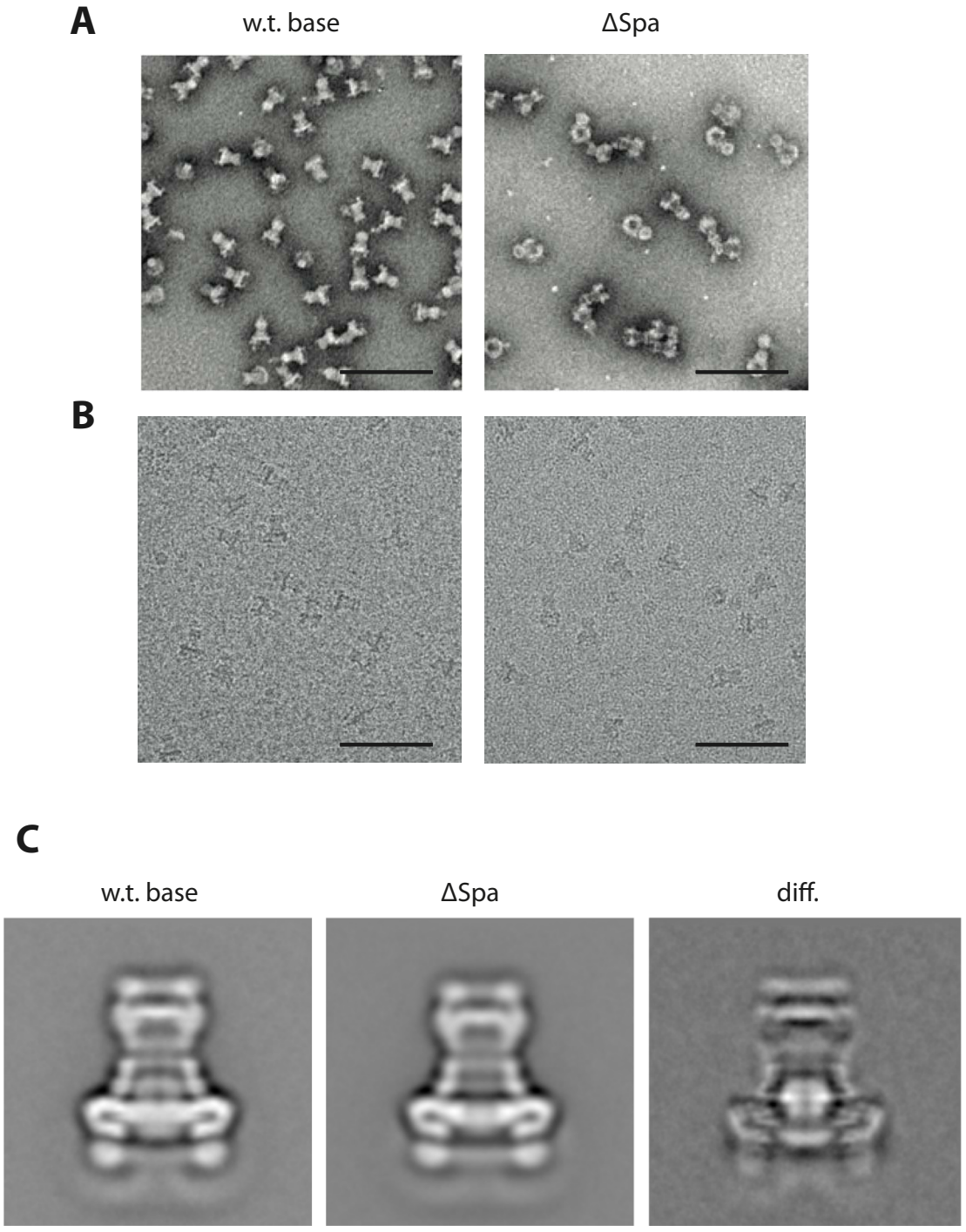

Figure 11. Visualization of ΔSpa bases by EM. (A) ΔSpa bases are less stable compared to w.t. bases, since they partially disassemble upon negative staining. **(B)** However, when using cryo-EM for visualization, ΔSpa bases do not disassemble. Bar = 100nm. (**C)** Single particle analysis of w.t. and ΔSpa bases reveal strong differences within cup and socket region.

6.3.3 ΔSpa bases lack NC cup and socket substructures

Images of w.t. and ΔSpa bases were collected using cryo-EM and single particle analysis was performed for structural comparison (Fig. 11C). For generating a 2D-average only low-tilt particle projections (beta angle: 88-92 degrees) obtained by projection matching were selected. By comparison of w.t. and ΔSpa bases one could observe distinct differences in the lower part of the mutant bases, where a prominent density was absent. This density corresponds to a NC substructure also called cup and socket, positioned right in the center of the base, touching the PrgH/K rings from the inside (Schraidt et al. 2011). Which proteins comprise the cup and socket is still remaining an open question.

In order to further refine the structural differences of the ΔSpa base missing density, 3D maps of w.t. and ΔSpa bases were created using the whole dataset of ~ 40 000 particles for angular reconstitution. The ΔSpa volume was subtracted from the w.t. structure thereby generating a difference map of both 3D structures (Fig. 12. 1. - Fig. 12. 4.). The difference map confirmed the results from the 2D analysis and represented cup and socket as the main dissimilarity between w.t. and ΔSpa bases. Longitudinal sections through both structures showed that except from the basal center ΔSpa bases were not distinguishable from w.t (Fig. 12.5A), also observed by looking at the similar 3D surface views of ΔSpa and w.t. bases. Structural differences could only be observed internally and were depicted in the 3D enlargement of the basal center by overlaying w.t. and ΔSpa structures highlighting cup and socket (Fig. 12. 5B).

These results are the first proof that the export apparatus proteins (Spa/InvA proteins) play a role in the establishment of the cup and socket region. It still remains to be shown, whether these proteins are structural elements forming this region, and if so, which of them corresponds to which area of the cup and socket substructure.

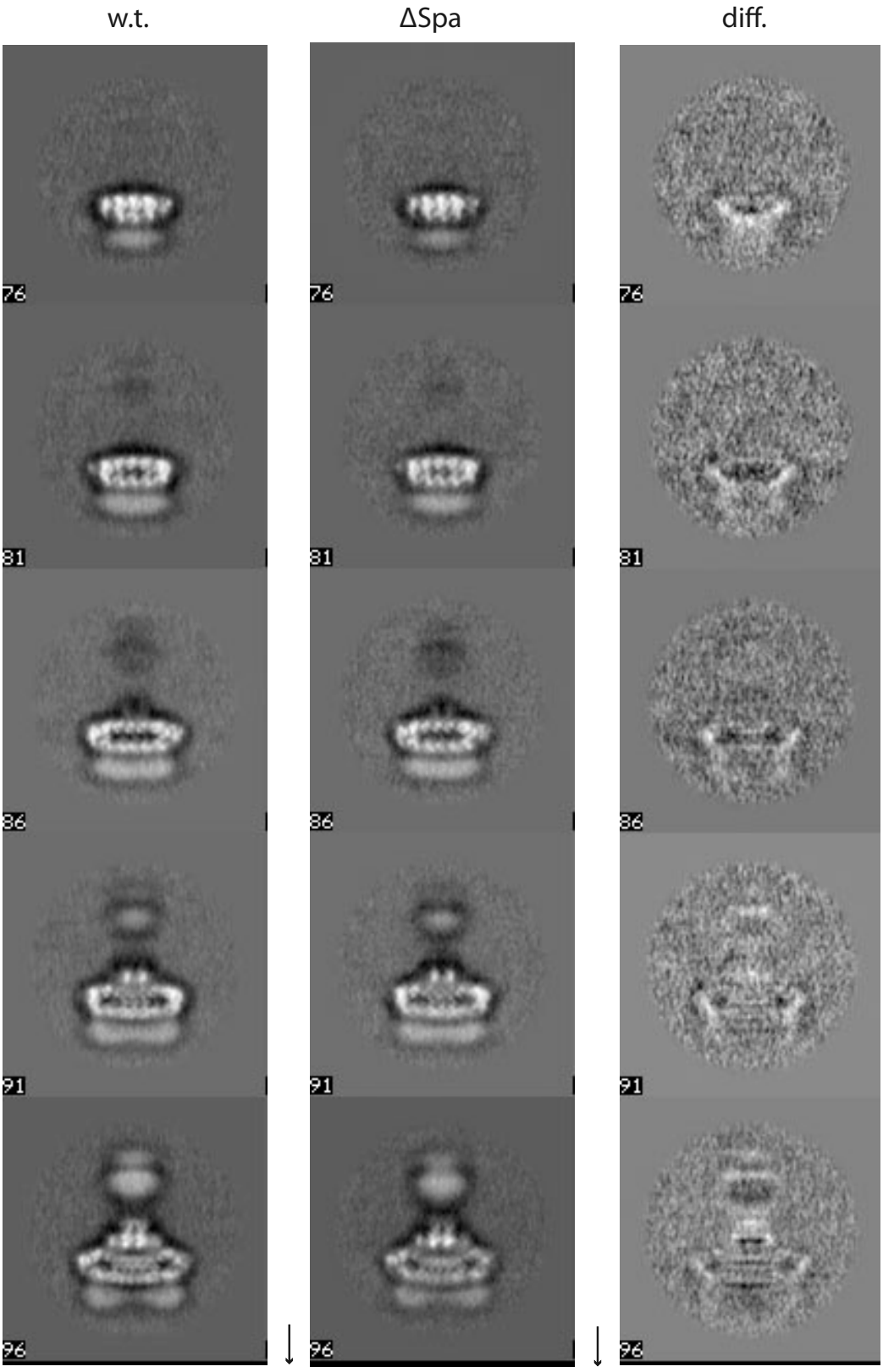

Figure 12. 1. 3D reconstruction of ΔSpa compared to w.t. bases. Display of longitudinal sections through the 3D structure of ΔSpa compared to w.t. bases and corresponding difference map reveal cup and socket as missing substructure in ΔSpa bases. Sections = 256, display = every fifth section from 76-96.

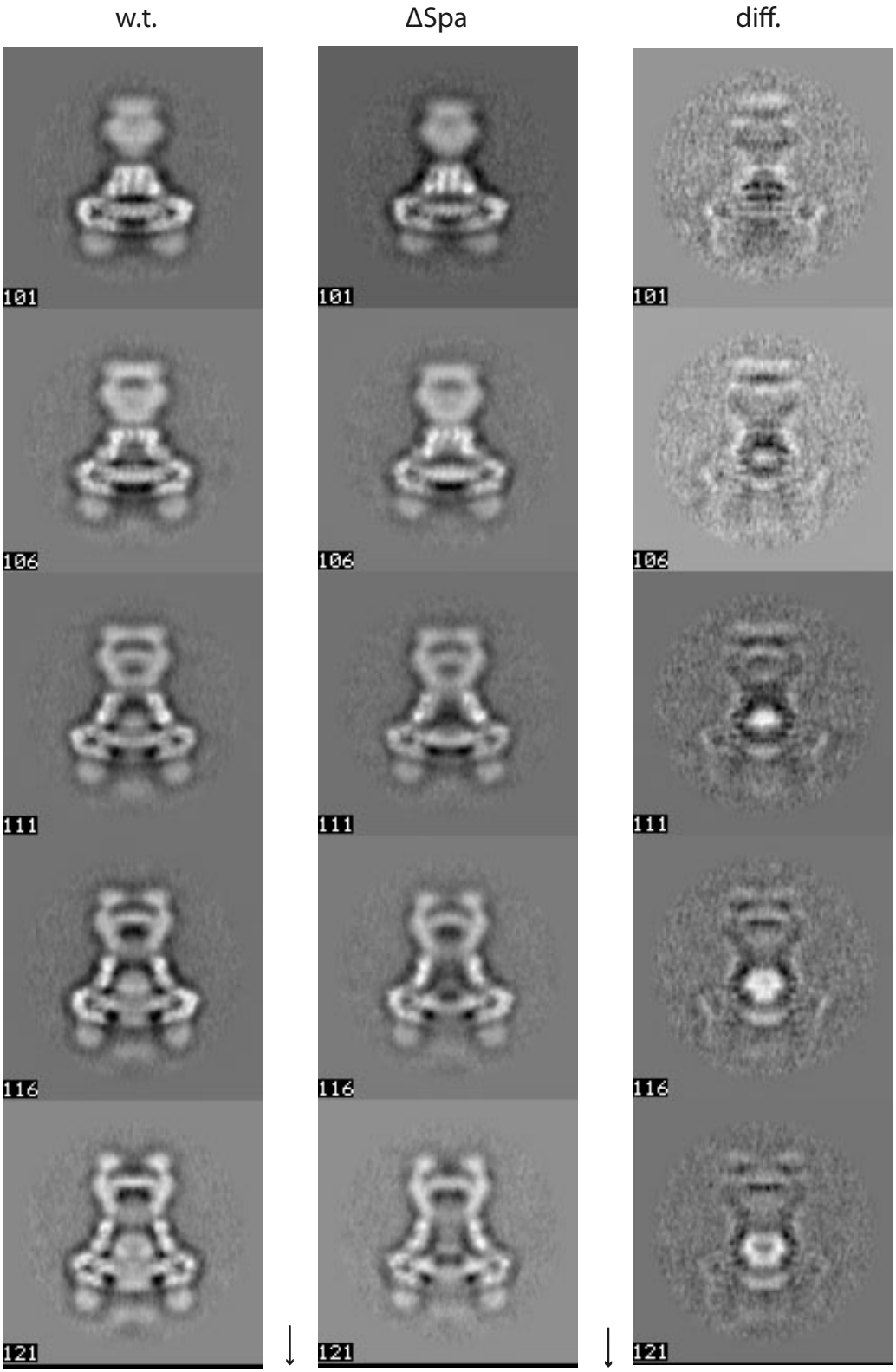

Figure 12. 2. 3D reconstruction of ΔSpa compared to w.t. bases. Display of longitudinal sections through the 3D structure of ΔSpa compared to w.t. bases and corresponding difference map (diff.) reveal cup and socket as missing substructure in ΔSpa bases. Sections = 256, display = every fifth section from 101-121.

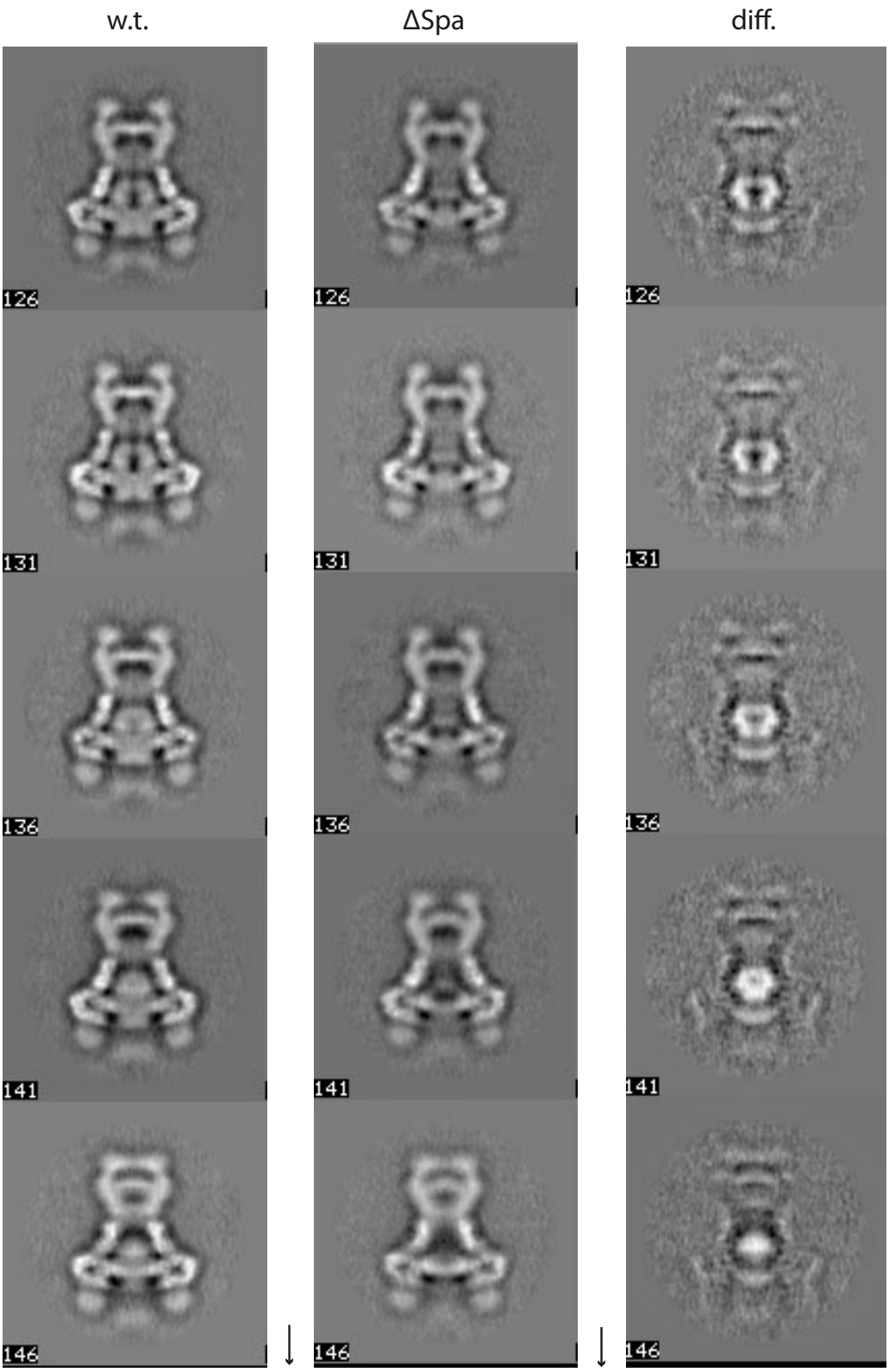

Figure 12. 3. 3D reconstruction of ΔSpa compared to w.t. bases. Display of longitudinal sections through the 3D structure of ΔSpa compared to w.t. bases and corresponding difference map reveal cup and socket as missing substructure in ΔSpa bases. Sections = 256, display = every fifth section from 126-146.

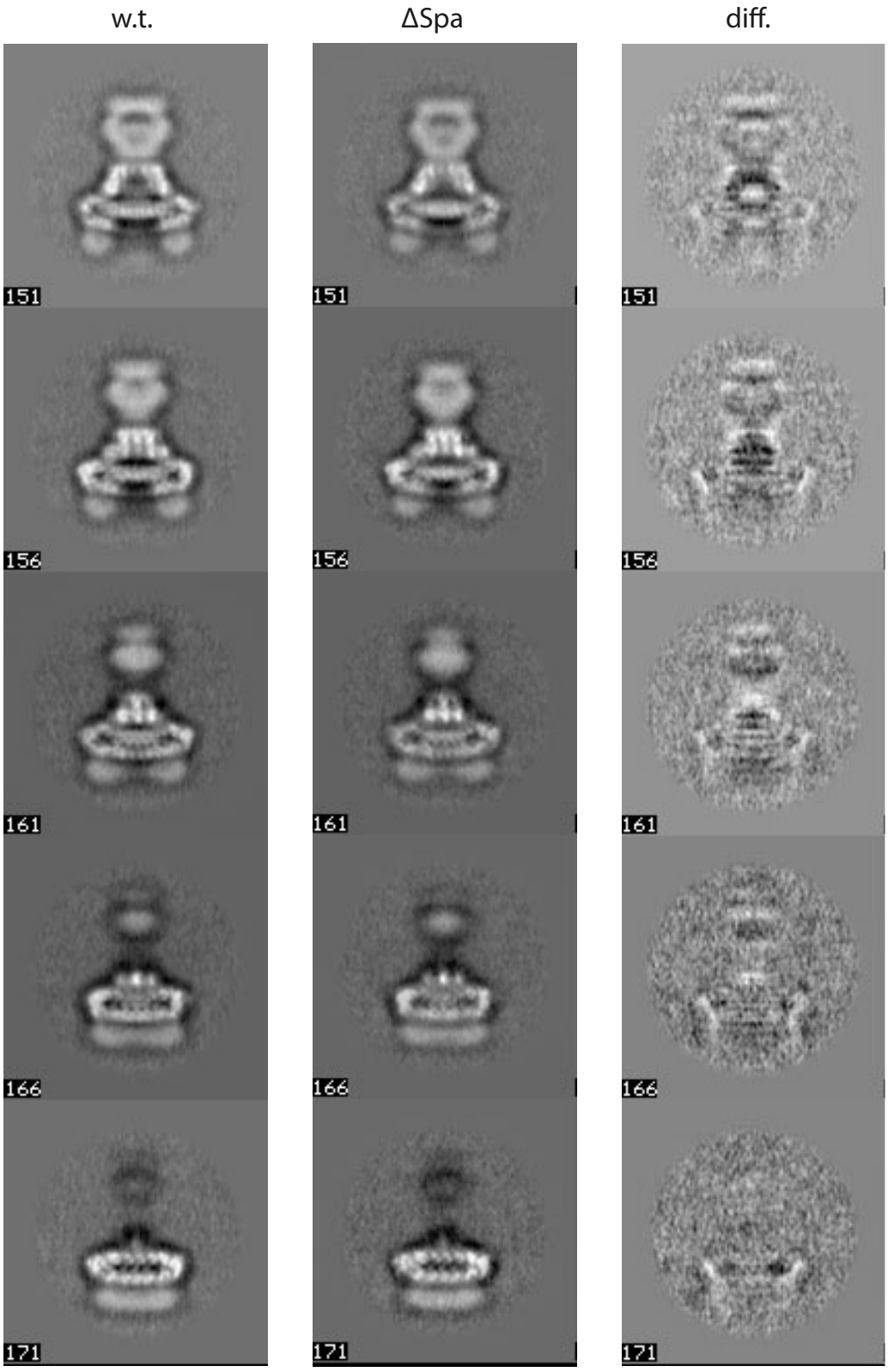

Figure 12. 4. 3D reconstruction of ΔSpa compared to w.t. bases. Display of longitudinal sections through the 3D structure of ΔSpa compared to w.t. bases and corresponding difference map reveal cup and socket as missing substructure in ΔSpa bases. Sections = 256, display = every fifth section from 151-171.

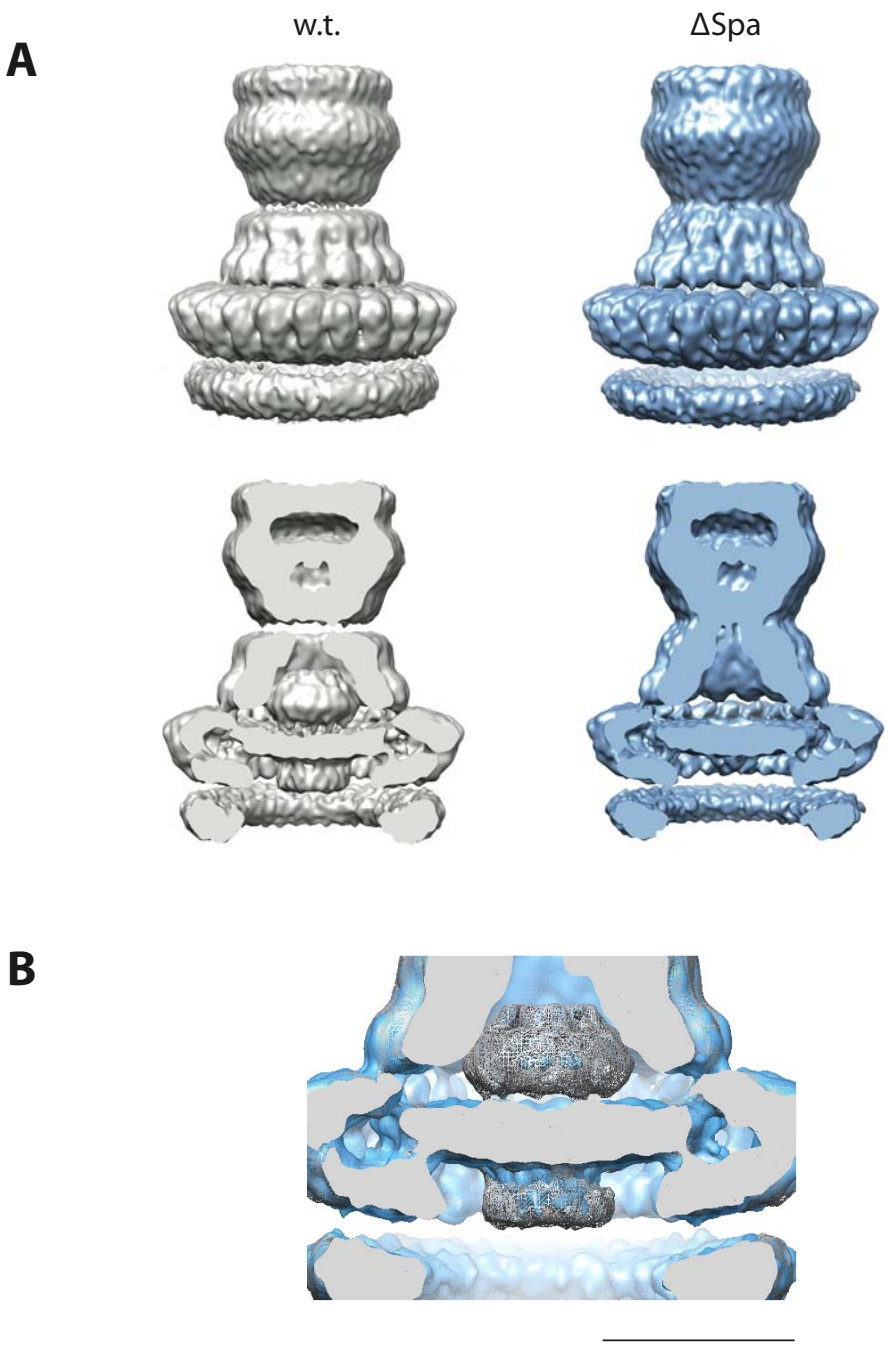

Figure 12. 5. 3D reconstruction of ΔSpa compared to w.t. bases. (A) 3D resonstruction of ΔSpa and w.t. bases shows, that their surface views are indistinguishable. The structural difference can only be seen by looking at a section through the base, which reveals that cup and socket are absent in the ΔSpa base. **(B)** The overlay of both 3D structures in a section view shows the additional density within cup and socket region (mesh, grey). Bar = 10nm.

6.3.4. EM reveals different phenotypes of individual Spa/InvA mutants

The missing substructure of the Spa/InvA depleted NC base prompted us to investigate the effect of removing the Spa/InvA proteins individually. As previously reported, the individual mutant strains were incapable of building fully assembled NC as assayed by the presence of NCs in the membrane of osmotically shocked cells by EM, confirming that each of the export apparatus proteins is essential for secretion of substrates including rod and needle proteins (Sukhan et al. 2001).

NC bases from Δ*spaP* (SB1902), Δ*spaQ* (SB1903), Δ*spaR* (SB1904), Δ*spaS* (SB1905) and Δ*invA* (SB1901) were purified according to the same protocol used for the Δ*spa*. As shown by negative stain EM the individual mutant bases display different stability: only disassembled base substructures could be visualized by negative stain EM in the cases of Δ*spa* (lacking SpaP, SpaQ, SpaR, SpaS, InvA), Δ*spaP*, Δ*spaQ* and Δ*spaR* (Fig. 13. 1., left panel). On the other hand, ΔSpaS and ΔInvA bases remained stable upon negative stain treatment, suggesting different structural composition of the various mutants (Fig. 13. 2., left panel). Thus, negative stain EM could be used to investigate the stability of the individual Spa/InvA mutants and revealed first phenotypical differences between the various mutant base structures.

For structural analysis it was necessary to use a milder method than negative stain which did not cause disassembly of the less stable mutants. As in the case of ΔSpa, ΔSpaP, ΔSpaQ and ΔSpaR, bases remained assembled upon vitrification and could be visualized together with the other mutants ΔSpaS and ΔInvA individually by Cryo-EM (Fig. 13.1., right panel).

Subsequent single particle analysis revealed distinct structural differences between the single mutants defining two main groups: while the unstable ΔSpaP, ΔSpaQ and ΔSpaR bases lacked a cup and socket like ΔSpa (empty base), the structures of stable ΔSpaS and ΔInvA contained cup and socket (filled base) as seen in the 2D-class averages (Fig. 13. 2., right panel).

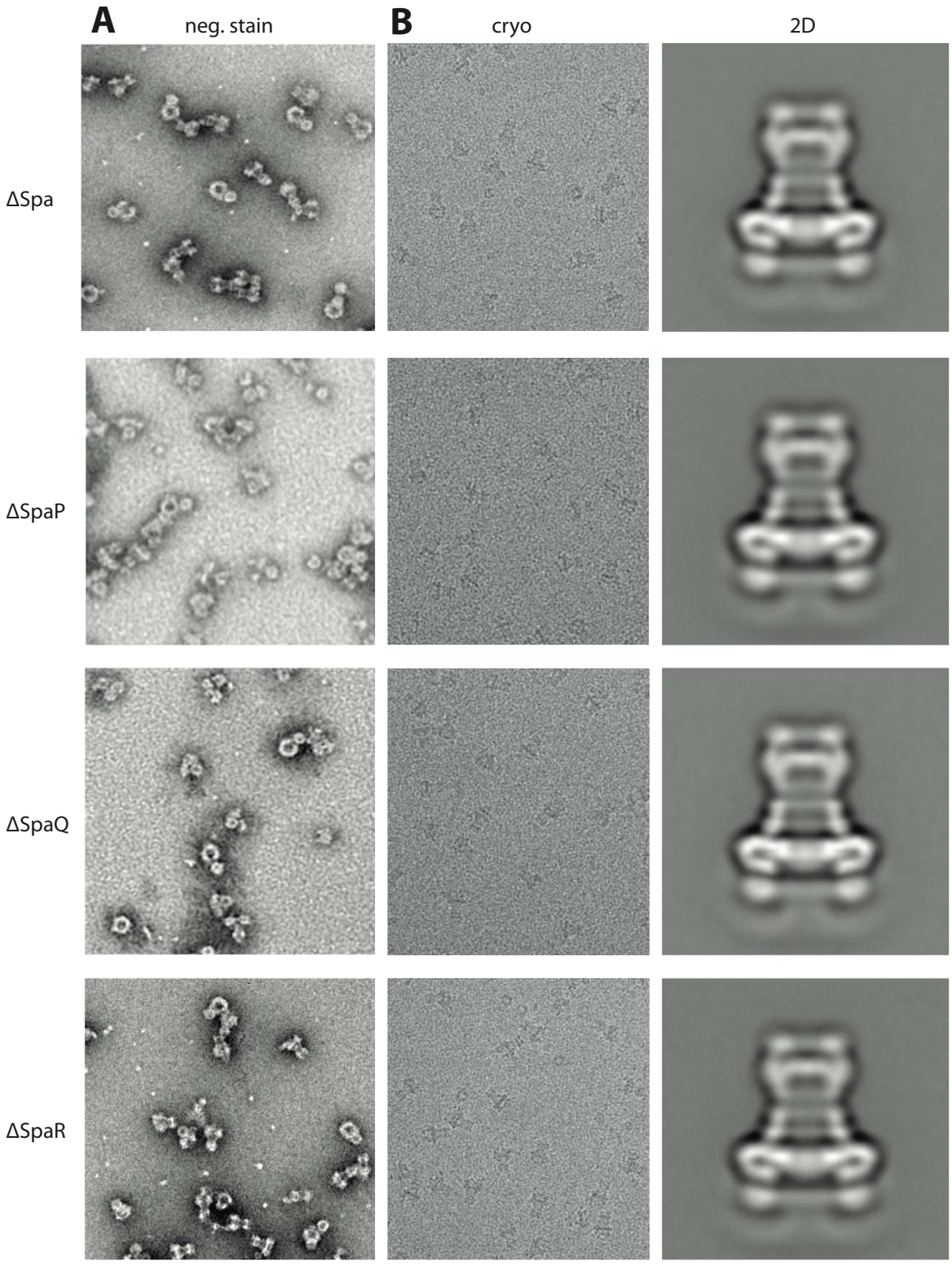

Figure 13. 1. (A) Using negative stain imaging to test for stable and unstable export apparatus mutants. ΔSpaP, ΔSpaQ and ΔSpaR bases disassembled upon negative staining (left panel), they were less stable compared to w.t. bases and behaved like ΔSpa bases. Bar = 50nm. **(B) Cryo-EM and single particle analysis of export apparatus mutants.** ΔSpaP, ΔSpaQ, ΔSpaR stayed assembled upon vitrification and cryo-EM (middle panel) and had an empty base phenotype as shown by class averages (right panel) of all upright particles.

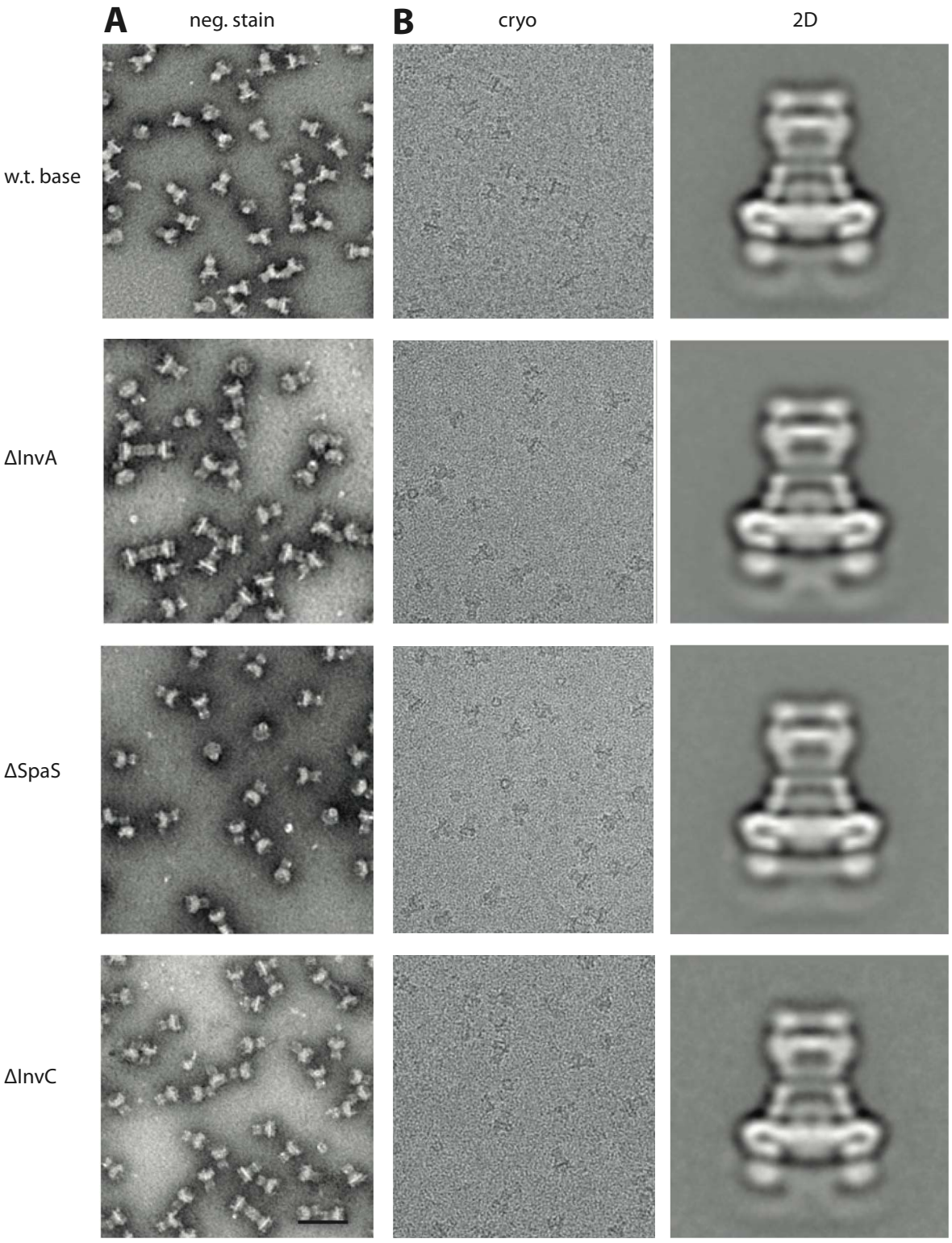

Figure 13. 2. (A) Using negative stain imaging to test for stable and unstable export apparatus mutants. ΔInvA, ΔSpaS and ΔInvC bases were indistinguishable from w.t. and stayed assembled upon negative staining (left panel). Bar = 50nm. **(B) Cryo-EM and single particle analysis of export apparatus mutants.** ΔInvA, ΔSpaS and ΔInvC bases were imaged via cryo-EM (middle panel). ΔSpaS had and intermediate phenotype, whereas ΔInvA and ΔInvC showed an filled base phenotype as shown by class averages of all upright particles (right panel).

6.3.5. ΔSpaS bases show empty and filled base phenotype

Eigenimage analysis was used to investigate the structural differences of the individual export apparatus mutants in more detail and to search for potential heterogeneity within the data sets (Fig. 14). For this purpose only untilted images were used and by applying an image mask, only variation in the cup and socket region was taken into account in the analysis.

This analysis confirmed a homogenous population of empty bases for ΔSpa, ΔInvA, ΔSpaP, ΔSpaQ, ΔSpaR and filled bases for w.t. base and ΔInvA. However, in the case of ΔSpaS, the second eigenimage showed a higher intensity within cup and socket region, pointing out that the strongest difference of compared particles occured within this substructure. Therefore the datasets of all mutants were reinvestigated. Previously generated ΔSpa and w.t. 2D averages served as empty and filled references for cross-correlation based multi reference alignment (MRA) of 200 classes. Using this approach, the analysis revealed an intermediate phenotype for ΔSpa bases, made up by 74% filled versus 26% empty bases within the ΔSpa data, (Fig. 15). This is in contrast to the other mutant complexes analyzed, in which case the dominant phenotype accounted for at least 98% of the generated classes.

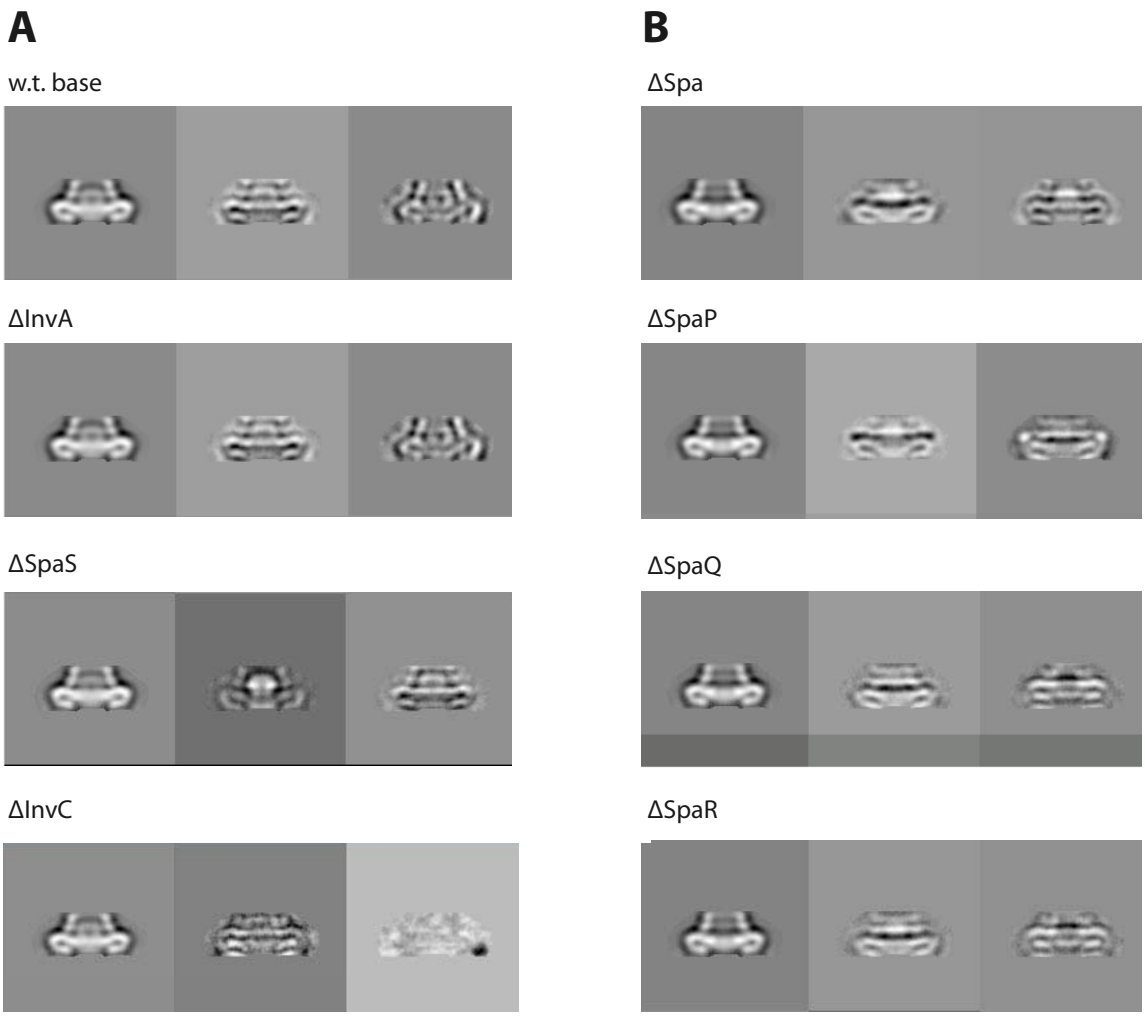

Figure 14. Eigenimage analysis of individual export apparatus mutants reveals heterogeneity within ΔSpaS dataset. (A) ΔInvA, ΔSpaS and ΔInvC bases showed a filled base phenotype, seen on the first eigenimage. The second eigenimage shows the strongest variations whithin the dataset. The second ΔInvA and ΔInvC eigenimages were comparable to w.t., whereas the ΔSpaS data contained distinct variations within cup and socket. **(B)** ΔSpaP, Δ SpaQ and ΔSpaR behaved like ΔSpa bases, showing an empty base phenotype and similar eigenimages. Images were provided by Matthias Brunner.

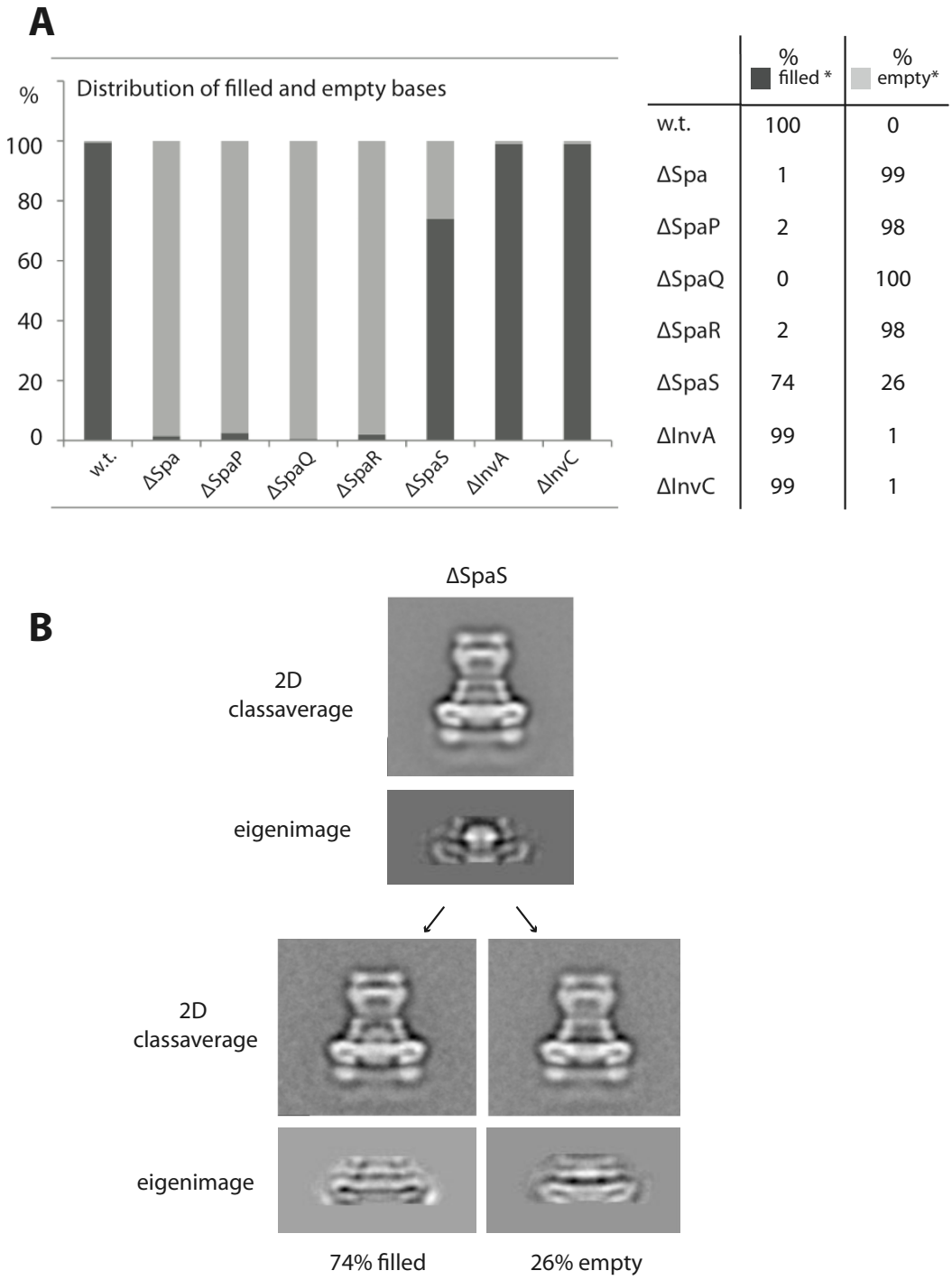

Figure 15. ΔSpaS shows empty and filled base phenotype. (A) Multi reference alignment (MRA) of empty and filled bases with 200 subclasses of ΔSpaP, ΔSpaQ, ΔSpaR, ΔInvA and ΔInvC bases confirmed a homogenous dataset and showing a clear phenotype (>98% filled or empty bases, respectively). In case of ΔSpaS a heterogenous dataset was found, as previously indicated by eigenimage analysis: 74% filled and 26% empty phenotype bases. **(B)** The Δ*spaS* strain was able to build up bases containing cup and socket (74%), as seen in the class average of all upright particles but also an emtpy subpoluation (26%) was found within the dataset. Images were provided by Matthias Brunner. * Values were rounded to the unit's digit.

6.3.6. ΔInvA and ΔSpaS samples contain the export apparatus protein SpaP as shown by MS analysis

Aliquots of the samples used for cryo-EM studies were also subjected to MS analysis to determine their protein composition with regard to NC and export apparatus proteins compared to w.t. composition (Fig. 16, Fig 17.1. -17.5., for peptide list see appendix). In ΔSpa, ΔSpaP, ΔSpaQ and ΔSpaR samples, only the base proteins InvG, PrgH and PrgK were detected, whereas in the ΔSpaS and ΔInvA samples (filled base phenotype), either InvA or SpaS were identified, respectively. The other two export apparatus proteins, SpaQ and SpaR, were not found in the sample. Taking into account that within the w.t. sample only two peptides of both SpaQ and SpaR were found, it cannot be excluded that these proteins are also present in the mutant bases but just not detected. However, with SpaP being the only common protein detectable in all strains showing the cup and socket region, we conclude that SpaP is most likely involved in building up this NC substructure.

	w.t.	ΔSpa	ΔSpaP	ΔSpaQ	ΔSpaR	ΔSpaS	ΔInvA	ΔInvC
	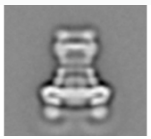	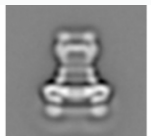		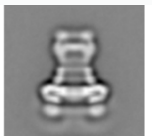	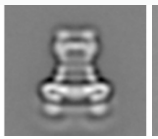	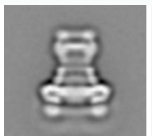		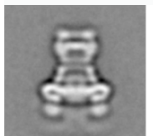
	filled	empty	empty	empty	empty	inter-mediate	filled	filled
InvG	85% 54	34% 19	11% 7	56% 29	43% 25	64% 33	35% 20	64% 38
PrgH	69% 32	53% 32	29% 16	64% 39	71% 37	75% 34	53% 32	98% 49
PrgK	69% 14	48% 12	23% 6	65% 18	55% 16	53% 16	35% 11	78% 24
PrgJ	75% 9	n.f.	n.f.	n.f.	n.f.	n.f.	n.f.	n.f.
PrgI	100% 9	n.f.	n.f.	n.f.	n.f.	n.f.	n.f.	n.f.
SpaP	34% 12	n.f.	n.f.	n.f.	n.f.	22% 8	12% 4	24% 11
SpaQ	22% **2**	n.f.	n.f.	n.f.	n.f.	**n.f.***	**n.f.***	**n.f.***
SpaR	5% **1**	n.f.	n.f.	n.f.	n.f.	**n.f.***	**n.f.***	**n.f.***
SpaS	3% **1**	n.f.	n.f.	n.f.	n.f.	n.f.	6% 2	2% 1
InvA	27% 18	n.f.	n.f.	n.f.	n.f.	14% 9	n.f.	17% 10

Figure 16. Mass spec analysis of w.t., ΔSpa, ΔSpaP, ΔSpaQ, ΔSpaR, ΔSpaS, ΔinvA and ΔinvC bases and corresponding 2D classaverages. The table presents the sequence coverage (black) and unique peptides (red) of the NC proteins InvG, PrgH, PrgK, PrgJ, PrgI and export apparatus proteins SpaP, SpaQ, SpaR, SpaS and InvA found in the purified sample as well as the 2D classaverages of the individual mutant bases. The protein amounts subjected to mass spectrometry analysis were normalized to w.t. level. For SpaQ only 2 and for SpaR only 1 peptide was found, highlighted in blue (list of peptides in appendix). n.f. = not found, *two biological replicates were analyzed two times independently.

ΔSpa

InvG

Sequence Coverage: **34%** Unique Peptides: 19

```
  1 MKTHILLARV LACAALVLVT PGYSSEKIPV TGSGFVAKDD SLRTFFDAMA
 51 LQLKEPVIVS KMAARKKITG NFEFHDPNAL LEKLSLQLGL IWYFDGQAIY
101 IYDASEMRNA VVSLRNVSLN EFNNFLKRSG LYNKNYPLRG DNRKGTFYVS
151 GPPVYVDMVV NAATMMDKQN DGIELGRQKI GVMRLNNTFV GDRTYNLRDQ
201 KMVIPGIATA IERLLQGEEQ PLGNIVSSEP PAMPAFSANG EKGKAANYAG
251 GMSLQEALKQ NAAAGNIKIV AYPDTNSLLV KGTAEQVHFI EMLVKALDVA
301 KRHVELSLWI VDLNKSDLER LGTSWSGSIT IGDKLGVSLN QSSISTLDGS
351 RFIAAVNALE EKKQATVVSR PVLLTQENVP AIFDNNRTFY TKLIGERNVA
401 LEHVTYGTMI RVLPRFSADG QIEMSLDIED GNDKTPQSDT TTSVDALPEV
451 GRTLISTIAR VPHGKSLLVG GYTRDANTDT VQSIPFLGKL PLIGSLFRYS
501 SKNKSNVVRV FMIEPKEIVD PLTPDASESV NNILKQSGAW SGDDKLQKWV
551 RVYLDRGQEA IK
```

PrgH

Sequence Coverage: **53%** Unique Peptides: 32

```
  1 METSKEKTIT SPGPYIVRLL NSSLNGCEFP LLTGRTLFVV GQSDALTASG
 51 QLPDIPADSF FIPLDHGGVN FEIQVDTDAT EIILHELKEG NSESRSVQLN
101 TPIQVGELLI LIRPESEPWV PEQPEKLETS AKKNEPRFKN GIVAALAGFF
151 ILGIGTVGTL WILNSPQRQA AELDSLLGQE KERFQVLPGR DKMLYVAAQN
201 ERDTLWARQV LARGDYDKNA RVINENEENK RISIWLDTYY PQLAYYRIHF
251 DEPRKPVFWL SRQRNTMSKK ELEVLSQKLR ALMPYADSVN ITLMDDVTAA
301 GQAEAGLKQQ ALPYSRRNHK GGVTFVIQGA LDDVEILRAR QFVDSYYRTW
351 GGRYVQFAIE LKDDWLKGRS FQYGAEGYIK MSPGHWYFPS PL
```

PrgK

Sequence Coverage: **48%** Unique Peptides: 12

```
  1 MIRRYLYTFL LVMTLAGCKD KDLLKGLDQE QANEVIAVLQ MHNIEANKID
 51 SGKLGYSITV AEPDFTAAVY WIKTYQLPPR PRVEIAQMFP ADSLVSSPRA
101 EKARLYSAIE QRLEQSLQTM EGVLSARVHI SYDIDAGENG RPPKPVHLSA
151 LAVYERGSPL AHQISDIKRF LKNSFADVDY DNISVVLSER SDAQLQAPGT
201 PVKRNSFATS WIVLIILLSV MSAGFGVWYY KNHYARNKKG ITADDKAKSS
251 NE
```

ΔSpaP

InvG

Sequence Coverage: **11%** Unique Peptides: 7

```
  1 MKTHILLARV LACAALVLVT PGYSSEKIPV TGSGFVAKDD SLRTFFDAMA
 51 LQLKEPVIVS KMAARKKITG NFEFHDPNAL LEKLSLQLGL IWYFDGQAIY
101 IYDASEMRNA VVSLRNVSLN EFNNFLKRSG LYNKNYPLRG DNRKGTFYVS
151 GPPVYVDMVV NAATMMDKQN DGIELGRQKI GVMRLNNTFV GDRTYNLRDQ
201 KMVIPGIATA IERLLQGEEQ PLGNIVSSEP PAMPAFSANG EKGKAANYAG
251 GMSLQEALKQ NAAAGNIKIV AYPDTNSLLV KGTAEQVHFI EMLVKALDVA
301 KRHVELSLWI VDLNKSDLER LGTSWSGSIT IGDKLGVSLN QSSISTLDGS
351 RFIAAVNALE EKKQATVVSR PVLLTQENVP AIFDNNRTFY TKLIGERNVA
401 LEHVTYGTMI RVLPRFSADG QIEMSLDIED GNDKTPQSDT TTSVDALPEV
451 GRTLISTIAR VPHGKSLLVG GYTRDANTDT VQSIPFLGKL PLIGSLFRYS
501 SKNKSNVVRV FMIEPKEIVD PLTPDASESV NNILKQSGAW SGDDKLQKWV
551 RVYLDRGQEA IK
```

PrgH

Sequence Coverage: **29%** Unique Peptides: 16

```
  1 METSKEKTIT SPGPYIVRLL NSSLNGCEFP LLTGRTLFVV GQSDALTASG
 51 QLPDIPADSF FIPLDHGGVN FEIQVDTDAT EIILHELKEG NSESRSVQLN
101 TPIQVGELLI LIRPESEPWV PEQPEKLETS AKKNEPRFKN GIVAALAGFF
151 ILGIGTVGTL WILNSPQRQA AELDSLLGQE KERFQVLPGR DKMLYVAAQN
201 ERDTLWARQV LARGDYDKNA RVINENEENK RISIWLDTYY PQLAYYRIHF
251 DEPRKPVFWL SRQRNTMSKK ELEVLSQKLR ALMPYADSVN ITLMDDVTAA
301 GQAEAGLKQQ ALPYSRRNHK GGVTFVIQGA LDDVEILRAR QFVDSYYRTW
351 GGRYVQFAIE LKDDWLKGRS FQYGAEGYIK MSPGHWYFPS PL
```

PrgK

Sequence Coverage: **23%** Unique Peptides: 6

```
  1 MIRRYLYTFL LVMTLAGCKD KDLLKGLDQE QANEVIAVLQ MHNIEANKID
 51 SGKLGYSITV AEPDFTAAVY WIKTYQLPPR PRVEIAQMFP ADSLVSSPRA
101 EKARLYSAIE QRLEQSLQTM EGVLSARVHI SYDIDAGENG RPPKPVHLSA
151 LAVYERGSPL AHQISDIKRF LKNSFADVDY DNISVVLSER SDAQLQAPGT
201 PVKRNSFATS WIVLIILLSV MSAGFGVWYY KNHYARNKKG ITADDKAKSS
251 NE
```


Figure 17.1. Peptide coverage of NC and export apparatus proteins found in purified bases from Δ*spa* and Δ*spaP* strains. Peptides originating from NC ring proteins InvG, PrgH and PrgK, but no export apparatus proteins were identified.

ΔSpaQ

InvG

Sequence coverage: 56% Unique Peptides: 29

```
  1 MKTHILLARV LACAALVLVT PGYSSEKIPV TGSGFVAKDD SLRTFFDAMA
 51 LQLKEPVIVS KMAARKKITG NFEFHDPNAL LEKLSLQLGL IWYFDGQAIY
101 IYDASEMRNA VVSLRNVSLN EFNNFLKRSG LYNKNYPLRG DNRKGTFYVS
151 GPPVYVDMVV NAATMMDKQN DGIELGRQKI GVMRLNNTFV GDRTYNLRDQ
201 KMVIPGIATA IERLLQGEEQ PLGNIVSSEP PAMPAFSANG EKGKAANYAG
251 GMSLQEALKQ NAAAGNIKIV AYPDTNSLLV KGTAEQVHFI EMLVKALDVA
301 KRHVELSLWI VDLNKSDLER LGTSWSGSIT IGDKLGVSLN QSSISTLDGS
351 RFIAAVNALE EKKQATVVSR PVLLTQENVP AIFDNNRTFY TKLIGERNVA
401 LEHVTYGTMI RVLPRFSADG QIEMSLDIED GNDKTPQSDT TTSVDALPEV
451 GRTLISTIAR VPHGKSLLVG GYTRDANTDT VQSIPFLGKL PLIGSLFRYS
501 SKNKSNVVRV FMIEPKEIVD PLTPDASESV NNILKQSGAW SGDDKLQKWV
551 RVYLDRGQEA IK
```

PrgH

Sequence coverage: 64% Unique Peptides: 39

```
  1 METSKEKTIT SPGPYIVRLL NSSLNGCEFP LLTGRTLFVV GQSDALTASG
 51 QLPDIPADSF FIPLDHGGVN FEIQVDTDAT EIILHELKEG NSESRSVQLN
101 TPIQVGELLI LIRPESEPWV PEQPEKLETS AKKNEPRFKN GIVAALAGFF
151 ILGIGTVGTL WILNSPQRQA AELDSLLGQE KERFQVLPGR DKMLYVAAQN
201 ERDTLWARQV LARGDYDKNA RVINENEENK RISIWLDTYY PQLAYYRIHF
251 DEPRKPVFWL SRQRNTMSKK ELEVLSQKLR ALMPYADSVN ITLMDDVTAA
301 GQAEAGLKQQ ALPYSRRNHK GGVTFVIQGA LDDVEILRAR QFVDSYYRTW
351 GGRYVQFAIE LKDDWLKGRS FQYGAEGYIK MSPGHWYFPS PL
```

PrgK

Sequence coverage: 65% Unique Peptides: 18

```
  1 MIRRYLYTFL LVMTLAGCKD KDLLKGLDQE QANEVIAVLQ MHNIEANKID
 51 SGKLGYSITV AEPDFTAAVY WIKTYQLPPR PRVEIAQMFP ADSLVSSPRA
101 EKARLYSAIE QRLEQSLQTM EGVLSARVHI SYDIDAGENG RPPKPVHLSA
151 LAVYERGSPL AHQISDIKRF LKNSFADVDY DNISVVLSER SDAQLQAPGT
201 PVKRNSFATS WIVLIILLSV MSAGFGVWYY KNHYARNKKG ITADDKAKSS
251 NE
```

ΔSpaR

InvG

Sequence coverage: 39% Unique Peptides: 25

```
  1 MKTHILLARV LACAALVLVT PGYSSEKIPV TGSGFVAKDD SLRTFFDAMA
 51 LQLKEPVIVS KMAARKKITG NFEFHDPNAL LEKLSLQLGL IWYFDGQAIY
101 IYDASEMRNA VVSLRNVSLN EFNNFLKRSG LYNKNYPLRG DNRKGTFYVS
151 GPPVYVDMVV NAATMMDKQN DGIELGRQKI GVMRLNNTFV GDRTYNLRDQ
201 KMVIPGIATA IERLLQGEEQ PLGNIVSSEP PAMPAFSANG EKGKAANYAG
251 GMSLQEALKQ NAAAGNIKIV AYPDTNSLLV KGTAEQVHFI EMLVKALDVA
301 KRHVELSLWI VDLNKSDLER LGTSWSGSIT IGDKLGVSLN QSSISTLDGS
351 RFIAAVNALE EKKQATVVSR PVLLTQENVP AIFDNNRTFY TKLIGERNVA
401 LEHVTYGTMI RVLPRFSADG QIEMSLDIED GNDKTPQSDT TTSVDALPEV
451 GRTLISTIAR VPHGKSLLVG GYTRDANTDT VQSIPFLGKL PLIGSLFRYS
501 SKNKSNVVRV FMIEPKEIVD PLTPDASESV NNILKQSGAW SGDDKLQKWV
551 RVYLDRGQEA IK
```

PrgH

Sequence coverage: 63% Unique Peptides: 37

```
  1 METSKEKTIT SPGPYIVRLL NSSLNGCEFP LLTGRTLFVV GQSDALTASG
 51 QLPDIPADSF FIPLDHGGVN FEIQVDTDAT EIILHELKEG NSESRSVQLN
101 TPIQVGELLI LIRPESEPWV PEQPEKLETS AKKNEPRFKN GIVAALAGFF
151 ILGIGTVGTL WILNSPQRQA AELDSLLGQE KERFQVLPGR DKMLYVAAQN
201 ERDTLWARQV LARGDYDKNA RVINENEENK RISIWLDTYY PQLAYYRIHF
251 DEPRKPVFWL SRQRNTMSKK ELEVLSQKLR ALMPYADSVN ITLMDDVTAA
301 GQAEAGLKQQ ALPYSRRNHK GGVTFVIQGA LDDVEILRAR QFVDSYYRTW
351 GGRYVQFAIE LKDDWLKGRS FQYGAEGYIK MSPGHWYFPS PL
```

PrgK

Sequence coverage: 50% Unique Peptides: 16

```
  1 MIRRYLYTFL LVMTLAGCKD KDLLKGLDQE QANEVIAVLQ MHNIEANKID
 51 SGKLGYSITV AEPDFTAAVY WIKTYQLPPR PRVEIAQMFP ADSLVSSPRA
101 EKARLYSAIE QRLEQSLQTM EGVLSARVHI SYDIDAGENG RPPKPVHLSA
151 LAVYERGSPL AHQISDIKRF LKNSFADVDY DNISVVLSER SDAQLQAPGT
201 PVKRNSFATS WIVLIILLSV MSAGFGVWYY KNHYARNKKG ITADDKAKSS
251 NE
```

Figure 17. 2. Peptide coverage of NC and export apparatus proteins found in purified bases from *ΔspaQ* and *ΔspaR* strains.
Peptides originating from NC ring proteins InvG, PrgH and PrgK, but no export apparatus proteins were identified.

ΔSpaS

InvG

Sequence Coverage: **64%** Unique Peptides: 33

```
  1 MKTHILLARV LACAALVLVT PGYSSEKIPV TGSGFVAKDD SLRTFFDAMA
 51 LQLKEPVIVS KMAARKKITG NFEFHDPNAL LEKLSLQLGL IWYFDGQAIY
101 IYDASEMRNA VVSLRNVSLN EFNNFLKRSG LYNKNYPLRG DNRKGTFYVS
151 GPPVYVDMVV NAATMMDKQN DGIELGRQKI GVMRLNNTFV GDRTYNLRDQ
201 KMVIPGIATA IERLLQGEEQ PLGNIVSSEP PAMPAFSANG EKGKAANYAG
251 GMSLQEALKQ NAAAGNIKIV AYPDTNSLLV KGTAEQVHFI EMLVKALDVA
301 KRHVELSLWI VDLNKSDLER LGTSWSGSIT IGDKLGVSLN QSSISTLDGS
351 RFIAAVNALE EKKQATVVSR PVLLTQENVP AIFDNNRTFY TKLIGERNVA
401 LEHVTYGTMI RVLPRFSADG QIEMSLDIED GNDKTPQSDT TTSVDALPEV
451 GRTLISTIAR VPHGKSLLVG GYTRDANTDT VQSIPFLGKL PLIGSLFRYS
501 SKNKSNVVRV FMIEPKEIVD PLTPDASESV NNILKQSGAW SGDDKLQKWV
551 RVYLDRGQEA IK
```

PrgH

Sequence Coverage: **72%** Unique Peptides: 34

```
  1 METSKEKTIT SPGPYIVRLL NSSLNGCEFP LLTGRTLFVV GQSDALTASG
 51 QLPDIPADSF FIPLDHGGVN FEIQVDTDAT EIILHELKEG NSESRSVQLN
101 TPIQVGELLI LIRPESEPWV PEQPEKLETS AKKNEPRFKN GIVAALAGFF
151 ILGIGTVGTL WILNSPQRQA AELDSLLGQE KERFQVLPGR DKMLYVAAQN
201 ERDTLWARQV LARGDYDKNA RVINENEENK RISIWLDTYY PQLAYYRIHF
251 DEPRKPVFWL SRQRNTMSKK ELEVLSQKLR ALMPYADSVN ITLMDDVTAA
301 GQAEAGLKQQ ALPYSRRNHK GGVTFVIQGA LDDVEILRAR QFVDSYYRTW
351 GGRYVQFAIE LKDDWLKGRS FQYGAEGYIK MSPGHWYFPS PL
```

PrgK

Sequence Coverage: **53%** Unique Peptides: 16

```
  1 MIRRYLYTFL LVMTLAGCKD KDLLKGLDQE QANEVIAVLQ MHNIEANKID
 51 SGKLGYSITV AEPDFTAAVY WIKTYQLPPR PRVEIAQMFP ADSLVSSPRA
101 EKARLYSAIE QRLEQSLQTM EGVLSARVHI SYDIDAGENG RPPKPVHLSA
151 LAVYERGSPL AHQISDIKRF LKNSFADVDY DNISVVLSER SDAQLQAPGT
201 PVKRNSFATS WIVLIILLSV MSAGFGVWYY KNHYARNKKG ITADDKAKSS
251 NE
```

SpaP

Sequence Coverage: **22%** Unique Peptides: 8

```
  1 MGNDISLIAL LAFSTLLPFI IASGTCFVKF SIVFVMVRNA LGLQQIPSNM
 51 TLNGVALLLS MFVMWPIMHD AYVYFEDEDV TFNDISSLSK HVDEGLDGYR
101 DYLIKYSDRE LVQFFENAQL KRQYGEETET VKRDKDEIEK PSIFALLPAY
151 ALSEIKSAFK IGFYLYLPFV VVDLVVSSVL LALGMMMMSP VTISTPIKLV
201 LFVALDGWTL LSKGLILQYM DIAT
```

InvA

Sequence Coverage: **14%** Unique Peptides: 9

```
  1 MLLSLLNSAR LRPELLILVL MVMIISMFVI PLPTYLVDFL IALNIVLAIL
 51 VFMGSFYIDR ILSFSTFPAV LLITTLFRLA LSISTSRLIL IEADAGEIIA
101 TFGQFVIGDS LAVGFVVFSI VTVVQFIVIT KGSERVAEVA ARFSLDGMPG
151 KQMSIDADLK AGIIDADAAR ERRSVLERES QLYGSFDGAM KFIKGDAIAG
201 IIIIFVNFIG GISVGMTRHG MDLSSALSTY TMLTIGDGLV AQIPALLIAI
251 SAGFIVTRVN GDSDNMGRNI MTQLLNNPFV LVVTAILTIS MGTLPGFPLP
301 VFVILSVVLS VLFYFKFREA KRSAAKPKTS KGEQPLSIEE KEGSSLGLIG
351 DLDKVSTETV PLILLVPKSR REDLEKAQLA ERLRSQFFID YGVRLPEVLL
401 RDGEGLDDNS IVLLINEIRV EQFTVYFDLM RVVNYSDEVV SFGINPTIHQ
451 QGSSQYFWVT HEEGEKLREL GYVLRNALDE LYHCLAVTLA RNVNEYFGIQ
501 ETKHMLDQLE AKFPDLLKEV LRHATVQRIS EVLQRLLSER VSVRNMKLIM
551 EALALWAPRE KDVINLVEHI RGAMARYICH KFANGGELRA VMVSAEVEDV
601 IRKGIRQTSG STFLSLDPEA SANLMDLITL KLDDLLIAHK DLVLLTSVDV
651 RRFIKKMIEG RFPDLEVLSF GEIADSKSVN VIKT
```


Figure 17. 3. Peptide coverage of NC and export apparatus proteins found in purified bases from ΔSpaS strain. Peptides originating from NC ring proteins InvG, PrgH and PrgK as well as export apparatus proteins SpaP and InvA were identified. Peptides from SpaQ and SpaR were not detected.

ΔInvA

InvG

Sequence Coverage: **35%** Unique Peptides: **20**

```
  1 MKTHILLARV LACAALVLVT PGYSSEKIPV TGSGFVAKDD SLRTFFDAMA
 51 LQLKEPVIVS KMAARKKITG NFEFHDPNAL LEKLSLQLGL IWYFDGQAIY
101 IYDASEMRNA VVSLRNVSLN EFNNFLKRSG LYNKNYPLRG DNRKGTFYVS
151 GPPVYVDMVV NAATMMDKQN DGIELGRQKI GVMRLNNTFV GDRTYNLRDQ
201 KMVIPGIATA IERLLQGEEQ PLGNIVSSEP PAMPAFSANG EKGKAANYAG
251 GMSLQEALKQ NAAAGNIKIV AYPDTNSLLV KGTAEQVHFI EMLVKALDVA
301 KRHVELSLWI VDLNKSDLER LGTSWSGSIT IGDKLGVSLN QSSISTLDGS
351 RFIAAVNALE EKKQATVVSR PVLLTQENVP AIFDNNRTFY TKLIGERNVA
401 LEHVTYGTMI RVLPRFSADG QIEMSLDIED GNDKTPQSDT TTSVDALPEV
451 GRTLISTIAR VPHGKSLLVG GYTRDANTDT VQSIPFLGKL PLIGSLFRYS
501 SKNKSNVVRV FMIEPKEIVD PLTPDASESV NNILKQSGAW SGDDKLQKWV
551 RVYLDRGQEA IK
```

PrgH

Sequence Coverage: **53%** Unique Peptides: **32**

```
  1 METSKEKTIT SPGPYIVRLL NSSLNGCEFP LLTGRTLFVV GQSDALTASG
 51 QLPDIPADSF FIPLDHGGVN FEIQVDTDAT EIILHELKEG NSESRSVQLN
101 TPIQVGELLI LIRPESEPWV PEQPEKLETS AKKNEPRFKN GIVAALAGFF
151 ILGIGTVGTL WILNSPQRQA AELDSLLGQE KERFQVLPGR DKMLYVAAQN
201 ERDTLWARQV LARGDYDKNA RVINENEENK RISIWLDTYY PQLAYYRIHF
251 DEPRKPVFWL SRQRNTMSKK ELEVLSQKLR ALMPYADSVN ITLMDDVTAA
301 GQAEAGLKQQ ALPYSRRNHK GGVTFVIQGA LDDVEILRAR QFVDSYYRTW
351 GGRYVQFAIE LKDDWLKGRS FQYGAEGYIK MSPGHWYFPS PL
```

PrgK

Sequence Coverage: **35%** Unique Peptides: **11**

```
  1 MIRRYLYTFL LVMTLAGCKD KDLLKGLDQE QANEVIAVLQ MHNIEANKID
 51 SGKLGYSITV AEPDFTAAVY WIKTYQLPPR PRVEIAQMFP ADSLVSSPRA
101 EKARLYSAIE QRLEQSLQTM EGVLSARVHI SYDIDAGENG RPPKPVHLSA
151 LAVYERGSPL AHQISDIKRF LKNSFADVDY DNISVVLSER SDAQLQAPGT
201 PVKRNSFATS WIVLIILLSV MSAGFGVWYY KNHYARNKKG ITADDKAKSS
251 NE
```

SpaP

Sequence Coverage: **12%** Unique Peptides: **4**

```
  1 MGNDISLIAL LAFSTLLPFI IASGTCFVKF SIVFVMVRNA LGLQQIPSNM
 51 TLNGVALLLS MFVMWPIMHD AYVYFEDEDV TFNDISSLSK HVDEGLDGYR
101 DYLIKYSDRE LVQFFENAQL KRQYGEETET VKRDKDEIEK PSIFALLPAY
151 ALSEIKSAFK IGFYLYLPFV VVDLVVSSVL LALGMMMMSP VTISTPIKLV
201 LFVALDGWTL LSKGLILQYM DIAT
```

SpaS

Sequence Coverage: **6%** Unique Peptides: **2**

```
  1 MSSNKTEKPT KKRLEDSAKK GQSFKSKDLI IACLTLGGIA YLVSYGSFNE
 51 FMGIIKIIIA DNFDQSMADY SLAVFGIGLK YLIPFMLLCL VCSALPALLQ
101 AGFVLATEAL KPNLSALNPV EGAKKLFSMR TVKDTVKTLL YLSSFVVAAI
151 ICWKKYKVEI FSQLNGNIVG IAVIWRELLL ALVLTCLACA LIVLLLDAIA
201 EYFLTMKDMK MDKEEVKREM KEQEGNPEVK SKRREVHMEI LSEQVKSDIE
251 NSRLIVANPT HITIGIYFKP ELMPIPMISV YETNQRALAV RAYAEKVGVP
301 VIVDIKLARS LFKTHRRYDL VSLEEIDEVL RLLVWLEEVE NAGKDVIQPQ
351 ENEVRH
```

Figure 17. 4. Peptide coverage of NC and export apparatus proteins found in purified bases from Δ*invA* strain. Peptides originating from NC ring proteins InvG, PrgH and PrgK as well as export apparatus proteins SpaP and SpaS were identified. Peptides from SpaQ and SpaR were not detected.

ΔInvC

InvG

Sequence Coverage: 64% Unique Peptides: 38

```
  1 MKTHILLARV LACAALVLVT PGYSSEKIPV TGSGFVAKDD SLRTFFDAMA
 51 LQLKEPVIVS KMAARKKITG NFEFHDPNAL LEKLSLQLGL IWYFDGQAIY
101 IYDASEMRNA VVSLRNVSLN EFNNFLKRSG LYNKNYPLRG DNRKGTFYVS
151 GPPVYVDMVV NAATMMDKQN DGIELGRQKI GVMRLNNTFV GDRTYNLRDQ
201 KMVIPGIATA IERLLQGEEQ PLGNIVSSEP PAMPAFSANG EKGKAANYAG
251 GMSLQEALKQ NAAAGNIKIV AYPDTNSLLV KGTAEQVHFI EMLVKALDVA
301 KRHVELSLWI VDLNKSDLER LGTSWSGSIT IGDKLGVSLN QSSISTLDGS
351 RFIAAVNALE EKKQATVVSR PVLLTQENVP AIFDNNRTFY TKLIGERNVA
401 LEHVTYGTMI RVLPRFSADG QIEMSLDIED GNDKTPQSDT TTSVDALPEV
451 GRTLISTIAR VPHGKSLLVG GYTRDANTDT VQSIPFLGKL PLIGSLFRYS
501 SKNKSNVVRV FMIEPKEIVD PLTPDASESV NNILKQSGAW SGDDKLQKWV
551 RVYLDRGQEA IK
```

PrgH

Sequence Coverage: 97% Unique Peptides: 49

```
  1 METSKEKTIT SPGPYIVRLL NSSLNGCEFP LLTGRTLFVV GQSDALTASG
 51 QLPDIPADSF FIPLDHGGVN FEIQVDTDAT EIILHELKEG NSESRSVQLN
101 TPIQVGELLI LIRPESEPWV PEQPEKLETS AKKNEPRFKN GIVAALAGFF
151 ILGIGTVGTL WILNSPQRQA AELDSLLGQE KERFQVLPGR DKMLYVAAQN
201 ERDTLWARQV LARGDYDKNA RVINENEENK RISIWLDTYY PQLAYYRIHF
251 DEPRKPVFWL SRQRNTMSKK ELEVLSQKLR ALMPYADSVN ITLMDDVTAA
301 GQAEAGLKQQ ALPYSRRNHK GGVTFVIQGA LDDVEILRAR QFVDSYYRTW
351 GGRYVQFAIE LKDDWLKGRS FQYGAEGYIK MSPGHWYFPS PL
```

PrgK

Sequence Coverage: 78% Unique Peptides: 24

```
  1 MIRRYLYTFL LVMTLAGCKD KDLLKGLDQE QANEVIAVLQ MHNIEANKID
 51 SGKLGYSITV AEPDFTAAVY WIKTYQLPPR PRVEIAQMFP ADSLVSSPRA
101 EKARLYSAIE QRLEQSLQTM EGVLSARVHI SYDIDAGENG RPPKPVHLSA
151 LAVYERGSPL AHQISDIKRF LKNSFADVDY DNISVVLSER SDAQLQAPGT
201 PVKRNSFATS WIVLIILLSV MSAGFGVWYY KNHYARNKKG ITADDKAKSS
251 NE
```

SpaP

Sequence Coverage: 97% Unique Peptides: 11

```
  1 MGNDISLIAL LAFSTLLPFI IASGTCFVKF SIVFVMVRNA LGLQQIPSNM
 51 TLNGVALLLS MFVMWPIMHD AYVYFEDEDV TFNDISSLSK HVDEGLDGYR
101 DYLIKYSDRE LVQFFENAQL KRQYGEETET VKRDKDEIEK PSIFALLPAY
151 ALSEIKSAFK IGFYLYLPFV VVDLVVSSVL LALGMMMMSP VTISTPIKLV
201 LFVALDGWTL LSKGLILQYM DIAT
```

SpaS

Sequence Coverage: 2% Unique Peptides: 1

```
  1 MSSNKTEKPT KKRLEDSAKK GQSFKSKDLI IACLTLGGIA YLVSYGSFNE
 51 FMGIIKIIIA DNFDQSMADY SLAVFGIGLK YLIPFMLLCL VCSALPALLQ
101 AGFVLATEAL KPNLSALNPV EGAKKLFSMR TVKDTVKTLL YLSSFVVAAI
151 ICWKKYKVEI FSQLNGNIVG IAVIWRELLL ALVLTCLACA LIVLLLDAIA
201 EYFLTMKDMK MDKEEVKREM KEQEGNPEVK SKRREVHMEI LSEQVKSDIE
251 NSRLIVANPT HITIGIYFKP ELMPIPMISV YETNQRALAV RAYAEKVGVP
301 VIVDIKLARS LFKTHRRYDL VSLEEIDEVL RLLVWLEEVE NAGKDVIQPQ
351 ENEVRH
```

InvA

Sequence Coverage: 17% Unique Peptides: 10

```
  1 MLLSLLNSAR LRPELLILVL MVMIISMFVI PLPTYLVDFL IALNIVLAIL
 51 VFMGSFYIDR ILSFSTFPAV LLITTLFRLA LSISTSRLIL IEADAGEIIA
101 TFGQFVIGDS LAVGFVVFSI VTVVQFIVIT KGSERVAEVA ARFSLDGMPG
151 KQMSIDADLK AGIIDADAAR ERRSVLERES QLYGSFDGAM KFIKGDAIAG
201 IIIIFVNFIG GISVGMTRHG MDLSSALSTY TMLTIGDGLV AQIPALLIAI
251 SAGFIVTRVN GDSDNMGRNI MTQLLNNPFV LVVTAILTIS MGTLPGFPLP
301 VFVILSVVLS VLFYFKFREA KRSAAKPKTS KGEQPLSIEE KEGSSLGLIG
351 DLDKVSTETV PLILLVPKSR REDLEKAQLA ERLRSQFFID YGVRLPEVLL
401 RDGEGLDDNS IVLLINEIRV EQFTVYFDLM RVVNYSDEVV SFGINPTIHQ
451 QGSSQYFWVT HEEGEKLREL GYVLRNALDE LYHCLAVTLA RNVNEYFGIQ
501 ETKHMLDQLE AKFPDLLKEV LRHATVQRIS EVLQRLLSER VSVRNMKLIM
551 EALALWAPRE KDVINLVEHI RGAMARYICH KFANGGELRA VMVSAEVEDV
601 IRKGIRQTSG STFLSLDPEA SANLMDLITL KLDDLLIAHK DLVLLTSVDV
651 RRFIKKMIEG RFPDLEVLSF GEIADSKSVN VIKT
```

Figure 17. 5. Peptide coverage of NC and export apparatus proteins found in purified bases from Δ*invC* strain. Peptides originating from NC ring proteins InvG, PrgH and PrgK as well as export apparatus proteins SpaP, SpaS and were identified. Peptides from SpaQ and SpaR were not detected.

6.4. Approaches to localize InvA and SpaS within the NC structure

InvA and SpaS homologs were subject to a variety of studies revealing interaction between their C-terminal domains as well as interaction with cytoplasmic proteins such as the ATPase (Zhu et al. 2002, VanArnam et al. 2004). These findings prompted us to investigate InvA and SpaS association with the NC for future structural analysis and localization studies.

6.4.1. InvA is associated with the NC

InvA was suggested to be more weakly associated to the NC than SpaS (Wagner et al. 2010). Although it was possible to pull down NCs by immunoprecipitation with an antibody targeted against the FLAG-tag on InvA C-terminus (strain SB1906), the purified sample included a minor fraction of free InvA not incorporated into the NC as shown by Blue Native-PAGE analysis. A loose attachment of InvA would imply that conventionally purified NCs do not all contain InvA or at least not the same amount and are therefore structurally heterogeneous, making it more difficult to localize and perform structural analysis on such complexes.

Thus, InvA association with the NC was reinvestigated by starting with the immunoprecipitation of InvA-FLAG, but under slightly different conditions than published by Wagner et al. 2010 (see Methods). Either purified NC or DDM-solubilized membranes were used as input for the immunoprecipitaion. DDM was reported to have little impact on InvA disassociation. As judged by negative stain EM and immunoblotting, both methods yielded a similar amount of NC (Fig. 18). Further analysis of the InvA containing elution fraction by sucrose gradient centrifugation revealed free InvA-FLAG in addition to NC incorporated InvA-FLAG, which is in agreement with the prior observation of Wagner et al. 2010 (Fig. 19). Thus, one could argue that the free InvA fraction represents free InvA abundant in the solubilized membrane. On the other hand, the same experiment was performed with NCs purified by CsCl (density) and sucrose gradient (size), which also contained free InvA-FLAG. Taken together, this suggests that InvA is loosely attached to the NC and dissociates from the complex in the process of subsequent purification.

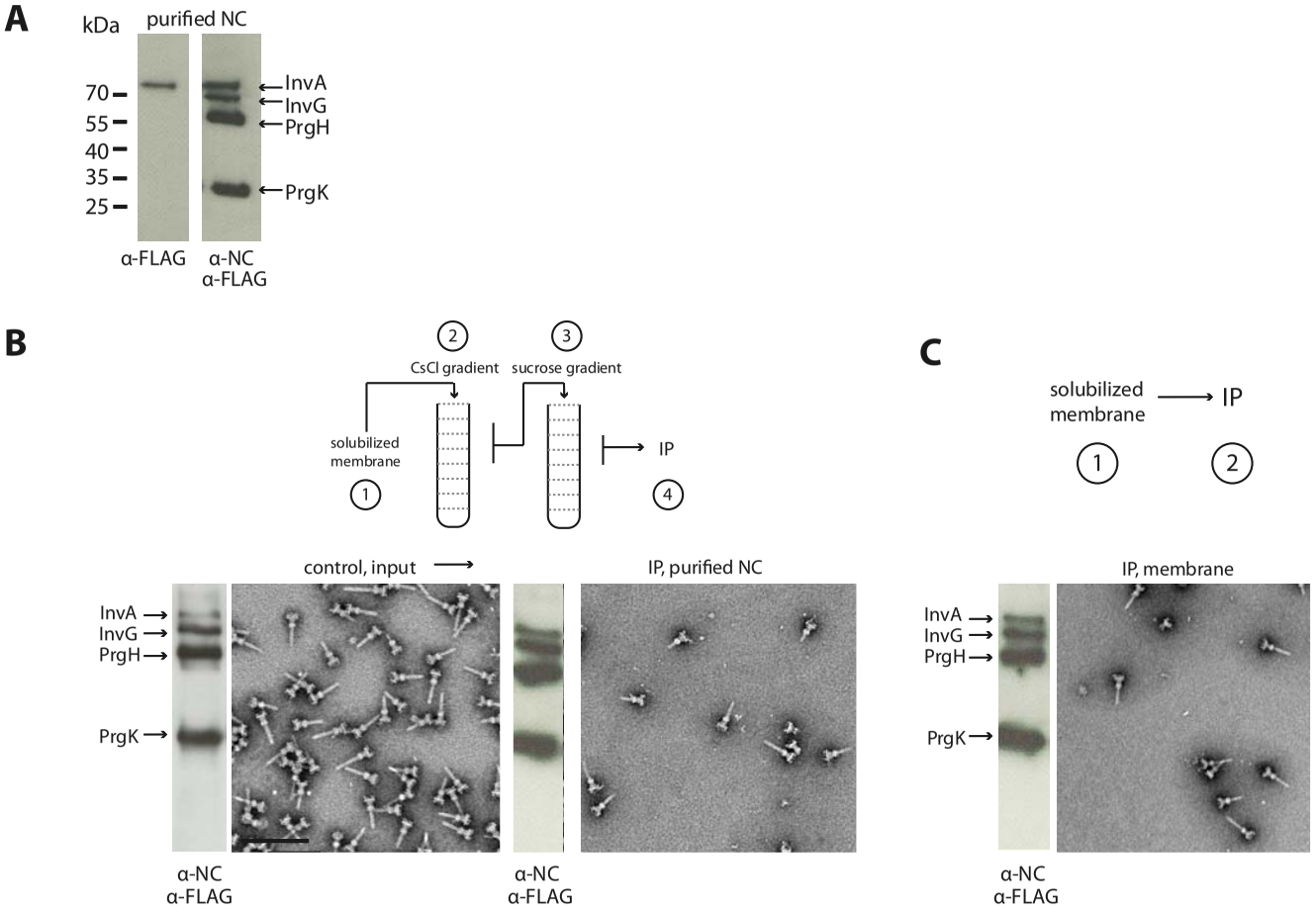

Figure 18. Purification of NC containing InvA-FLAG. (A) Purified NC was analyzed by immunoblotting and sequentially incubated with anti-FLAG and anti-NC antibody to detect InvA-FLAG and NC proteins respectively. **(B)** Purified NC (CsCl/sucrose) was diluted 1:30 and negatively stained (positive control). The fraction was analyzed by immunoblotting with anti-NC antibody and anti-FLAG antibody. NC was immunoprecipitated (IP) from purified NC and and negatively stained. 20 µl of the elution fraction were analyzed by immunoblotting with anti-NC antibody and anti-FLAG antibody. **(C)** NC was immunoprecipitated from solubilized membrane fraction; elution fraction 1 was negatively stained and 20 µl of the same fraction were used for immunoblotting with anti-NC antibody and anti-FLAG antibody. Bar = 100nm.

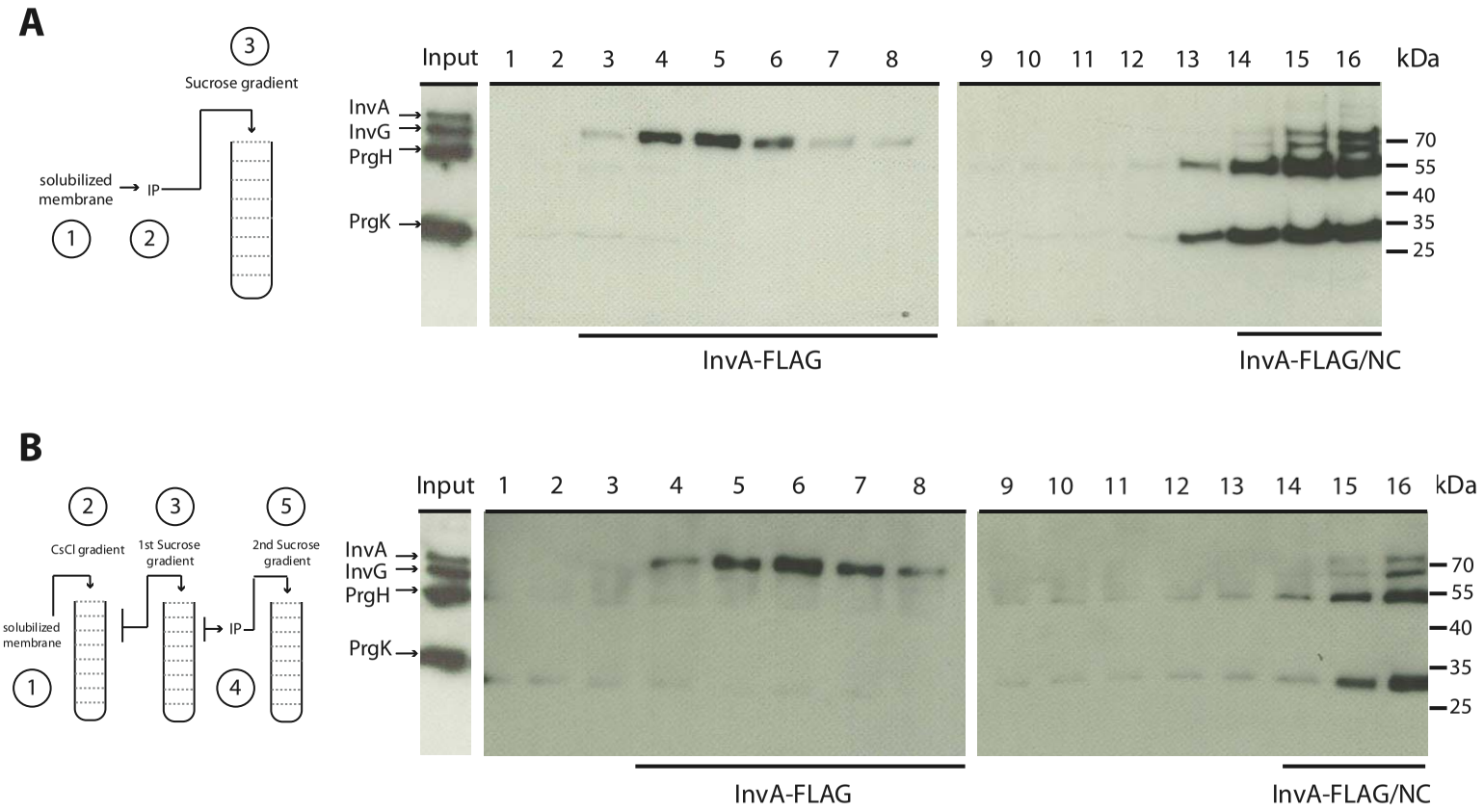

Figure 19. InvA-FLAG is weakly associated to the NC. (A) NC was purified by immunoprecipitation (IP) of InvA-FLAG from DDM-solubilized membrane fraction and loaded on a sucrose gradient (10-25% sucrose w/v). InvA-FLAG was detected in fractions 3 to 8, with peak fractions 4 to 6. NC and incorporated InvA-FLAG were found in fractions 14 to 16. **(B)** NC was immunoprecipitated from purified NC (CsCl/sucrose gradient), with LDAO as detergent and was loaded on a sucrose gradient (10-25% sucrose w/v). InvA-FLAG was detected in fractions 4 to 8, with peak fractions 5 to 7. NC and incorporated InvA-FLAG were found in fractions 14 to 16.

Neither the conventional NC purification nor the immunoprecipitation from purified NC/ membrane are therefore appropriate to obtain a homogenous InvA containing NC sample suitable to be used for structural studies.

6.4.2. SpaS is more tightly associated to the NC than InvA

SpaS undergoes auto-cleavage and is proposed to mediate a switch in the substrate secretion profile of the T3SS (Zarivach et al. 2008). To prevent this switch and the following C-terminal cleavage, an autocatalytic mutant was used for tagging SpaS at the C-terminus (SpaS-N258A FLAG, SB1769). It was shown that its functionality is reduced to secretion of early substrates such as PrgJ, PrgI and InvJ, thus the strain is still able to build up fully assembled NCs (Fig. 20).

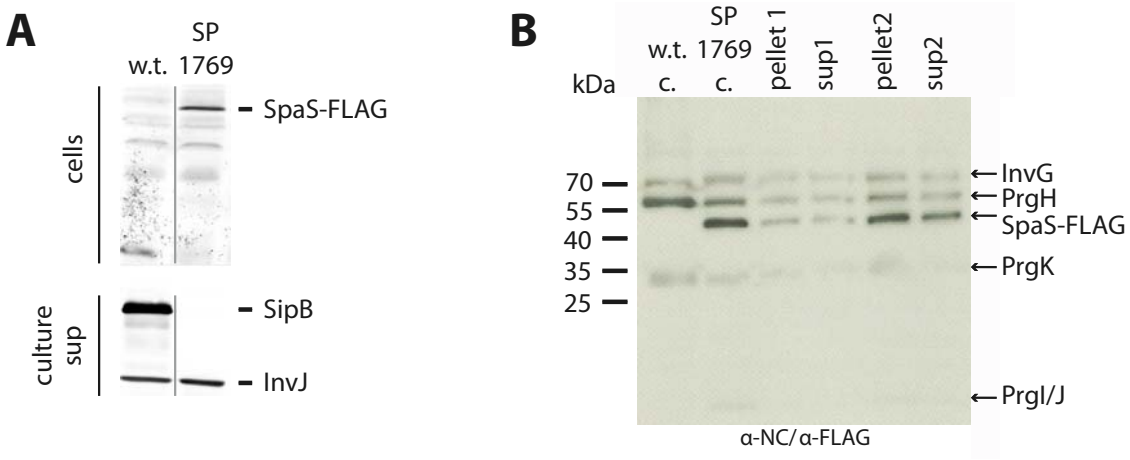

Figure 20. SpaS-FLAG strain (SP1769 - switch mutant) is functional and NCs containing SpaS-FLAG can be purified. (A) SpaS-FLAG could be detected by anti-FLAG antibody in SpaS-FLAG strain SP1769 cells (top). The mutant strain was functional for secretion of an early substrate like InvJ, found in the precipitated culture supernatant by immunoblotting (culture sup, bottom), but no secretion of SipB was detected (late substrate). Immunoblot was kindly provided by Samuel Wagner. **(B)** Purification steps before immunoprecipitation of SpaS-FLAG; pellet1 and sup1 originated from the first centrifugation step to remove cell debris, whereas pellet2 and sup2 resulted from the subsequent ultracentrifugation step (see Methods). SpaS-FLAG was detected through the whole purification. Pellet2 was solubilized and further used as immunoprecipitation input.

At first, SpaS-FLAG containing NCs were purified applying our conventional purification protocol. As shown in Figure 20, SpaS-FLAG was detected throughout the entire purification procedure and was not lost upon detergent treatment and ultracentrifugation as reported previously (Wagner et al. 2010). In order to obtain a homogenous sample of SpaS-FLAG containing NCs, NCs were immunoprecipitated either from purified NC or from the solubilized membrane fraction and the elution fractions were compared with each other by negative stain imaging and immunoblotting (Fig. 21). In both cases it was possible to pull down NCs, however, pull-down from the membrane fraction was more efficient than pull-down from purified NC.

The elution fraction (input = membrane) was further analyzed by sucrose gradient centrifugation to test whether SpaS-FLAG dissociated from the complex similarly to InvA-FLAG. Consistent with the observation of Wagner et al. (2010), SpaS-FLAG was only detected within the NC containing fraction (Fig. 22, fraction 14, 15), which is in sharp contrast to InvA. Although membrane was used as input for the experiment, free SpaS-FLAG was not detected, suggesting that all SpaS is incorporated into NCs at the starting point of the purification. These results indicate that SpaS is more tightly associated to the NC than InvA, at least at the time before switching substrate specificity.

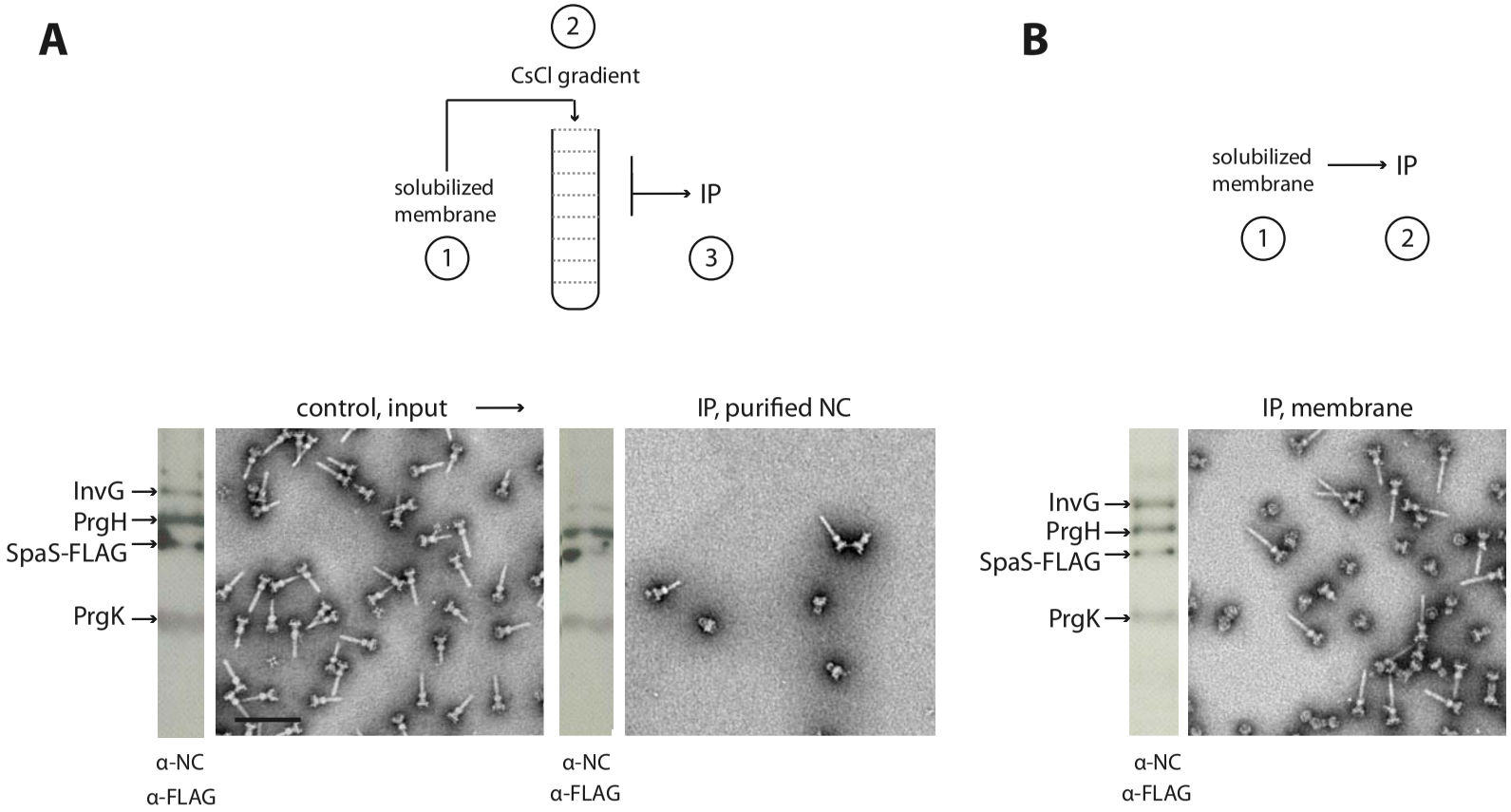

Figure 21. Purifcation of NC containing SpaS-FLAG followed by EM. (A) NCs containing SpaS-FLAG were purified via gradient centrifugation, fraction 4 was negatively stained and SpaS-FLAG and NC proteins were detected via immublotting (control, input). NC was immunoprecipitated (IP) from purified NC and 20µl of the elution fraction were analyzed by immunoblotting against SpaS-FLAG and NC; the same fraction was negatively stained. **(B)** NC was immunoprecipitated from solubilized membrane fraction; 10µl of the elution fraction were analyzed by immublotting against SpaS-FLAG and NC and was negatively stained. Bar = 100nm.

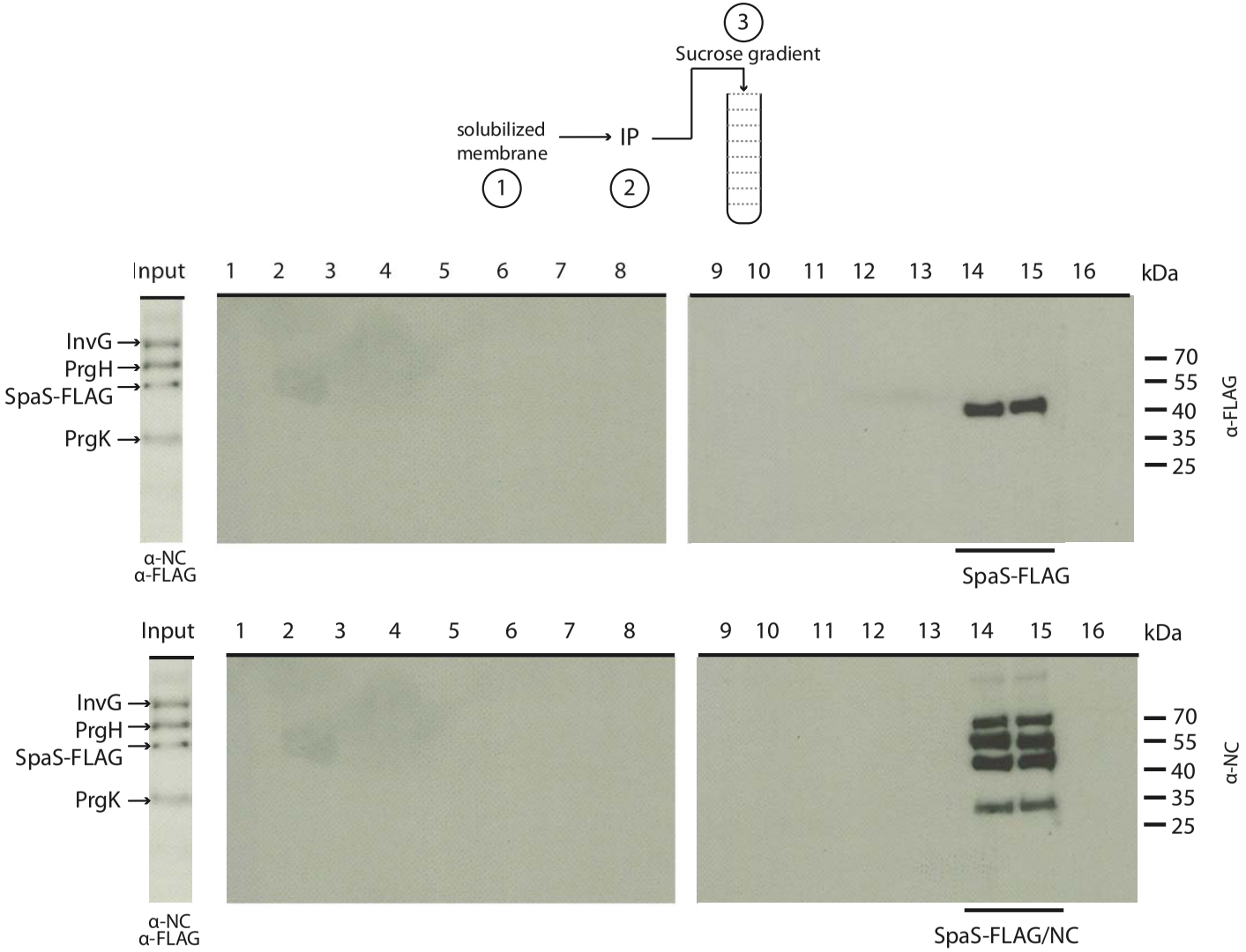

Figure 22. SpaS-FLAG is associated with the NC. NC was purified by immunoprecipitation (IP) of SpaS-FLAG from LDAO-solubilized membrane fraction and loaded on a sucrose gradient (10-25% sucrose w/v). NC and incorporated SpaS-FLAG were found in fractions 14 and 15.

6.4.3. SpaS is incorporated into bases and NCs

SpaS incorporation was moreover confirmed by the quantification of SpaS-FLAG immunoprecipitation. Here, relative amounts of PrgH, InvG (= NC standards) and SpaS-FLAG from the input fraction (= 100%) were compared to the amounts found in the elution fraction (Fig. 23). There was no significant enrichment of SpaS-FLAG, which supported the previous finding that in this experiment starting material NCs consist of mostly SpaS-FLAG. Furthermore these results indicate that SpaS is a structural component of bases and NCs and support a model in which SpaS is incorporated into the complex early in its assembly.

6.4.4. Immunoprecipitated SpaS-FLAG complexes are structurally different to conventionally purified wild type complexes

SpaS-FLAG immunoprecipitation could be optimized and SpaS-FLAG was shown to be stably incorporated into the NC. Therefore the sample could be used for further structural analysis. Eluted NCs and bases (Fig. 24A) were vitrified and used for cryo-EM and single particle analysis.

The structural analysis revealed that SpaS-FLAG-complexes are different from w.t. in certain areas of the complex (cup, OR1, IR2) (Fig. 24B). In particular, densities at the cup are more pronounced when compared to w.t., indicating that this additional density most likely originates from the uncleaved C-terminal SpaS-FLAG peptide and/or from an impairment of conformational changes at the cup. Structural deviations observed in other parts of the complex (OR1, IR2), which are composed of the outer membrane protein InvG or the cytoplasmically localized domains of PrgH and PrgK, emerged most likely as the result of different experimental conditions (immunoprecipitation) during which the activity of the detergent LDAO is less active compared to complex purifications using salt (CsCl) gradients.

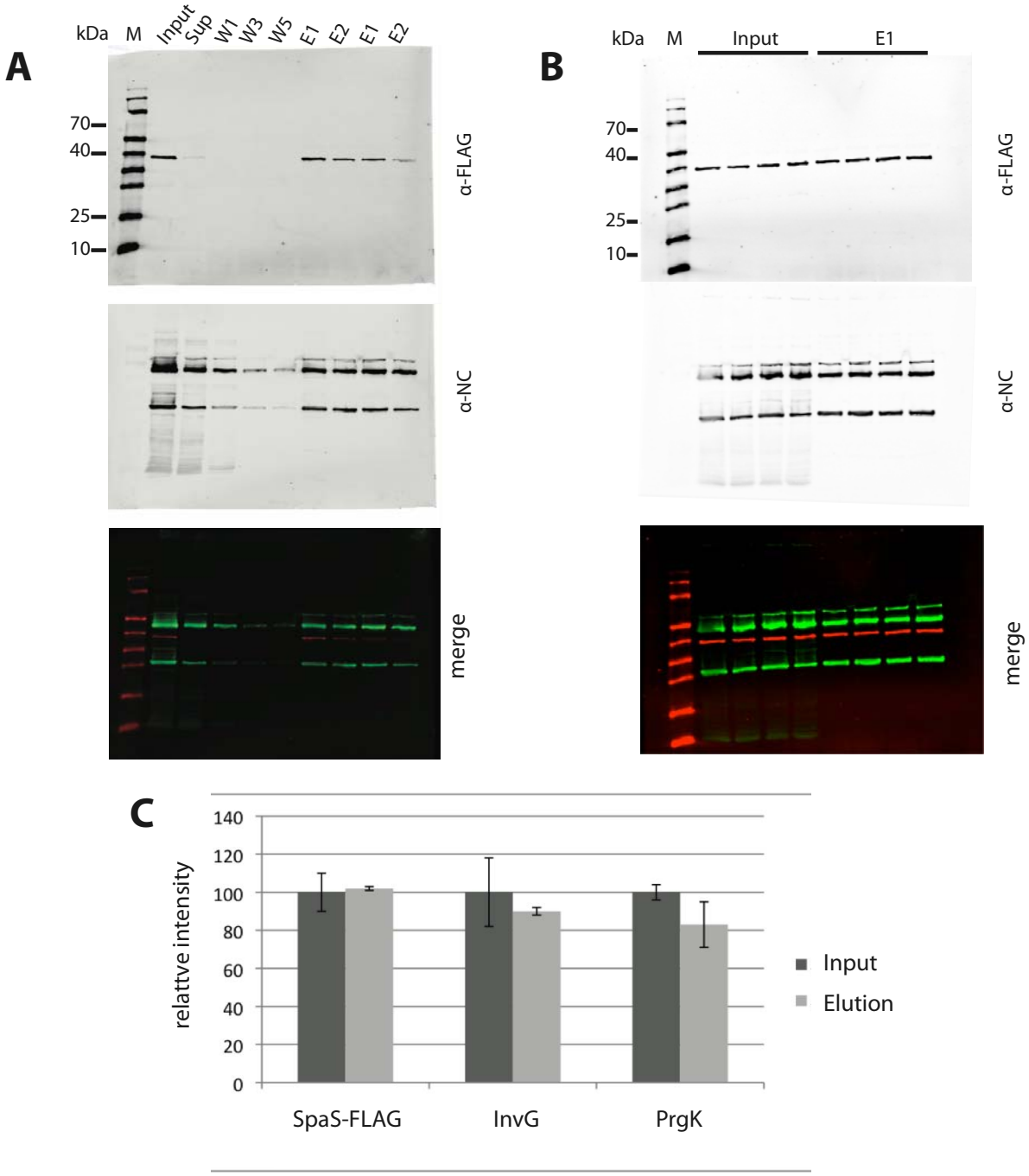

Figure 23. The majority of NC and bases contain SpaS-FLAG. (A) Purification steps during immunoprecipitaion (IP); input, supernatant (Sup), wash 1 (W1), wash 3 (W3), wash 5 (W5), elution fraction 1 (E1), elution fraction 2 (E2). M = marker. SpaS-FLAG can be used to pull down NC. **(B)** Immunoblot used for IP quantification (four replicates of equal volume of input and elution fraction, respectively). **(C)** Quantification of relative amounts of protein found in input fraction compaired to elution fraction using the Licor Odyssey quantification tool; PrgK and InvG were used as inner standards. The relative amount of SpaS-FLAG containing NCs is not significantly enriched by IP, standard deviations were calculated from four individual lanes with equal amount of sample.

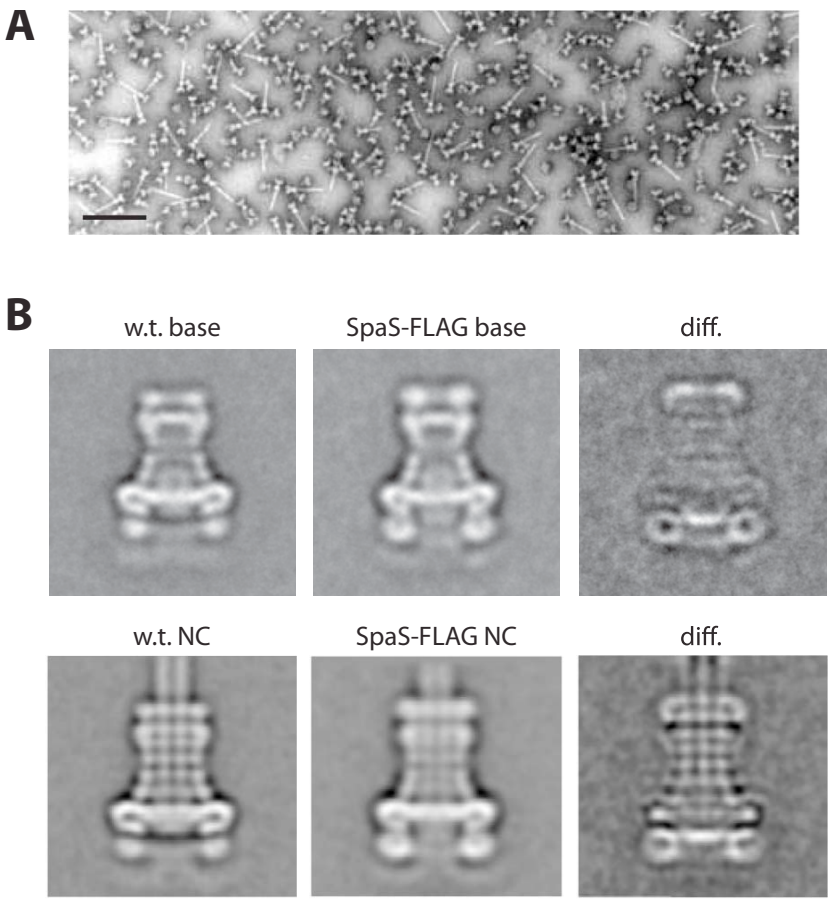

Figure 24. Single particle analysis of SpaS-FLAG containing bases and NCs reveals structural differences to w.t. (A) Elution fraction containing bases and NCs were negatively stained and the same sample was subsequently vitrified for cryo-EM. **(B)** Class averages of w.t. compared to SpaS-FLAG complexes, NCs as well as bases, are shown. By looking at the corresponding difference map (diff.) the structural variation becomes visible in upper/lower rings and cup region.

6.5. The ATPase InvC is not required to build up cup and socket region

The secretion process via the T3SS is energized by the ATPase InvC, which is involved in recognizing and unfolding of substrates prior to translocation, consequently required for the rod and needle filament formation (Sukhan et al. 2001, Galan and Wolf-Watz 2006). InvC is not part of the inner membrane proteins but has been shown to be a peripherally associated to the membrane (Akeda and Galan 2005).

In order to investigate the role of InvC in building up cup and socket region, bases from a strain lacking InvC (Δ*invC*, SB917) were purified. These bases are as stable as w.t. upon negative stain treatment, indicating that they contain cup and socket (Fig. 13. 2., left panel). Cryo-EM and single particle analyses were performed as for the other Δ*spa*/Δ*invA* mutant strains. As the stable core structure implied, the resulting class averages indeed revealed a filled-base phenotype for ΔInvC bases (Fig. 13. 2., right panel). These results indicate that InvC is not involved in building up a cup and socket region, supporting the idea that cup and socket are formed at an early point during assembly.

VII DISCUSSION AND PERSPECTIVES

VII. Discussion and Perspectives

7.1. Export apparatus - a defined structure within the NC?

The inner membrane proteins SpaP, SpaQ, SpaR, SpaS and InvA were termed export apparatus relating to their functional implication during secretion. But also the other membrane proteins, InvG, PrgH and PrgK are essential for T3S and therefore a functional assignment is not enough to define the export apparatus as such.

It has been suggested many times in literature, that the export apparatus could be located within the cup and socket region of the NC (Blocker et al. 2001, Zenk et al. 2007, Wagner et al. 2010). Thus, a structural approach could aid with showing whether they build a defined complex within the NC.

Studying InvA revealed disassociation of the protein during the applied purification procedure suggesting that it is most likely weakly associated to the NC. However, it is probable that InvA needs additional stabilizing proteins present in vivo. A potential group of proteins are known interaction partners from the flagellar system, such as OrgB, InvI or InvC (Zhu et al. 2002). OrgB has been shown to be a part of the sorting platform (Lara-Tejero et al. 2011), implying that InvA could be also involved in substrate selection and/or transport.

SpaS on the other hand is an integral component of bases and NCs, yet the ΔSpa mutant bases contained filled bases indistinguishable from w.t. and an empty base populations. Taking into account, that the stoichiometry of SpaS is still unknown and assuming a rather low abundance and flexible C-terminal regions it is likely that it cannot be seen in the current structure of the NC, explaining the w.t.-like base structures. The empty base population might indicate a minor cooperative role of SpaS on the assembly of cup and socket.

The fact, that SpaP is present in all the filled base mutants strengthens the hypothesis that at least SpaP could be part of cup and socket. SpaP, SpaQ and SpaR were shown to build subcomplexes and were detected in the w.t. NC sample, therefore it is still probable that SpaQ and SpaR are present within the filled bases of Δ*invA* and Δ*spaS* but are just not detected.

Whether cup and socket are the structures defining the export apparatus, remains to be formally demonstrated. Nevertheless, we could provide with the initial tools to investigate the export apparatus proteins regarding their influence on the NC structure as well as the basis for future structural analysis of the export apparatus.

7.2. The involvement of export apparatus proteins and InvC in the assembly of the NC

The pipeline of T3SS assembly has been investigated by different approaches in different model organisms and homologous systems (Jones et al. 1990, Kubori et al. 2000, Sukhan et al. 2001). Among those studies, genetic analysis have shown that depletion of the export apparatus proteins results in loss of secretion. However, these mutant strains were still able to form base structures and therefore the export apparatus proteins were placed at the end of the base assembly.

Structural analysis of the individual mutant bases provided here, give a more detailed view of the export apparatus proteins and their role during the NC assembly.
In all three mutant bases, ΔSpaP, ΔSpaQ, ΔSpaR (empty base phenotype), we only found the ring proteins InvG, PrgH and PrgK among the NC and the export apparatus proteins. This shows that, if one of these three export apparatus proteins is knocked out the other two are also not present. This is in accordance with the idea that SpaP, SpaQ and SpaR are tightly bound to each other (Wagner et al. 2010). It furthermore shows that they can only act as a trimer and are essential for cup and socket formation. Lacking cup and socket within the base resulted in less stable bases suggesting that these substructures enhance the interaction between outer and inner rings.
The other mutants, ΔInvA, ΔSpaS and ΔInvC displayed a filled base phenotype, implying that they are dispensable for cup and socket assembly.

The current working model of export apparatus and NC assembly (Wagner et al. 2010) was confirmed and refined by the structural analysis of the individual Spa mutants (Fig. 25A). This model presents the export apparatus proteins SpaP, SpaQ and SpaR as assembly nucleators, which form an initial complex, as they were also shown to promote PrgH/PrgK ring formation. SpaS joins the trimeric complex as an enhancing factor for PrgH/PrgK ring formation and substrate specificity switch, while InvA not being necessary for efficient inner ring formation, is added at a later time point as a potential moderator of interaction with

cytoplasmic proteins like InvC or OrgB (Warrall et al. 2010, Zarivach et al. 2008). The inner ring and outer ring are formed and InvC is employed for secretion of the inner rod and the needle filament, which are the last components to complete the structure of a fully assembled NC (Fig. 25B). Thus, the inner membrane proteins are inserted into the membrane via the Sec-system in an InvC independent manner.

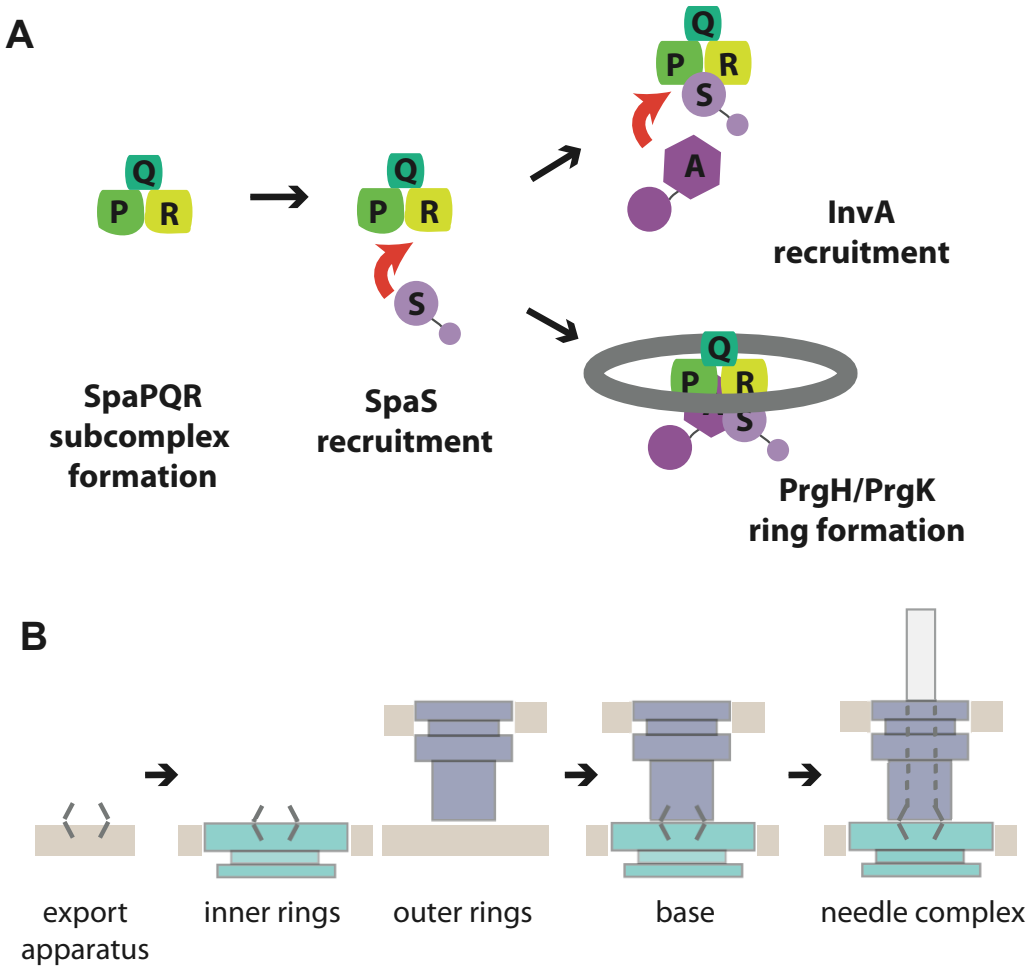

Figure 25. Working model of export apparatus and NC assembly (adapted from Wagner et al. 2010). (A) SpaP, SpaQ and SpaR form a subcomplex. Recruitment of SpaS promotes PrgH/PrgK ring formation but appears not to be necessary for it. InvA joins the complex but is not important for ring formation efficiency. **(B)** The export apparatus proteins seem to be the nucleator for the NC assembly and promote inner ring formation. Formation of outer rings completes base assembly. Building up inner rod and needle filament is the last step of NC assembly.

7.3. Localisation of the export apparatus proteins within the NC

This work demonstrates that the export apparatus proteins SpaP, SpaQ and SpaR are essential for cup and socket formation, and that SpaS is integrated into the NC structures. However, it still remains to be clearly shown whether they all are themselves structural elements or act as regulators for building up this NC substructure.

Within the w.t. sample only two peptides of each, SpaQ and SpaR, were found, which might be due to them being the smallest membrane proteins within the sample and having a low abundance. Moreover they are highly hydrophobic, around 50% of the SpaQ and SpaR are predicted to be transmembrane, in contrary to InvA with 25% and SpaS with 29% predicted transmembrane region (Uniprot accession numbers see appendix). Thus, the sample preparation for mass spectrometry still has to be optimized. To further increase protein coverage and the chance to find missed peptides, it is possible to use a less specific protease, such as chymotrypsin, elastase or proteinase K creating shorter peptides (Speers et al. 2004, Rietschel et al. 2009). Besides changing sample preparation, increasing the amount of protein analyzed should be also beneficial for a better detection.

Labeling studies would be an effective way to determine, whether SpaP, SpaQ and SpaR are indeed the structural elements forming cup and socket. Nano-gold labeling of His-tagged proteins has shown to be a powerful technique to solve the topology of several NC components (Schraidt et al. 2010). In combination with cross linking and mass spec analysis, it could also be used to investigate the topology of the export apparatus proteins. Since cup and socket are located in the center of the lower base in contact with the InvG, PrgH/PrgK rings (Fig. 26), it is possible to find cross links between the ring proteins with known orientation and the export apparatus proteins. However, this approach could be challenging due to the low abundance, unknown accessibility and hydrophobicity of the export apparatus proteins. Therefore it will be necessary to enrich the export apparatus proteins within the sample first using e.g. affinity purification. In order to study the stoichiometry of the SpaP,

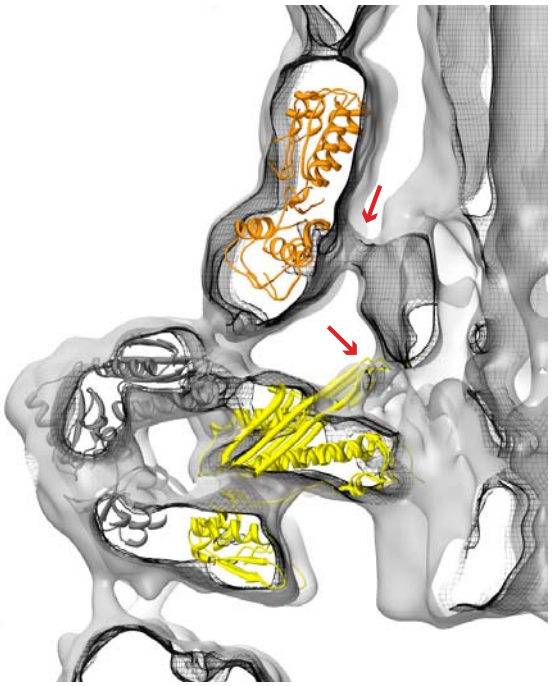

Figure 26. Cup and socket are connected to NC ring structures. By looking at the longitudinal section of the NC (~ 10 Å resolution), it becomes visible that PrgK and InvG are connected to the cup and socket region via brigding densities indicated by the red arrows (Schraidt and Marlovits 2011, EMDB:1875).

SpaQ and SpaR complex, one could think of testing in vitro complex formation and native mass spectrometry.

To localize InvA and SpaS, it would be useful to get a sample of preferably homogenous protein content. One way to do so was tagging InvA and SpaS individually at the C-terminus and perform immunoprecipitation to pull down InvA or SpaS containing NCs only.

Nevertheless, although InvA dissociates during the applied purification, it would be possible to perform labeling studies on the pulled down InvA containing NCs. But with an uncertain amount of InvA, the whole procedure would be very time consuming and therefore the purification conditions should be optimized first before starting further analysis. It is probable that a different detergent can assist on circumventing InvA disassociation. Another way could be using crosslinking of InvA to the complex to overcome the problem of uncontrollable protein disassociation.

In contrast to InvA, SpaS is tightly bound to the NC and is present in most fully assembled bases and NCs at the timepoint of starting the experimental procedures. With SpaS-FLAG being accessible as shown by immunoprecipitation, it should be possible to perform labeling on the purified sample in the future.

7.4. Structure of the SpaS autocatalytic mutant NC

The structure of immunoprecipitated SpaS-FLAG bases differed from w.t. within upper and lower rings of the base, areas which are most likely membrane associated, as well as within the cup region itself. Sani et al. (2007) reported in their study on Shigella NCs the effect of different detergent concentrations on their resulting negative stain structures. They have observed similar variations in the upper and lower parts of the complexes at lower detergent concentrations. Not only the concentration of the applied detergent but also the salt concentration of the used buffer is crucial to the detergent's solubilization efficiency (Corrin and Harkins 1948). Higher salt concentrations lead to a change of the critical micelle concentration of the detergent, therefore changing the detergent's efficiency. The NC purification includes CsCl gradient centrifugation, which enhances the strength of LDAO and is more stringent than the immunoprecipitation. Therefore the extra densities seen in upper and lower rings of the immunoprecipitated complexes could be additional proteins or even membrane remnants still present under milder conditions.

Having used a strain with a mutation in SpaS, not able to undergo the substrate specificity switch, we could assume that the difference we see within the cup region is due to missing conformational changes usually caused before or by the switch. Because we have shown by immunprecipitation, that SpaS-FLAG was present in most NCs we could perform single particle analysis on conventionally purified SpaS-FLAG NCs and test whether we still see the same differences in contrast to w.t.. If so, it is very likely that the autocatalytic mutant SpaS causes the structural variance.

Taken together, our studies provided the basis for structural analysis of autocatalytic mutant SpaS-FLAG containing NCs. The next steps would be generating a high resolution structure of the mutant NC as well as labeling of SpaS-FLAG, which could be used to eventually localize the protein within the NC.

VIII CONCLUSIVE REMARKS

VIII. Conclusive remarks

The importance of the export apparatus proteins as central components in the process of substrate switching and type III secretion becomes apparent. This study shows that the export apparatus proteins are associated with the needle complex and, more specifically, that SpaP, SpaQ and SpaR are essential for cup and socket formation, acting presumably as a trimetric complex. Moreover, with SpaP being present in all base structures exhibiting a cup and socket structure, our data indicates that SpaP is a structural component of this region. Further studies nonetheless need to formally determine the localization of SpaP, SpaQ and SpaR.

With this work providing knowledge and tools for addressing these questions, it seems realistic that within the next years a precise map of all structural components of the needle complex will be drawn. Such a map should not only provide knowledge about assembly and protein-protein interactions but also should advance experiments targeting their function and the mechanism of type III secretion. While we are aware that this work is just one step, we are confident that it is an important step on the way to design alternative antibacterial strategies to antibiotics and to establish a micro-injection tool based on type III secretion.

IX. Literature

[1] A. M. Abdallah, N. C. Gey van Pittius, P. A. D. Champion, J. Cox, J. Luirink, C. M. J. E. Vandenbroucke-Grauls, B. J. Appelmelk, and W. Bitter. Type vii secretion–mycobacteria show the way. *Nat Rev Microbiol*, 5(11):883–91, Nov 2007.

[2] Y. Akeda and J. E. Galán. Chaperone release and unfolding of substrates in type iii secretion. *Nature*, 437(7060):911–5, Oct 2005.

[3] F. R. Balkwill, J. Roskams, L. Rogers. Lab Ref: A handbook of recipes, reagents, and other reference tools for use at the bench. *Cold Spring Harbor Laboratory Press*, 2002.

[4] G. Bange, N. Kümmerer, C. Engel, G. Bozkurt, K. Wild, and I. Sinning. Flha provides the adaptor for coordinated delivery of late flagella building blocks to the type iii secretion system. *Proc Natl Acad Sci U S A*, 107(25):11295–300, Jun 2010.

[5] W. Bitter, E. N. G. Houben, D. Bottai, P. Brodin, E. J. Brown, J. S. Cox, K. Derbyshire, S. M. Fortune, L.-Y. Gao, J. Liu, N. C. Gey van Pittius, A. S. Pym, E. J. Rubin, D. R. Sherman, S. T. Cole, and R. Brosch. Systematic genetic nomenclature for type vii secretion systems. *PLoS Pathog*, 5(10):e1000507, Oct 2009.

[6] A. Blocker, N. Jouihri, E. Larquet, P. Gounon, F. Ebel, C. Parsot, P. Sansonetti, and A. Allaoui. Structure and composition of the shigella flexneri "needle complex", a part of its type iii secreton. *Mol Microbiol*, 39(3):652–63, Feb 2001.

[7] A. Blocker, K. Komoriya, and S.-I. Aizawa. Type iii secretion systems and bacterial flagella: insights into their function from structural similarities. *Proc Natl Acad Sci U S A*, 100(6):3027–30, Mar 2003.

[8] A. Botteaux, C. A. Kayath, A.-L. Page, N. Jouihri, M. Sani, E. Boekema, L. Biskri, C. Parsot, and A. Allaoui. The 33 carboxyl-terminal residues of spa40 orchestrate the multi-step assembly process of the type iii secretion needle complex in shigella flexneri. *Microbiology*, 156(Pt 9): 2807–17, Sep 2010.

[9] J. E. Bröms, A.-L. Forslund, A. Forsberg, and M. S. Francis. Dissection of homologous translocon operons reveals a distinct role for yopd in type iii secretion by yersinia pseudotuberculosis. *Microbiology*, 149(Pt 9):2615–26, Sep 2003.

[10] P. Broz, C. A. Mueller, S. A. Müller, A. Philippsen, I. Sorg, A. Engel, and G. R. Cornelis. Function and molecular architecture of the yersinia injectisome tip complex. *Mol Microbiol*, 65(5):1311–20, Sep 2007.

[11] M. J. Brunner. Structural studies of the Salmonella SPI-1 type III secretion apparatus. Diploma thesis, University of Vienna, June 2009.

[12] M. Chami, I. Guilvout, M. Gregorini, H. W. Rémigy, S. A. Müller, M. Valerio, A. Engel, A. P. Pugsley, and N. Bayan. Structural insights into the secretin puld and its trypsin-resistant core. *J Biol Chem*, 280(45):37732–41, Nov 2005.

[13] J. Z. Chen and N. Grigorieff. Signature: a single-particle selection system for molecular electron microscopy. *J Struct Biol*, 157(1):168–73, Jan 2007.

[14] B. Coburn, I. Sekirov, and B. B. Finlay. Type iii secretion systems and disease. *Clin Microbiol Rev*, 20(4):535–49, Oct 2007.

[15] C. M. Collazo and J. E. Galán. Requirement for exported proteins in secretion through the invasion-associated type iii system of salmonella typhimurium. *Infect Immun*, 64(9):3524–31, Sep 1996.

[16] R. F. Collins, L. Davidsen, J. P. Derrick, R. C. Ford, and T. Tønjum. Analysis of the pilq secretin from neisseria meningitidis by transmission electron microscopy reveals a dodecameric quaternary structure. *J Bacteriol*, 183(13):3825–32, Jul 2001.

[17] F. S. Cordes, K. Komoriya, E. Larquet, S. Yang, E. H. Egelman, A. Blocker, and S. M. Lea. Helical structure of the needle of the type iii secretion system of shigella flexneri. *J Biol Chem*, 278(19):17103–7, May 2003.

[18] M. L. Corrin and W. D. Harkins. The effect of salts on the critical concentration for the formation of micelles in colloidal electrolytes. *J Am Chem Soc*, 69(3):683–8, Mar 1947.

[19] J. E. Deane, P. Roversi, F. S. Cordes, S. Johnson, R. Kenjale, S. Daniell, F. Booy, W. D. Picking, W. L. Picking, A. J. Blocker, and S. M. Lea. Molecular model of a type iii secretion system needle: Implications for host-cell sensing. *Proc Natl Acad Sci U S A*, 103(33):12529–33, Aug 2006.

[20] U. Derewenda, A. Mateja, Y. Devedjiev, K. M. Routzahn, A. G. Evdokimov, Z. S. Derewenda, and D. S. Waugh. The structure of yersinia pestis v-antigen, an essential virulence factor and mediator of immunity against plague. *Structure*, 12(2):301–6, Feb 2004.

[21] A. Diepold, M. Amstutz, S. Abel, I. Sorg, U. Jenal, and G. R. Cornelis. Deciphering the assembly of the yersinia type iii secretion injectisome. *EMBO J*, 29(11):1928–40, Jun 2010.

[22] A. J. M. Driessen and N. Nouwen. Protein translocation across the bacterial cytoplasmic membrane. *Annu Rev Biochem*, 77:643–67, 2008.

[23] M. Erhardt and K. T. Hughes. C-ring requirement in flagellar type iii secretion is bypassed by flhdc upregulation. *Mol Microbiol*, 75(2):376–93, Jan 2010.

[24] M. Erhardt, K. Namba, and K. T. Hughes. Bacterial nanomachines: the flagellum and type iii injectisome. *Cold Spring Harb Perspect Biol*, 2(11):a000299, Nov 2010.

[25] P. T. Erskine, M. J. Knight, A. Ruaux, H. Mikolajek, N. Wong Fat Sang, J. Withers, R. Gill, S. P. Wood, M. Wood, G. C. Fox, and J. B. Cooper. High resolution structure of bipd: an invasion protein associated with the type iii secretion system of burkholderia pseudomallei. *J Mol Biol*, 363(1):125–36, Oct 2006.

[26] F. Fan, K. Ohnishi, N. R. Francis, and R. M. Macnab. The flip and flir proteins of salmonella typhimurium, putative components of the type iii flagellar export apparatus, are located in the flagellar basal body. *Mol Microbiol*, 26(5):1035–46, Dec 1997.

[27] J. Frank and M. Radermacher. Three-dimensional reconstruction of single particles negatively stained or in vitreous ice. *Ultramicroscopy*, 46(1-4):241–62, Oct 1992.

[28] J. E. Galán and H. Wolf-Watz. Protein delivery into eukaryotic cells by type iii secretion machines. *Nature*, 444(7119):567–73, Nov 2006.

[29] V. E. Galkin, W. H. Schmied, O. Schraidt, T. C. Marlovits, and E. H. Egelman. The structure of the salmonella typhimurium type iii secretion system needle shows divergence from the flagellar system. *J Mol Biol*, 396(5):1392–7, Mar 2010.

[30] A. Gauthier and B. B. Finlay. Translocated intimin receptor and its chaperone interact with atpase of the type iii secretion apparatus of enteropathogenic escherichia coli. *J Bacteriol*, 185(23): 6747–55, Dec 2003.

[31] I. Gentschev, G. Dietrich, and W. Goebel. The e. coli alpha-hemolysin secretion system and its use in vaccine development. *Trends Microbiol*, 10(1):39–45, Jan 2002.

[32] B. González-Pedrajo, T. Minamino, M. Kihara, and K. Namba. Interactions between c ring proteins and export apparatus components: a possible mechanism for facilitating type iii protein export. *Mol Microbiol*, 60(4):984–98, May 2006.

[33] H. L. Hamilton, N. M. Domìnguez, K. J. Schwartz, K. T. Hackett, and J. P. Dillard. Neisseria gonorrhoeae secretes chromosomal dna via a novel type iv secretion system. *Mol Microbiol*, 55(6):1704–21, Mar 2005.

[34] I. Hansen-Wester and M. Hensel. Salmonella pathogenicity islands encoding type iii secretion systems. *Microbes Infect*, 3(7):549–59, Jun 2001.

[35] A. Haraga, M. B. Ohlson, and S. I. Miller. Salmonellae interplay with host cells. *Nat Rev Microbiol*, 6(1):53–66, Jan 2008.

[36] C. S. Hayes, S. K. Aoki and D. A. Low. Bacterial contact-dependent delivery systems. *Annu Rev Genet*, 44: 71-90, 2010.

[37] A. Heijne, M. F. Gerhards, J. G. A. M. Blomjous, and A. van der Sluys Veer. Episodes of abdominal pain. *Neth J Med*, 69(5):222–8, May 2011.

[38] J. L. Hodgkinson, A. Horsley, D. Stabat, M. Simon, S. Johnson, P. C. A. da Fonseca, E. P. Morris, J. S. Wall, S. M. Lea, and A. J. Blocker. Three-dimensional reconstruction of the shigella t3ss transmembrane regions reveals 12-fold symmetry and novel features throughout. *Nat Struct Mol Biol*, 16(5):477–85, May 2009.

[39] T. Izoré, V. Job, and A. Dessen. Biogenesis, regulation, and targeting of the type iii secretion system. *Structure*, 19(5):603–12, May 2011.

[40] S. Johnson, P. Roversi, M. Espina, A. Olive, J. E. Deane, S. Birket, T. Field, W. D. Picking, A. J. Blocker, E. E. Galyov, W. L. Picking, and S. M. Lea. Self-chaperoning of the type iii secretion system needle tip proteins ipad and bipd. *J Biol Chem*, 282(6):4035–44, Feb 2007.

[41] C. J. Jones and R. M. Macnab. Flagellar assembly in salmonella typhimurium: analysis with temperature-sensitive mutants. *J Bacteriol*, 172(3):1327–39, Mar 1990.

[42] C. J. Jones, R. M. Macnab, H. Okino, and S. Aizawa. Stoichiometric analysis of the flagellar hook-(basal-body) complex of salmonella typhimurium. *J Mol Biol*, 212(2):377–87, Mar 1990.

[43] J. A. Kenniston, T. A. Baker, J. M. Fernandez, and R. T. Sauer. Linkage between atp consumption and mechanical unfolding during the protein processing reactions of an aaa+ degradation machine. *Cell*, 114(4):511–20, Aug 2003.

[44] T. G. Kimbrough and S. I. Miller. Contribution of salmonella typhimurium type iii secretion components to needle complex formation. *Proc Natl Acad Sci U S A*, 97(20):11008–13, Sep 2000.

[45] T. Kubori, A. Sukhan, S. I. Aizawa, and J. E. Galán. Molecular characterization and assembly of the needle complex of the salmonella typhimurium type iii protein secretion system. *Proc Natl Acad Sci U S A*, 97(18):10225–30, Aug 2000.

[46] M. Lara-Tejero and J. E. Galán. Salmonella enterica serovar typhimurium pathogenicity island 1-encoded type iii secretion system translocases mediate intimate attachment to nonphagocytic cells. *Infect Immun*, 77(7):2635–42, Jul 2009.

[47] M. Lara-Tejero, J. Kato, S. Wagner, X. Liu, and J. E. Galán. A sorting platform determines the order of protein secretion in bacterial type iii systems. *Science*, 331(6021):1188–91, Mar 2011.

[48] M. Lilic, C. M. Quezada, and C. E. Stebbins. A conserved domain in type iii secretion links the cytoplasmic domain of inva to elements of the basal body. *Acta Crystallogr D Biol Crystallogr*, 66(Pt 6):709–13, Jun 2010.

[49] R. L. Lucas and C. A. Lee. Unravelling the mysteries of virulence gene regulation in salmonella typhimurium. *Mol Microbiol*, 36(5):1024–33, Jun 2000.

[50] T. C. Marlovits, T. Kubori, M. Lara-Tejero, D. Thomas, V. M. Unger, and J. E. Galán. Assembly of the inner rod determines needle length in the type iii secretion injectisome. *Nature*, 441(7093): 637–40, Jun 2006.

[51] T. C. Marlovits, T. Kubori, A. Sukhan, D. R. Thomas, J. E. Galán, and V. M. Unger. Structural insights into the assembly of the type iii secretion needle complex. *Science*, 306(5698):1040–2, Nov 2004.

[52] J. Mazar and P. A. Cotter. New insight into the molecular mechanisms of two-partner secretion. *Trends Microbiol*, 15(11):508–15, Nov 2007.

[53] E. J. McGhie, L. C. Brawn, P. J. Hume, D. Humphreys, and V. Koronakis. Salmonella takes control: effector-driven manipulation of the host. *Curr Opin Microbiol*, 12(1):117–24, Feb 2009.

[54] T. Minamino and R. M. MacNab. Interactions among components of the salmonella flagellar export apparatus and its substrates. *Mol Microbiol*, 35(5):1052–64, Mar 2000.

[55] T. Minamino and K. Namba. Distinct roles of the flii atpase and proton motive force in bacterial flagellar protein export. *Nature*, 451(7177):485–8, Jan 2008.

[56] J. A. Mindell and N. Grigorieff. Accurate determination of local defocus and specimen tilt in electron microscopy. *J Struct Biol*, 142(3):334–47, Jun 2003.

[57] T. Morita-Ishihara, M. Ogawa, H. Sagara, M. Yoshida, E. Katayama, and C. Sasakawa. Shigella spa33 is an essential c-ring component of type iii secretion machinery. *J Biol Chem*, 281(1):599–607, Jan 2006.

[58] C. A. Mueller, P. Broz, and G. R. Cornelis. The type iii secretion system tip complex and translocon. *Mol Microbiol*, 68(5):1085–95, Jun 2008.

[59] N. Nouwen, N. Ranson, H. Saibil, B. Wolpensinger, A. Engel, A. Ghazi, and A. P. Pugsley. Secretin puld: association with pilot puls, structure, and ion-conducting channel formation. *Proc Natl Acad Sci U S A*, 96(14):8173–7, Jul 1999.

[60] K. Ohnishi, F. Fan, G. J. Schoenhals, M. Kihara, and R. M. Macnab. The flio, flip, fliq, and flir proteins of salmonella typhimurium: putative components for flagellar assembly. *J Bacteriol*, 179(19):6092–9, Oct 1997.

[61] N. Opalka, R. Beckmann, N. Boisset, M. N. Simon, M. Russel, and S. A. Darst. Structure of the filamentous phage piv multimer by cryo-electron microscopy. *J Mol Biol*, 325(3):461–70, Jan 2003.

[62] M. Radermacher, T. Wagenknecht, R. Grassucci, J. Frank, M. Inui, C. Chadwick, and S. Fleischer. Cryo-em of the native structure of the calcium release channel/ryanodine receptor from sarcoplasmic reticulum. *Biophys J*, 61(4):936–40, Apr 1992.

[63] B. Rietschel, S. Bornemann, T. N. Arrey, D. Baeumlisberger, M. Karas, and B. Meyer. Membrane protein analysis using an improved peptic in-solution digestion protocol. *Proteomics*, 9(24): 5553–7, Dec 2009.

[64] K. E. Riordan and O. Schneewind. Yscu cleavage and the assembly of yersinia type iii secretion machine complexes. *Mol Microbiol*, 68(6):1485–501, Jun 2008.

[65] Y. Saijo-Hamano, K. Imada, T. Minamino, M. Kihara, M. Shimada, A. Kitao, and K. Namba. Structure of the cytoplasmic domain of flha and implication for flagellar type iii protein export. *Mol Microbiol*, 76(1):260–8, Apr 2010.

[66] M. Sandkvist. Biology of type ii secretion. *Mol Microbiol*, 40(2):271–83, Apr 2001.

[67] M. Sani, A. Allaoui, F. Fusetti, G. T. Oostergetel, W. Keegstra, and E. J. Boekema. Structural organization of the needle complex of the type iii secretion apparatus of shigella flexneri. *Micron*, 38(3):291–301, 2007.

[68] O. Schraidt, M. D. Lefebre, M. J. Brunner, W. H. Schmied, A. Schmidt, J. Radics, K. Mechtler, J. E. Galán, and T. C. Marlovits. Topology and organization of the salmonella typhimurium type iii secretion needle complex components. *PLoS Pathog*, 6(4):e1000824, Apr 2010.

[69] O. Schraidt and T. C. Marlovits. Three-dimensional model of salmonella's needle complex at subnanometer resolution. *Science*, 331(6021):1192–5, Mar 2011.

[70] O. Schraidt. Structural dissection of the *Salmonella typhimurium* type III secretion needle complex. Dissertation, University of Vienna, October 2010.

[71] A. E. Speers and C. C. Wu. Proteomics of integral membrane proteins–theory and application. *Chem Rev*, 107(8):3687–714, Aug 2007.

[72] T. Spreter, C. K. Yip, S. Sanowar, I. André, T. G. Kimbrough, M. Vuckovic, R. A. Pfuetzner, W. Deng, A. C. Yu, B. B. Finlay, D. Baker, S. I. Miller, and N. C. J. Strynadka. A conserved structural motif mediates formation of the periplasmic rings in the type iii secretion system. *Nat Struct Mol Biol*, 16(5):468–76, May 2009.

[73] C. B. Stone, D. L. Johnson, D. C. Bulir, J. D. Gilchrist, and J. B. Mahony. Characterization of the putative type iii secretion atpase cdsn (cpn0707) of chlamydophila pneumoniae. *J Bacteriol*, 190(20):6580–8, Oct 2008.

[74] A. Sukhan, T. Kubori, J. Wilson, and J. E. Galán. Genetic analysis of assembly of the salmonella enterica serovar typhimurium type iii secretion-associated needle complex. *J Bacteriol*, 183(4): 1159–67, Feb 2001.

[75] P. Troisfontaines and G. R. Cornelis. Type iii secretion: more systems than you think. *Physiology (Bethesda)*, 20:326–39, Oct 2005.

[76] J. S. Van Arnam, J. L. McMurry, M. Kihara, and R. M. Macnab. Analysis of an engineered salmonella flagellar fusion protein, flir-flhb. *J Bacteriol*, 186(8):2495–8, Apr 2004.

[77] G. von Heijne. The signal peptide. *J Membr Biol*, 115(3):195–201, May 1990.

[78] S. Wagner, L. Königsmaier, M. Lara-Tejero, M. Lefebre, T. C. Marlovits, and J. E. Galán. Organization and coordinated assembly of the type iii secretion export apparatus. *Proc Natl Acad Sci U S A*, 107(41):17745–50, Oct 2010.

[79] Y. Wang, A. N. Ouellette, C. W. Egan, T. Rathinavelan, W. Im, and R. N. De Guzman. Differences in the electrostatic surfaces of the type iii secretion needle proteins prgi, bsal, and mxih. *J Mol Biol*, 371(5):1304–14, Aug 2007.

[80] M. W. Wood, M. A. Jones, P. R. Watson, S. Hedges, T. S. Wallis, and E. E. Galyov. Identification of a pathogenicity island required for salmonella enteropathogenicity. *Mol Microbiol*, 29(3):883–91, Aug 1998.

[81] M. W. Wood, R. Rosqvist, P. B. Mullan, M. H. Edwards, and E. E. Galyov. Sope, a secreted protein of salmonella dublin, is translocated into the target eukaryotic cell via a sip-dependent mechanism and promotes bacterial entry. *Mol Microbiol*, 22(2):327–38, Oct 1996.

[82] L. J. Worrall, E. Lameignere, and N. C. J. Strynadka. Structural overview of the bacterial injectisome. *Curr Opin Microbiol*, 14(1):3–8, Feb 2011.

[83] L. J. Worrall, M. Vuckovic, and N. C. J. Strynadka. Crystal structure of the c-terminal domain of the salmonella type iii secretion system export apparatus protein inva. *Protein Sci*, 19(5):1091–6, May 2010.

[84] C. K. Yip, T. G. Kimbrough, H. B. Felise, M. Vuckovic, N. A. Thomas, R. A. Pfuetzner, E. A. Frey, B. B. Finlay, S. I. Miller, and N. C. J. Strynadka. Structural characterization of the molecular platform for type iii secretion system assembly. *Nature*, 435(7042):702–7, Jun 2005.

[85] R. Zarivach, W. Deng, M. Vuckovic, H. B. Felise, H. V. Nguyen, S. I. Miller, B. B. Finlay, and N. C. J. Strynadka. Structural analysis of the essential self-cleaving type iii secretion proteins escu and spas. *Nature*, 453(7191):124–7, May 2008.

[86] R. Zarivach, M. Vuckovic, W. Deng, B. B. Finlay, and N. C. J. Strynadka. Structural analysis of a prototypical atpase from the type iii secretion system. *Nat Struct Mol Biol*, 14(2):131–7, Feb 2007.

[87] S. F. Zenk, D. Stabat, J. L. Hodgkinson, A. K. J. Veenendaal, S. Johnson, and A. J. Blocker. Identification of minor inner-membrane components of the shigella type iii secretion system 'needle complex'. *Microbiology*, 153(Pt 8):2405–15, Aug 2007.

[88] L. Zhang, Y. Wang, W. L. Picking, W. D. Picking, and R. N. De Guzman. Solution structure of monomeric bsal, the type iii secretion needle protein of burkholderia pseudomallei. *J Mol Biol*, 359(2):322–30, Jun 2006.

[89] K. Zhu, B. González-Pedrajo, and R. M. Macnab. Interactions among membrane and soluble components of the flagellar export apparatus of salmonella. *Biochemistry*, 41(30):9516–24, Jul 2002.

X. Curriculum Vitae

Curriculum vitae	**Lisa Königsmaier**
Date of Birth	16.10.1982
Nationality	Austria

Education

March 2007 – June 2011	**Institute of Molecular Biotechnology of the Austrian Academy of Sciences, Vienna, Austria** PhD thesis in structural biology, Vienna Biocenter PhD program (Boehringer Ingelheim Fonds Fellowship Dec. 2007 – March 2010)
Nov. 2004 - July 2006	**University of Salzburg, Austria** MSc Genetics and Biotechnology, average grade: 1.0 (excellent)
Feb. 2005 - July 2005	**University of Rome, Italy** Exchange semester (Erasmus program)
Oct. 2001 - Nov 2004	**University of Salzburg, Austria** BSc Genetics and Molecular Biology, average grade: 1.7 (good)
1993 - 2001	**Gymnasium der Kreuzschwestern Linz**, **Austria**

Research Experience

March 2009- now	**PhD thesis at the Institute of Molecular Biotechnology of the Austrian Academy of Sciences, Vienna, Austria** - PhD Thesis: Structural and functional analysis of type III secretion system - Supervisor: Dr. Thomas Marlovits
Sept. 2005 - June 2006	**Diploma thesis at the Max Planck Institute of Biochemistry, Munich, Germany** **-** Analysis of Fatty Acid Metabolism in Halophilic Archaea - Supervisors: Dr. Dieter Oesterhelt and Dr. Helga Stan-Lotter
Nov. 2004	**Research Project at the University of Salzburg, Austria** - Research project on ageing in yeast - Supervisor: Dr. Michael Breitenbach
July - Aug. 2004	**Internship at the Max Planck Institute of Molecular Genetics, Berlin, Germany** - Research project: 'Genomic analyses of bac-clones in *Ornithorhynchus anatinus'* - Supervisors: Dr. Hans Lehrach and Dr. Heinz Himmelbauer

XI. Acknowledgements

I look back on my PhD studies and see an existing journey, with many lessons to learn, ups and downs, surprises and doubts. Through all this time, I was not alone and my work was supported by different people in many different ways.

My thanks go at first to Thomas Marlovits, who let me be part of his group, shared his knowledge and ideas with me and supported me during the last four years with his enthusiasm about science and the beauty of structural biology. I also want to thank Thomas for choosing great people for his team, whom I appreciate and for whom I hope the best for the future: Matthias Brunner, Jesus Fernandez-Rodriguez, Agata Kosarewicz, Johanna Radek, Julia Radics, Wolfgang Schmied, Oliver Schraidt and Wolfgang Weber. It was my pleasure to work with you all. Matthias, thank you for your help from the very beginning till the end of my PhD, from showing me around in the lab to helping me with processing and always having time for coffee, coke zero and nerd talk; Agata, thanks a lot for encouraging me and seeing the good parts of my project after a long day in the lab, for coffee breaks and distracting me from work with funny stories and great house parties; Jesus, thanks for always having an open ear and discussing my results, for being crazy and making our time as colorful and funny as it was; Julia, my special thanks also go to you, I have not only enjoyed working with you, also our friendship means a lot to me and I am lucky that I was able to work with such a good friend side by side. Olli, thanks for your positive attitude, our tea parties, for discussing the various drafts of this work and your constructive comments. Wolfi, thanks for being a good friend and co-worker and making me laugh countless times. Besides the core group, I would also like to thank the members of the Electron Microscopy Facility, Guenter Resch, who has introduced me to electron microscopy and shared his comprehensive knowledge with me, Marlene Brandstetter and Nicole Fellner, for their constant technical support and advice.

Moreover I would like to acknowledge Jorge Galan and Samuel Wagner for collaborating on the export apparatus project, for providing me with strains and discussing purification protocols. Thanks to Tim Clausen, Jan-Michael Peters and Peggy Stolt-Bergner for their scientific input and support as my PhD committee. My acknowledgements also include Boehringer Ingelheim Fonds for their financial support of this work.

During my time at IMBA, I met people who have become really important to me and played a special role during my PhD. Angi, thanks for being a very good friend, who supported me, scientifically and personally from the first day onwards in Vienna until the end of our PhDs. Vivien, thank you for always believing in me and sharing your life with me during our time in Vienna.

My last thanks go to my family and best friends. Franz, Johanna, Kim, Doris and Natalie, you accompanied me through my ups and down, helped me overcoming my doubts, trusted me and believed in my dreams.

XII. Appendix

12.1. List of T3SS homologs

Localisation	**Salmonella**	**Yersinia**	**Shigella**	**Flagellum**
	S.enterica SPI-1	*Yersinia* spp.	*Shigella* ssp.	*S.enterica*
extracellular				
needle/filament	PrgI	YscF	MxiH	FlgE?
OM/periplasm				
outer ring/secretin	InvG	YscC	MxiD	
rod	PrgJ	YscI	MxiI	
inner membrane				
inner ring	PrgK	YscJ	MxiJ	FliF
	PrgH	YscD	MxiG	FliG
export apparatus	SpaP	YscR	Spa24	FliP
	SpaQ	YscS	Spa9	FliQ
	SpaR	YscT	Spa29	FliR
	SpaS	YscU	Spa40	FlhB
	InvA	YscV	MxiA	FlhA
cytoplasm				
ATPase	InvC	YscN	Spa47	FliI
putative C-ring/ sorting platform	SpaO	YscQ	Spa33	FliM/N
	OrgA	YscK	MxiK	
	OrgB	YscL	MxiN	FliH
ATPase complex?	InvI	YscO	Spa13	FliJ

Table of T3SS homologs of *S. enterica* SPI-1, *Yersinia* spp., *Shigella* ssp. and the flagellum.

12.2. Uniprot accession numbers of Spa/InvA proteins

P40700 (SPAP_SALTY)

P0A1L7 (SPAQ_SALTY)

P40701 (SPAR_SALTY)

P40702 (SPAS_SALTY)

P0A1I3 (INVA_SALTY)

12.3. List of cryo-EM sessions/collected particles

SP63-dSpa

58_62
Number of 2D images: 0

63_67
Number of 2D images in file: 150

68_72
Number of 2D images in file: 637

73_77
Number of 2D images in file: 1863

78_82
Number of 2D images in file: 3745

83_87
Number of 2D images in file: 4662

88_92
Number of 2D images in file: 12454

93_97
Number of 2D images in file: 4864

98_102
Number of 2D images in file: 4158

103_107
Number of 2D images in file: 1829

108_112
Number of 2D images in file: 599

113_117
Number of 2D images in file: 154

118_122
Number of 2D images: 0

SP72-dSpaP

58_62
Number of 2D images: 0

63_67
Number of 2D images in file: 150

68_72
Number of 2D images in file: 637

73_77
Number of 2D images in file: 1863

78_82
Number of 2D images in file: 3745

83_87
Number of 2D images in file: 4662

88_92
Number of 2D images in file: 12454

93_97
Number of 2D images in file: 4864

98_102
Number of 2D images in file: 4158

103_107
Number of 2D images in file: 1829

108_112
Number of 2D images in file: 599

113_117
Number of 2D images in file: 154

118_122
Number of 2D images: 0

SP74-dInvA

58_62
Number of 2D images: 0

63_67
Number of 2D images in file: 132

68_72
Number of 2D images in file: 997

73_77
Number of 2D images in file: 2676

78_82
Number of 2D images in file: 3994

83_87
Number of 2D images in file: 3647

88_92
Number of 2D images in file: 7914

93_97
Number of 2D images in file: 3241

98_102
Number of 2D images in file: 3809

103_107
Number of 2D images in file: 2535

108_112
Number of 2D images in file: 1003

113_117
Number of 2D images in file: 132

118_122
Number of 2D images: 0

SP76-dSpaS

58_62
Number of 2D images: 0

63_67
Number of 2D images in file: 167

68_72
Number of 2D images in file: 602

73_77
Number of 2D images in file: 1193

78_82
Number of 2D images in file: 1710

83_87
Number of 2D images in file: 1567

88_92
Number of 2D images in file: 4325

93_97
Number of 2D images in file: 1537

98_102
Number of 2D images in file: 1644

103_107
Number of 2D images in file: 1120

108_112
Number of 2D images in file: 575

113_117
Number of 2D images in file: 177

118_122
Number of 2D images: 0

SP79-dSpaQ

58_62
Number of 2D images: 0

63_67
Number of 2D images in file: 84

68_72
Number of 2D images in file: 336

73_77
Number of 2D images in file: 983

78_82
Number of 2D images in file: 2396

83_87
Number of 2D images in file: 2748

88_92
Number of 2D images in file: 8673

93_97
Number of 2D images in file: 2857

98_102
Number of 2D images in file: 2882

103_107
Number of 2D images in file: 1086

108_112
Number of 2D images in file: 293

113_117
Number of 2D images in file: 91

118_122
Number of 2D images: 0

SP80-dSpaR

58_62
Number of 2D images: 0

63_67
Number of 2D images in file: 92

68_72
Number of 2D images in file: 306

73_77
Number of 2D images in file: 689

78_82
Number of 2D images in file: 1462

83_87
Number of 2D images in file: 2056

88_92
Number of 2D images in file: 7240

93_97
Number of 2D images in file: 2228

98_102
Number of 2D images in file: 1555

103_107
Number of 2D images in file: 789

108_112
Number of 2D images in file: 327

113_117
Number of 2D images in file: 112

118_122
Number of 2D images: 0

SP91-wt

58_62
Number of 2D images: 0

63_67
Number of 2D images in file: 816

68_72
Number of 2D images in file: 3256

73_77
Number of 2D images in file: 4727

78_82
Number of 2D images in file: 4920

83_87
Number of 2D images in file: 2530

88_92
Number of 2D images in file: 3712

93_97
Number of 2D images in file: 2209

98_102
Number of 2D images in file: 4199

103_107
Number of 2D images in file: 4412

108_112
Number of 2D images in file: 2882

113_117
Number of 2D images in file: 883

118_122
Number of 2D images: 0

SP99-dInvC

58_62
Number of 2D images: 0

63_67
Number of 2D images in file: 162

68_72
Number of 2D images in file: 785

73_77
Number of 2D images in file: 1546

78_82
Number of 2D images in file: 1955

83_87
Number of 2D images in file: 1000

88_92
Number of 2D images in file: 1241

93_97
Number of 2D images in file: 1106

98_102
Number of 2D images in file: 2186

103_107
Number of 2D images in file: 1776

108_112
Number of 2D images in file: 915

113_117
Number of 2D images in file: 139

118_122
Number of 2D images: 0

12.4. List of peptides found by MS

w.t.

>sp|P41783|PRGH_SALTY Protein prgH OS=Salmonella typhimurium

Unique Peptides: 32
Sequence Coverage: **69%**

Sequence	Start	Stop
(K)TITSPGPYIVR(L)	8	18
(R)LLNSSLNGcEFPLLTGR(T)	19	35
(R)SVQLNTPIQVGELLILIRPESEPWVPEQPEK(L)	96	126
(R)QAAELDSLLGQEK(E)	169	181
(K)ERFQVLPGR(D)	182	190
(K)ERFQVLPGRDK(M)	182	192
(R)FQVLPGR(D)	184	190
(R)FQVLPGRDK(M)	184	192
(K)MLYVAAQNER(D)	193	202
(K)MLYVAAQNERDTLWAR(Q)	193	208
(R)qVLARGDYDK(N)	209	218
(K)NARVINENEENK(R)	219	230
(R)VINENEENK(R)	222	230
(R)VINENEENKR(I)	222	231
(R)ISIWLDTYYPQLAYYR(I)	232	247
(R)IHFDEPR(K)	248	254
(R)KPVFWLSR(Q)	255	262
(K)KELEVLSQK(L)	270	278
(K)ELEVLSQK(L)	271	278
(R)ALMPYADSVNITLMDDVTAAGQAEAGLK(Q)	281	308
(K)qQALPYSR(R)	309	316
(K)GGVTFVIQGALDDVEILR(A)	321	338
(K)GGVTFVIQGALDDVEILRAR(Q)	321	340
(R)ARQFVDSYYR(T)	339	348
(R)ARQFVDSYYRTWGGR(Y)	339	353
(R)QFVDSYYR(T)	341	348
(R)QFVDSYYRTWGGR(Y)	341	353
(R)TWGGRYVQFAIELK(D)	349	362
(R)YVQFAIELK(D)	354	362
(R)YVQFAIELKDDWLK(G)	354	367
(K)GRSFQYGAEGYIK(M)	368	380
(R)SFQYGAEGYIK(M)	370	380
(K)MSPGHWYFPSPL(-)	381	392

invA685aa

Unique Peptides: 18
Sequence Coverage: **27%**

Sequence	Start	Stop
(K)GSERVAEVAAR(F)	132	142
(R)FSLDGMPGK(Q)	143	151
(K)QMSIDADLK(A)	152	160
(K)AGIIDADAAR(E)	161	170
(R)ESQLYGSFDGAMK(F)	179	191
(K)VSTETVPLILLVPK(S)	355	368
(K)SRREDLEK(A)	369	376
(R)LPEVLLR(D)	395	401
(R)DGEGLDDNSIVLLINEIR(V)	402	419
(K)LRELGYVLR(N)	467	475
(K)HMLDQLEAK(F)	504	512
(K)EVLRHATVQR(I)	519	528

(K)IVAYPDTNSLLVK(G)	269	281
(K)GTAEQVHFIEMLVK(A)	282	295
(K)RHVELSLWIVDLNK(S)	302	315
(R)HVELSLWIVDLNK(S)	303	315
(K)SDLERLGTSWSGSITIGDK(L)	316	334
(R)LGTSWSGSITIGDK(L)	321	334
(K)LGVSLNQSSISTLDGSR(F)	335	351
(K)LGVSLNQSSISTLDGSRFIAAVNALEEK(K)	335	362
(R)FIAAVNALEEK(K)	352	362
(R)FIAAVNALEEKK(Q)	352	363
(K)qATVVSRPVLLTQENVPAIFDNNR(T)	364	387
(R)TFYTK(L)	388	392
(K)LIGERNVALEHVTYGTMIR(V)	393	411
(R)NVALEHVTYGTMIR(V)	398	411
(R)NVALEHVTYGTMIRVLPR(F)	398	415
(R)FSADGQIEMSLDIEDGNDK(T)	416	434
(R)FSADGQIEMSLDIEDGNDKTPQSDTTTSVDALPEVGR(T	416	452
(K)TPQSDTTTSVDALPEVGR(T)	435	452
(R)TLISTIAR(V)	453	460
(R)TLISTIARVPHGK(S)	453	465
(K)SLLVGGYTR(D)	466	474
(K)SLLVGGYTRDANTDTVQSIPFLGK(L)	466	489
(R)DANTDTVQSIPFLGK(L)	475	489
(K)LPLIGSLFR(Y)	490	498
(K)SNVVRVFMIEPK(E)	505	516
(R)VFmIEPK(E)	510	516
(K)EIVDPLTPDASESVNNILK(Q)	517	535
(K)QSGAWSGDDK(L)	536	545
(K)QSGAWSGDDKLQK(W)	536	548
(K)WVRVYLDRGQEAIK(-)	549	562
(R)VYLDRGQEAIK(-)	552	562

>sp|P35672|INVG_SALTY Protein invG OS=Salmonella typhimurium

Unique Peptides: 54

Sequence Coverage: **85%**

Sequence	Start	Stop
(K)IPVTGSGFVAK(D)	28	38
(K)IPVTGSGFVAKDDSLR(T)	28	43
(K)DDSLRTFFDAMALQLK(E)	39	54
(R)TFFDAmALQLK(E)	44	54
(K)KITGNFEFHDPNALLEK(L)	67	83
(K)ITGNFEFHDPNALLEK(L)	68	83
(K)LSLQLGLIWYFDGQAIYIYDASEMR(N)	84	108
(R)NAVVSLRNVSLNEFNNFLK(R)	109	127
(R)NVSLNEFNNFLK(R)	116	127
(K)RSGLYNK(N)	128	134
(K)NYPLRGDNR(K)	135	143
(R)KGTFYVSGPPVYVDMVVNAATmMDK(Q)	144	168
(K)GTFYVSGPPVYVDMVVNAATMmDK(Q)	145	168
(K)QNDGIELGR(Q)	169	177
(K)qNDGIELGRQK(I)	169	179
(K)IGVMRLNNTFVGDR(T)	180	193
(K)IGVMRLNNTFVGDRTYNLR(D)	180	198
(R)LNNTFVGDR(T)	185	193
(R)LNNTFVGDRTYNLR(D)	185	198
(R)LNNTFVGDRTYNLRDQK(M)	185	201
(R)TYNLRDQK(M)	194	201
(K)MVIPGIATAIER(L)	202	213
(K)AANYAGGMSLQEALK(Q)	245	259
(K)qNAAAGNIK(I)	260	268

(K)IVAYPDTNSLLVK(G)	269	281
(K)GTAEQVHFIEMLVK(A)	282	295
(K)RHVELSLWIVDLNK(S)	302	315
(R)HVELSLWIVDLNK(S)	303	315
(K)SDLERLGTSWSGSITIGDK(L)	316	334
(R)LGTSWSGSITIGDK(L)	321	334
(K)LGVSLNQSSISTLDGSR(F)	335	351
(K)LGVSLNQSSISTLDGSRFIAAVNALEEK(K)	335	362
(R)FIAAVNALEEK(K)	352	362
(R)FIAAVNALEEKK(Q)	352	363
(K)qATVVSRPVLLTQENVPAIFDNNR(T)	364	387
(R)TFYTK(L)	388	392
(K)LIGERNVALEHVTYGTMIR(V)	393	411
(R)NVALEHVTYGTMIR(V)	398	411
(R)NVALEHVTYGTMIRVLPR(F)	398	415
(R)FSADGQIEMSLDIEDGNDK(T)	416	434
(R)FSADGQIEMSLDIEDGNDKTPQSDTTTSVDALPEVGR(T)	416	452
(K)TPQSDTTTSVDALPEVGR(T)	435	452
(R)TLISTIAR(V)	453	460
(R)TLISTIARVPHGK(S)	453	465
(K)SLLVGGYTR(D)	466	474
(K)SLLVGGYTRDANTDTVQSIPFLGK(L)	466	489
(R)DANTDTVQSIPFLGK(L)	475	489
(K)LPLIGSLFR(Y)	490	498
(K)SNVVRVFMIEPK(E)	505	516
(R)VFmIEPK(E)	510	516
(K)EIVDPLTPDASESVNNILK(Q)	517	535
(K)QSGAWSGDDK(L)	536	545
(K)QSGAWSGDDKLQK(W)	536	548
(K)WVRVYLDRGQEAIK(-)	549	562
(R)VYLDRGQEAIK(-)	552	562

>sp|P41784|PRGI_SALTY Protein prgI OS=Salmonella typhimurium

Unique Peptides: 9
Sequence Coverage: **100%**

Sequence	Start	Stop
(-)mATPWSGYLDDVSAK(F)	1	15
(M)ATPWSGYLDDVSAK(F)	2	15
(K)FDTGVDNLQTQVTEALDK(L)	16	33
(K)LAAKPSDPALLAAYQSK(L)	34	50
(K)LSEYNLYR(N)	51	58
(K)LSEYNLYRNAQSNTVK(V)	51	66
(R)NAQSNTVKVFK(D)	59	69
(K)VFKDIDAAIIQNFR(-)	67	80
(K)DIDAAIIQNFR(-)	70	80

spaP224aa

Unique Peptides: 12
Sequence Coverage: **34%**

Sequence	Start	Stop
(K)HVDEGLDGYR(D)	91	100
(K)HVDEGLDGYRDYLIK(Y)	91	105
(K)YSDRELVQFFENAQLK(R)	106	121

(K)YSDRELVQFFENAQLKR(Q)	106	122
(R)ELVQFFENAQLK(R)	110	121
(R)ELVQFFENAQLKR(Q)	110	122
(K)RQYGEETETVK(R)	122	132
(K)RQYGEETETVKR(D)	122	133
(R)qYGEETETVK(R)	123	132
(R)QYGEETETVKR(D)	123	133
(R)DKDEIEKPSIFALLPAYALSEIK(S)	134	156
(K)GLILQYMDIAT(-)	214	224

>sp|P41785|PRGJ_SALTY Protein prgJ OS=Salmonella typhimurium

Unique Peptides: 9
Sequence Coverage: **75%**

Sequence	Start	Stop
(M)SIATIVPENAVIGQAVNIR(S)	2	20
(R)SMETDIVSLDDR(L)	21	32
(R)LLQAFSGSAIATAVDK(Q)	33	48
(K)QTITNRIEDPNLVTDPK(E)	49	65
(R)IEDPNLVTDPK(E)	55	65
(R)KGVGAVETLLR(-)	90	100
(R)KGVGAVETLLRS(-)	90	101
(K)GVGAVETLLR(-)	91	100
(K)GVGAVETLLRS(-)	91	101

spaQ86aa

Unique Peptides: 2
Sequence Coverage: **22%**

Sequence	Start	Stop
(-)MDDLVFAGNK(A)	1	10
(R)qVIFLALAK(-)	77	85

spaR263aa

Unique Peptides: 1
Sequence Coverage: **5%**

Sequence	Start	Stop
(R)LSFQATGLSSWFYER(G)	242	256

spaS356aa

Unique Peptides: 1
Sequence Coverage: **3%**

Sequence	Start	Stop
(R)EVHMEILSEQVK(S)	235	246

ΔSpa

>sp|P41783|PRGH_SALTY Protein prgH OS=Salmonella typhimurium

Unique Peptides: 32
Sequence Coverage: **53%**

Sequence	Start	Stop
(-)METSKEKTITSPGPYIVR(L)	1	18
(K)EKTITSPGPYIVR(L)	6	18
(K)TITSPGPYIVR(L)	8	18
(K)LETSAKKNEPR(F)	127	137
(R)QAAELDSLLGQEK(E)	169	181
(R)qAAELDSLLGQEKER(F)	169	183
(R)FQVLPGR(D)	184	190
(R)FQVLPGRDK(M)	184	192
(R)DKMLYVAAQNER(D)	191	202
(K)MLYVAAQNER(D)	193	202
(K)MLYVAAQNERDTLWAR(Q)	193	208
(R)DTLWAR(Q)	203	208
(R)QVLARGDYDK(N)	209	218
(R)qVLARGDYDKNAR(V)	209	221
(R)GDYDKNAR(V)	214	221
(R)VINENEENK(R)	222	230
(R)VINENEENKR(I)	222	231
(R)ISIWLDTYYPQLAYYR(I)	232	247
(R)IHFDEPR(K)	248	254
(R)KPVFWLSR(Q)	255	262
(R)NTmSKKELEVLSQK(L)	265	278
(K)KELEVLSQK(L)	270	278
(K)KELEVLSQKLR(A)	270	280
(K)ELEVLSQKLR(A)	271	280
(R)ALMPYADSVNITLMDDVTAAGQAEAGLK(Q)	281	308
(R)ALMPYADSVNITLmDDVTAAGQAEAGLKQQALPYSR(R)	281	316
(K)QQALPYSR(R)	309	316
(R)ARQFVDSYYR(T)	339	348
(R)QFVDSYYR(T)	341	348
(K)GRSFQYGAEGYIK(M)	368	380
(R)SFQYGAEGYIK(M)	370	380
(K)MSPGHWYFPSPL(-)	381	392

>sp|P41786|PRGK_SALTY Lipoprotein prgK OS=Salmonella typhimurium

Unique Peptides: 12
Sequence Coverage: **48%**

Sequence	Start	Stop
(K)TYQLPPRPR(V)	74	82
(R)VEIAQmFPADSLVSSPR(A)	83	99
(R)LYSAIEQR(L)	105	112
(R)LEQSLQTMEGVLSAR(V)	113	127
(R)GSPLAHQISDIK(R)	157	168
(R)GSPLAHQISDIKR(F)	157	169
(R)SDAQLQAPGTPVK(R)	191	203
(R)SDAQLQAPGTPVKR(N)	191	204
(R)NSFATSWIVLIILLSVMSAGFGVWYYKNHYAR(N)	205	236
(K)KGITADDKAK(S)	239	248
(K)GITADDKAK(S)	240	248
(K)GITADDKAKSSNE(-)	240	252

>sp|P35672|INVG_SALTY Protein invG OS=Salmonella typhimurium

Unique Peptides: 19
Sequence Coverage: **34%**

Sequence	Start	Stop
(K)IPVTGSGFVAK(D)	28	38
(K)IPVTGSGFVAKDDSLR(T)	28	43
(R)TFFDAMALQLK(E)	44	54
(R)TFFDAMALQLKEPVIVSK(M)	44	61
(R)NAVVSLR(N)	109	115
(R)NVSLNEFNNFLK(R)	116	127
(R)NVSLNEFNNFLKR(S)	116	128
(R)SGLYNKNYPLR(G)	129	139
(R)LNNTFVGDR(T)	185	193
(K)mVIPGIATAIER(L)	202	213
(K)AANYAGGMSLQEALK(Q)	245	259
(K)IVAYPDTNSLLVK(G)	269	281
(R)FIAAVNALEEK(K)	352	362
(R)TLISTIAR(V)	453	460
(K)SLLVGGYTR(D)	466	474
(R)DANTDTVQSIPFLGK(L)	475	489
(R)VFMIEPK(E)	510	516
(K)QSGAWSGDDKLQK(W)	536	548
(R)VYLDRGQEAIK(-)	552	562

spaS356aa
not identified

spaP224aa
not identified

spaQ86aa
not identified

spaR263aa
not identified

invA685aa
not identified

>sp|P41784|PRGI_SALTY Protein prgI OS=Salmonella typhimurium
not identified

>sp|P41785|PRGJ_SALTY Protein prgJ OS=Salmonella typhimurium
not identified

ΔSpaP

>sp|P41783|PRGH_SALTY Protein prgH OS=Salmonella typhimurium

Unique Peptides: 16
Sequence Coverage: **29%**

Sequence	Start	Stop
(-)METSKEKTITSPGPYIVR(L)	1	18
(K)EKTITSPGPYIVR(L)	6	18
(K)TITSPGPYIVR(L)	8	18
(R)qAAELDSLLGQEK(E)	169	181
(R)QAAELDSLLGQEKER(F)	169	183
(R)FQVLPGR(D)	184	190
(R)FQVLPGRDK(M)	184	192
(K)mLYVAAQNER(D)	193	202
(R)DTLWAR(Q)	203	208
(R)qVLARGDYDK(N)	209	218
(R)qVLARGDYDKNAR(V)	209	221
(R)VINENEENKR(I)	222	231
(R)IHFDEPR(K)	248	254
(K)ELEVLSQKLR(A)	271	280
(K)QQALPYSR(R)	309	316
(R)qFVDSYYR(T)	341	348

>sp|P41786|PRGK_SALTY Lipoprotein prgK OS=Salmonella typhimurium

Unique Peptides: 6
Sequence Coverage: **23%**

Sequence	Start	Stop
(R)LYSAIEQR(L)	105	112
(R)LEQSLQTMEGVLSAR(V)	113	127
(R)GSPLAHQISDIK(R)	157	168
(R)GSPLAHQISDIKR(F)	157	169
(R)SDAQLQAPGTPVK(R)	191	203
(R)SDAQLQAPGTPVKR(N)	191	204

>sp|P35672|INVG_SALTY Protein invG OS=Salmonella typhimur

Unique Peptides: 7
Sequence Coverage: **11%**

Sequence	Start	Stop
(K)IPVTGSGFVAK(D)	28	38
(K)IPVTGSGFVAKDDSLR(T)	28	43
(R)NAVVSLR(N)	109	115
(K)IVAYPDTNSLLVK(G)	269	281
(R)FIAAVNALEEK(K)	352	362
(K)SLLVGGYTR(D)	466	474
(R)VYLDRGQEAIK(-)	552	562

spaS356aa
not identified

spaP224aa
not identified

spaQ86aa
not identified

spaR263aa
not identified

invA685aa
not identified

>sp|P41784|PRGI_SALTY Protein prgI OS=Salmonella typhimurium
not identified

>sp|P41785|PRGJ_SALTY Protein prgJ OS=Salmonella typhimurium
not identified

ΔSpaQ

>sp|P41783|PRGH_SALTY Protein prgH OS=Salmonella typhimurium

Unique Peptides: 39
Sequence Coverage: **64%**

Sequence	Start	Stop
(-)METSKEKTITSPGPYIVR(L)	1	18
(K)EKTITSPGPYIVR(L)	6	18
(K)TITSPGPYIVR(L)	8	18
(R)LLNSSLNGcEFPLLTGR(T)	19	35
(R)QAAELDSLLGQEK(E)	169	181
(R)QAAELDSLLGQEKER(F)	169	183
(R)FQVLPGR(D)	184	190
(R)FQVLPGRDK(M)	184	192
(R)FQVLPGRDKMLYVAAQNER(D)	184	202
(R)DKMLYVAAQNER(D)	191	202
(R)DKMLYVAAQNERDTLWAR(Q)	191	208
(K)mLYVAAQNER(D)	193	202
(K)MLYVAAQNERDTLWAR(Q)	193	208
(R)QVLARGDYDK(N)	209	218
(R)QVLARGDYDKNAR(V)	209	221
(R)VINENEENKR(I)	222	231
(R)VINENEENKRISIWLDTYYPQLAYYR(I)	222	247
(R)ISIWLDTYYPQLAYYR(I)	232	247
(R)IHFDEPR(K)	248	254
(R)IHFDEPRKPVFWLSR(Q)	248	262
(R)KPVFWLSR(Q)	255	262
(R)NTmSKKELEVLSQK(L)	265	278
(K)KELEVLSQK(L)	270	278
(K)KELEVLSQKLR(A)	270	280
(K)ELEVLSQKLR(A)	271	280
(R)ALmPYADSVNITLMDDVTAAGQAEAGLK(Q)	281	308
(R)ALMPYADSVNITLmDDVTAAGQAEAGLKQQALPYSR(R)	281	316
(R)ALMPYADSVNITLMDDVTAAGQAEAGLKQQALPYSRR(N)	281	317
(R)RNHKGGVTFVIQGALDDVEILR(A)	317	338
(R)NHKGGVTFVIQGALDDVEILR(A)	318	338
(K)GGVTFVIQGALDDVEILR(A)	321	338
(R)ARQFVDSYYR(T)	339	348
(R)QFVDSYYR(T)	341	348
(R)YVQFAIELK(D)	354	362
(R)YVQFAIELKDDWLK(G)	354	367
(R)YVQFAIELKDDWLKGR(S)	354	369
(K)GRSFQYGAEGYIK(M)	368	380
(R)SFQYGAEGYIK(M)	370	380
(K)MSPGHWYFPSPL(-)	381	392

invA685aa

Unique Peptides: 7
Sequence Coverage: **9%**

Sequence	Start	Stop
(K)QMSIDADLK(A)	152	160
(K)AGIIDADAAR(E)	161	170
(K)AGIIDADAARER(R)	161	172
(K)VSTETVPLILLVPK(S)	355	368
(R)LPEVLLR(D)	395	401
(R)NVNEYFGIQETK(H)	492	503
(R)AVMVSAEVEDVIR(K)	590	602

>sp|P41786|PRGK_SALTY Lipoprotein prgK OS=Salmonella typhimurium

Unique Peptides: 18
Sequence Coverage: **65%**

Sequence	Start	Stop
(K)GLDQEQANEVIAVLQMHNIEANK(I)	26	48
(K)GLDQEQANEVIAVLQMHNIEANKIDSGK(L)	26	53
(K)LGYSITVAEPDFTAAVYWIK(T)	54	73
(K)TYQLPPRPR(V)	74	82
(K)TYQLPPRPRVEIAQMFPADSLVSSPR(A)	74	99
(R)VEIAQMFPADSLVSSPR(A)	83	99
(R)VEIAQMFPADSLVSSPRAEK(A)	83	102
(R)VEIAQMFPADSLVSSPRAEKAR(L)	83	104
(R)LYSAIEQR(L)	105	112
(R)LEQSLQTMEGVLSAR(V)	113	127
(R)GSPLAHQISDIK(R)	157	168
(R)GSPLAHQISDIKR(F)	157	169
(R)FLKNSFADVDYDNISVVLSER(S)	170	190
(K)NSFADVDYDNISVVLSER(S)	173	190
(R)SDAQLQAPGTPVK(R)	191	203
(R)SDAQLQAPGTPVKR(N)	191	204
(K)KGITADDKAK(S)	239	248
(K)GITADDKAKSSNE(-)	240	252

>sp|P35672|INVG_SALTY Protein invG OS=Salmonella typhimurium

Unique Peptides: 29

Sequence Coverage: **56%**

Sequence	Start	Stop
(K)IPVTGSGFVAK(D)	28	38
(K)IPVTGSGFVAKDDSLR(T)	28	43
(K)DDSLRTFFDAMALQLKEPVIVSK(M)	39	61
(R)TFFDAMALQLK(E)	44	54
(K)ITGNFEFHDPNALLEK(L)	68	83
(R)NVSLNEFNNFLK(R)	116	127
(R)NVSLNEFNNFLKR(S)	116	128
(R)SGLYNKNYPLR(G)	129	139
(R)KGTFYVSGPPVYVDMVVNAATMMDK(Q)	144	168
(K)QNDGIELGR(Q)	169	177
(R)LNNTFVGDR(T)	185	193
(K)MVIPGIATAIER(L)	202	213
(K)AANYAGGMSLQEALK(Q)	245	259
(K)LGVSLNQSSISTLDGSR(F)	335	351
(R)FIAAVNALEEK(K)	352	362
(K)KQATVVSRPVLLTQENVPAIFDNNR(T)	363	387
(K)QATVVSRPVLLTQENVPAIFDNNR(T)	364	387
(R)NVALEHVTYGTMIR(V)	398	411
(K)TPQSDTTTSVDALPEVGR(T)	435	452
(R)TLISTIARVPHGK(S)	453	465
(K)LPLIGSLFR(Y)	490	498
(R)YSSKNKSNVVR(V)	499	509
(R)VFMIEPK(E)	510	516
(R)VFMIEPKEIVDPLTPDASESVNNILK(Q)	510	535
(K)EIVDPLTPDASESVNNILK(Q)	517	535
(K)QSGAWSGDDKLQK(W)	536	548
(K)QSGAWSGDDKLQKWVR(V)	536	551
(R)VYLDRGQEAIK(-)	552	562

spaP224aa

not identified

>sp|P41785|PRGJ_SALTY Protein prgJ OS=Salmonella typhimurium

not identified

spaQ86aa

not identified

spaR263aa

not identified

spaS356aa

not identified

ΔSpaR

>sp|P41783|PRGH_SALTY Protein prgH OS=Salmonella typhimurium

Unique Peptides: 37
Sequence Coverage: **71%**

Sequence	Start	Stop
(-)METSKEKTITSPGPYIVR(L)	1	18
(K)TITSPGPYIVR(L)	8	18
(R)LLNSSLNGcEFPLLTGR(T)	19	35
(R)SVQLNTPIQVGELLILIRPESEPWVPEQPEK(L)	96	126
(R)QAAELDSLLGQEK(E)	169	181
(R)QAAELDSLLGQEKER(F)	169	183
(R)FQVLPGR(D)	184	190
(R)FQVLPGRDK(M)	184	192
(R)FQVLPGRDKMLYVAAQNER(D)	184	202
(R)DKMLYVAAQNER(D)	191	202
(R)DKMLYVAAQNERDTLWAR(Q)	191	208
(K)mLYVAAQNER(D)	193	202
(K)MLYVAAQNERDTLWAR(Q)	193	208
(R)QVLARGDYDKNAR(V)	209	221
(R)VINENEENKR(I)	222	231
(R)VINENEENKRISIWLDTYYPQLAYYR(I)	222	247
(R)ISIWLDTYYPQLAYYR(I)	232	247
(R)IHFDEPR(K)	248	254
(R)IHFDEPRKPVFWLSR(Q)	248	262
(R)KPVFWLSR(Q)	255	262
(R)NTMSKKELEVLSQK(L)	265	278
(K)KELEVLSQK(L)	270	278
(K)KELEVLSQKLR(A)	270	280
(K)ELEVLSQK(L)	271	278
(K)ELEVLSQKLR(A)	271	280
(R)ALmPYADSVNITLMDDVTAAGQAEAGLK(Q)	281	308
(R)ALMPYADSVNITLMDDVTAAGQAEAGLKQQALPYSR(R)	281	316
(R)ALMPYADSVNITLMDDVTAAGQAEAGLKQQALPYSRR(N)	281	317
(R)RNHKGGVTFVIQGALDDVEILR(A)	317	338
(R)NHKGGVTFVIQGALDDVEILR(A)	318	338
(K)GGVTFVIQGALDDVEILR(A)	321	338
(R)QFVDSYYR(T)	341	348
(R)YVQFAIELKDDWLK(G)	354	367
(R)YVQFAIELKDDWLKGR(S)	354	369
(K)GRSFQYGAEGYIK(M)	368	380
(R)SFQYGAEGYIK(M)	370	380
(K)MSPGHWYFPSPL(-)	381	392

invA685aa

Unique Peptides: 4
Sequence Coverage: **7%**

Sequence	Start	Stop
(R)FSLDGMPGKQMSIDADLK(A)	143	160
(K)AGIIDADAAR(E)	161	170
(R)SQFFIDYGVR(L)	385	394
(R)AVMVSAEVEDVIR(K)	590	602

>sp|P41786|PRGK_SALTY Lipoprotein prgK OS=Salmonella typhimurium

Unique Peptides: 16
Sequence Coverage: **55%**

Sequence	Start	Stop	
(K)GLDQEQANEVIAVLQMHNIEANK(I)		26	48
(K)GLDQEQANEVIAVLQMHNIEANKIDSGK(L)		26	53
(K)TYQLPPRPR(V)		74	82
(R)VEIAQMFPADSLVSSPR(A)		83	99
(R)VEIAQMFPADSLVSSPRAEK(A)		83	102
(R)LYSAIEQR(L)		105	112
(R)LYSAIEQRLEQSLQTMEGVLSAR(V)		105	127
(R)LEQSLQTMEGVLSAR(V)		113	127
(R)GSPLAHQISDIK(R)		157	168
(R)GSPLAHQISDIKR(F)		157	169
(R)FLKNSFADVDYDNISVVLSER(S)		170	190
(K)NSFADVDYDNISVVLSER(S)		173	190
(R)SDAQLQAPGTPVK(R)		191	203
(R)SDAQLQAPGTPVKR(N)		191	204
(K)GITADDKAK(S)		240	248
(K)GITADDKAKSSNE(-)		240	252

>sp|P35672|INVG_SALTY Protein invG OS=Salmonella typhimurium

Unique Peptides: 25

Sequence Coverage: **43%**

Sequence	Start	Stop	
(K)IPVTGSGFVAK(D)		28	38
(K)IPVTGSGFVAKDDSLR(T)		28	43
(K)DDSLRTFFDAMALQLKEPVIVSK(M)		39	61
(R)TFFDAMALQLK(E)		44	54
(R)TFFDAMALQLKEPVIVSK(M)		44	61
(R)KKITGNFEFHDPNALLEK(L)		66	83
(K)KITGNFEFHDPNALLEK(L)		67	83
(K)ITGNFEFHDPNALLEK(L)		68	83
(R)NVSLNEFNNFLK(R)		116	127
(R)NVSLNEFNNFLKR(S)		116	128
(R)SGLYNKNYPLR(G)		129	139
(R)KGTFYVSGPPVYVDMVVNAATMMDK(Q)		144	168
(R)KGTFYVSGPPVYVDMVVNAATMMDKQNDGIELGR(Q)		144	177
(K)QNDGIELGR(Q)		169	177
(K)MVIPGIATAIER(L)		202	213
(K)AANYAGGMSLQEALK(Q)		245	259
(K)LGVSLNQSSISTLDGSR(F)		335	351
(R)NVALEHVTYGTMIR(V)		398	411
(K)TPQSDTTTSVDALPEVGR(T)		435	452
(R)TLISTIAR(V)		453	460
(K)SLLVGGYTR(D)		466	474
(K)LPLIGSLFR(Y)		490	498
(R)VFMIEPK(E)		510	516
(K)QSGAWSGDDKLQK(W)		536	548
(R)VYLDRGQEAIK(-)		552	562

>sp|P41784|PRGI_SALTY Protein prgI OS=Salmonella typhimurium

not identified

spaP224aa

not identified

>sp|P41785|PRGJ_SALTY Protein prgJ OS=Salmonella typhimurium

not identified

spaQ86aa

not identified

spaR263aa

not identified

spaS356aa

not identified

ΔSpaS

>sp|P41783|PRGH_SALTY Protein prgH OS=Salmonella typhimurium

Unique peptides: **34**
Sequence Coverage: **71%**

Sequence	Start	Stop
(-)mETSKEKTITSPGPYIVR(L)	1	18
(K)EKTITSPGPYIVR(L)	6	18
(K)TITSPGPYIVR(L)	8	18
(R)LLNSSLNGcEFPLLTGR(T)	19	35
(R)SVQLNTPIQVGELLILIRPESEPWVPEQPEK(L)	96	126
(R)SVQLNTPIQVGELLILIRPESEPWVPEQPEKLETSAK(K)	96	132
(R)qAAELDSLLGQEK(E)	169	181
(R)QAAELDSLLGQEKER(F)	169	183
(K)ERFQVLPGRDK(M)	182	192
(R)FQVLPGR(D)	184	190
(R)FQVLPGRDK(M)	184	192
(R)FQVLPGRDKMLYVAAQNER(D)	184	202
(K)mLYVAAQNER(D)	193	202
(K)MLYVAAQNERDTLWAR(Q)	193	208
(R)qVLARGDYDK(N)	209	218
(R)qVLARGDYDKNAR(V)	209	221
(R)VINENEENKR(I)	222	231
(R)ISIWLDTYYPQLAYYR(I)	232	247
(R)IHFDEPR(K)	248	254
(R)IHFDEPRKPVFWLSR(Q)	248	262
(R)KPVFWLSR(Q)	255	262
(R)NTMSKKELEVLSQK(L)	265	278
(K)KELEVLSQK(L)	270	278
(K)KELEVLSQKLR(A)	270	280
(K)ELEVLSQKLR(A)	271	280
(R)ALMPYADSVNITLMDDVTAAGQAEAGLK(Q)	281	308
(K)QQALPYSR(R)	309	316
(K)GGVTFVIQGALDDVEILR(A)	321	338
(R)ARQFVDSYYR(T)	339	348
(R)qFVDSYYR(T)	341	348
(R)YVQFAIELK(D)	354	362
(K)GRSFQYGAEGYIK(M)	368	380
(R)SFQYGAEGYIK(M)	370	380
(K)MSPGHWYFPSPL(-)	381	392

invA685aa

Unique peptides: **9**
Sequence Coverage: **14%**

Sequence	Start	Stop
(K)AGIIDADAAR(E)	161	170
(K)TSKGEQPLSIEEK(E)	329	341
(K)EGSSLGLIGDLDK(V)	342	354
(K)VSTETVPLILLVPK(S)	355	368
(R)SQFFIDYGVR(L)	385	394
(R)LPEVLLR(D)	395	401
(R)NVNEYFGIQETK(H)	492	503
(K)DVINLVEHIR(G)	562	571
(R)AVMVSAEVEDVIR(K)	590	602

>sp|P41786|PRGK_SALTY Lipoprotein prgK OS=Salmonella typhimurium

Unique peptides: **16**
Sequence Coverage: **54%**

Sequence	Start	Stop
(K)GLDQEQANEVIAVLQMHNIEANK(I)	26	48
(K)TYQLPPRPR(V)	74	82
(R)VEIAQMFPADSLVSSPR(A)	83	99
(R)VEIAQMFPADSLVSSPRAEK(A)	83	102
(R)VEIAQMFPADSLVSSPRAEKAR(L)	83	104
(R)AEKARLYSAIEQR(L)	100	112

(K)ARLYSAIEQR(L)	103	112
(R)LYSAIEQR(L)	105	112
(R)LEQSLQTMEGVLSAR(V)	113	127
(R)GSPLAHQISDIK(R)	157	168
(R)GSPLAHQISDIKR(F)	157	169
(K)NSFADVDYDNISVVLSER(S)	173	190
(R)SDAQLQAPGTPVK(R)	191	203
(R)SDAQLQAPGTPVKR(N)	191	204
(K)KGITADDKAK(S)	239	248
(K)GITADDKAKSSNE(-)	240	252

>sp|P35672|INVG_SALTY Protein invG OS=Salmonella typhimurium

Unique peptides: **33**
Sequence Coverage: **64%**

Sequence	Start	Stop
(K)IPVTGSGFVAK(D)	28	38
(K)IPVTGSGFVAKDDSLR(T)	28	43
(R)TFFDAMALQLK(E)	44	54
(R)TFFDAmALQLKEPVIVSK(M)	44	61
(K)KITGNFEFHDPNALLEK(L)	67	83
(K)ITGNFEFHDPNALLEK(L)	68	83
(R)NVSLNEFNNFLK(R)	116	127
(R)NVSLNEFNNFLKR(S)	116	128
(R)SGLYNKNYPLR(G)	129	139
(R)KGTFYVSGPPVYVDMVVNAATMMDK(Q)	144	168
(K)QNDGIELGR(Q)	169	177
(R)QKIGVMR(L)	178	184
(R)LNNTFVGDR(T)	185	193
(R)LNNTFVGDRTYNLRDQK(M)	185	201
(K)mVIPGIATAIER(L)	202	213
(K)AANYAGGMSLQEALK(Q)	245	259
(K)IVAYPDTNSLLVK(G)	269	281
(K)GTAEQVHFIEMLVK(A)	282	295

>sp|P41784|PRGI_SALTY Protein prgI OS=Salmonella typhimurium

not identified

spaP224aa

Unique peptides: **8**
Sequence Coverage: **22%**

Sequence	Start	Stop
(K)HVDEGLDGYR(D)	91	100
(K)HVDEGLDGYRDYLIK(Y)	91	105
(R)ELVQFFENAQLK(R)	110	121
(R)ELVQFFENAQLKR(Q)	110	122
(K)RQYGEETETVKR(D)	122	133
(R)QYGEETETVK(R)	123	132
(R)qYGEETETVKR(D)	123	133
(K)GLILQYMDIAT(-)	214	224

>sp|P41785|PRGJ_SALTY Protein prgJ OS=Salmonella typhimurium
not identified

spaQ86aa
not identified

spaR263aa
not identified

spaS356aa
not identified

ΔInvA

>sp|P41783|PRGH_SALTY Protein prgH OS=Salmonella typhimurium

Unique Peptides: 32
Sequence Coverage: **53%**

Sequence	Start	Stop
(-)METSKEKTITSPGPYIVR(L)	1	18
(K)EKTITSPGPYIVR(L)	6	18
(K)TITSPGPYIVR(L)	8	18
(K)LETSAKKNEPR(F)	127	137
(R)QAAELDSLLGQEK(E)	169	181
(R)QAAELDSLLGQEKER(F)	169	183
(R)FQVLPGR(D)	184	190
(R)FQVLPGRDK(M)	184	192
(R)DKMLYVAAQNER(D)	191	202
(K)mLYVAAQNER(D)	193	202
(K)MLYVAAQNERDTLWAR(Q)	193	208
(R)DTLWAR(Q)	203	208
(R)QVLARGDYDK(N)	209	218
(R)QVLARGDYDKNAR(V)	209	221
(R)GDYDKNAR(V)	214	221
(R)VINENEENK(R)	222	230
(R)VINENEENKR(I)	222	231
(R)ISIWLDTYYPQLAYYR(I)	232	247
(R)IHFDEPR(K)	248	254
(R)KPVFWLSR(Q)	255	262
(R)NTmSKKELEVLSQK(L)	265	278
(K)KELEVLSQK(L)	270	278
(K)KELEVLSQKLR(A)	270	280
(K)ELEVLSQK(L)	271	278
(K)ELEVLSQKLR(A)	271	280
(R)ALMPYADSVNITLMDDVTAAGQAEAGLKQQALPYSR(R)	281	316
(K)qQALPYSR(R)	309	316
(R)ARQFVDSYYR(T)	339	348
(R)QFVDSYYR(T)	341	348
(K)GRSFQYGAEGYIK(M)	368	380
(R)SFQYGAEGYIK(M)	370	380
(K)MSPGHWYFPSPL(-)	381	392

>sp|P41786|PRGK_SALTY Lipoprotein prgK OS=Salmonella typhimurium

Unique Peptides: 11
Sequence Coverage: **35%**

Sequence	Start	Stop
(K)TYQLPPRPR(V)	74	82
(R)VEIAQmFPADSLVSSPR(A)	83	99
(R)LYSAIEQR(L)	105	112
(R)LEQSLQTMEGVLSAR(V)	113	127
(R)GSPLAHQISDIK(R)	157	168
(R)GSPLAHQISDIKR(F)	157	169
(R)SDAQLQAPGTPVK(R)	191	203
(R)SDAQLQAPGTPVKR(N)	191	204
(K)KGITADDKAK(S)	239	248
(K)GITADDKAK(S)	240	248
(K)GITADDKAKSSNE(-)	240	252

>sp|P35672|INVG_SALTY Protein invG OS=Salmonella typhimurium

Unique Peptides: 20
Sequence Coverage: **35%**

Sequence	Start	Stop
(K)IPVTGSGFVAK(D)	28	38
(K)IPVTGSGFVAKDDSLR(T)	28	43
(R)TFFDAMALQLKEPVIVSK(M)	44	61
(K)EPVIVSK(M)	55	61
(R)NAVVSLR(N)	109	115
(R)NVSLNEFNNFLK(R)	116	127
(R)NVSLNEFNNFLKR(S)	116	128

(R)SGLYNKNYPLR(G)	129	139
(R)qKIGVMR(L)	178	184
(R)LNNTFVGDR(T)	185	193
(K)mVIPGIATAIER(L)	202	213
(K)AANYAGGMSLQEALK(Q)	245	259
(K)IVAYPDTNSLLVK(G)	269	281
(R)FIAAVNALEEK(K)	352	362
(R)TLISTIAR(V)	453	460
(K)SLLVGGYTR(D)	466	474
(R)DANTDTVQSIPFLGK(L)	475	489
(R)VFMIEPK(E)	510	516
(K)QSGAWSGDDKLQK(W)	536	548
(R)VYLDRGQEAIK(-)	552	562

spaS356aa

Unique Peptides: 2
Sequence Coverage: **6%**

Sequence	Start	Stop
(R)EMKEQEGNPEVK(S)	219	230
(R)EVHMEILSEQVK(S)	235	246

spaP224aa

Unique Peptides: 4
Sequence Coverage: **12%**

Sequence	Start	Stop
(K)HVDEGLDGYRDYLIK(Y)	91	105
(K)RQYGEETETVKR(D)	122	133
(R)qYGEETETVK(R)	123	132
(R)QYGEETETVKR(D)	123	133

spaQ86aa
not identified

spaR263aa
not identified

invA685aa
not identified

>sp|P41784|PRGI_SALTY Protein prgI OS=Salmonella typhimurium
not identified

>sp|P41785|PRGJ_SALTY Protein prgJ OS=Salmonella typhimurium
not identified

ΔInvC

>sp|P41783|PRGH_SALTY Protein prgH OS=Salmonella typhimurium

Unique Peptides: 49
Sequence Coverage: **98%**

Sequence	Start	Stop
(-)METSKEKTITSPGPYIVR(L)	1	18
(K)EKTITSPGPYIVR(L)	6	18
(K)TITSPGPYIVR(L)	8	18
(R)LLNSSLNGcEFPLLTGR(T)	19	35
(R)TLFVVGQSDALTASGQLPDIPADSFFIPLDHGGVNFEIQVDTDATEII LHELKEGNSESR(S)	36	95
(R)SVQLNTPIQVGELLILIRPESEPWVPEQPEK(L)	96	126
(R)SVQLNTPIQVGELLILIRPESEPWVPEQPEKLETSAK(K)	96	132
(K)LETSAKKNEPR(F)	127	137
(R)FKNGIVAALAGFFILGIGTVGTLWILNSPQR(Q)	138	168
(R)FKNGIVAALAGFFILGIGTVGTLWILNSPQRQAAELDSLLGQEK(E)	138	181
(R)FKNGIVAALAGFFILGIGTVGTLWILNSPQRQAAELDSLLGQEKER(F)	138	183
(K)NGIVAALAGFFILGIGTVGTLWILNSPQR(Q)	140	168
(R)qAAELDSLLGQEK(E)	169	181
(R)QAAELDSLLGQEKER(F)	169	183
(R)FQVLPGR(D)	184	190
(R)FQVLPGRDK(M)	184	192
(R)FQVLPGRDKMLYVAAQNER(D)	184	202
(R)DKmLYVAAQNER(D)	191	202
(R)DKMLYVAAQNERDTLWAR(Q)	191	208
(K)MLYVAAQNER(D)	193	202
(K)mLYVAAQNERDTLWAR(Q)	193	208
(R)DTLWAR(Q)	203	208
(R)QVLARGDYDK(N)	209	218
(R)qVLARGDYDKNAR(V)	209	221
(R)VINENEENK(R)	222	230
(R)VINENEENKR(I)	222	231
(R)ISIWLDTYYPQLAYYR(I)	232	247
(R)IHFDEPR(K)	248	254
(R)IHFDEPRKPVFWLSR(Q)	248	262
(R)KPVFWLSR(Q)	255	262
(K)PVFWLSR(Q)	256	262
(R)QRNTMSKKELEVLSQK(L)	263	278
(R)NTMSKKELEVLSQK(L)	265	278
(R)NTmSKKELEVLSQKLR(A)	265	280
(K)KELEVLSQK(L)	270	278
(K)KELEVLSQKLR(A)	270	280
(K)ELEVLSQKLR(A)	271	280
(R)ALMPYADSVNITLMDDVTAAGQAEAGLK(Q)	281	308
(R)ALMPYADSVNITLmDDVTAAGQAEAGLKQQALPYSR(R)	281	316
(R)ALmPYADSVNITLMDDVTAAGQAEAGLKQQALPYSRR(N)	281	317
(R)RNHKGGVTFVIQGALDDVEILR(A)	317	338
(R)NHKGGVTFVIQGALDDVEILR(A)	318	338
(K)GGVTFVIQGALDDVEILR(A)	321	338
(R)ARQFVDSYYR(T)	339	348
(R)YVQFAIELK(D)	354	362
(R)YVQFAIELKDDWLK(G)	354	367
(R)YVQFAIELKDDWLKGR(S)	354	369
(R)SFQYGAEGYIK(M)	370	380
(K)MSPGHWYFPSPL(-)	381	392

invA685aa

Unique Peptides: 10
Sequence Coverage: **17%**

Sequence	Start	Stop
(R)FSLDGmPGK(Q)	143	151
(K)AGIIDADAAR(E)	161	170
(K)TSKGEQPLSIEEK(E)	329	341
(K)EGSSLGLIGDLDKVSTETVPLILLVPK(S)	342	368
(K)VSTETVPLILLVPK(S)	355	368
(K)SRREDLEKAQLAER(L)	369	382
(R)LPEVLLR(D)	395	401
(R)NVNEYFGIQETK(H)	492	503
(R)AVMVSAEVEDVIR(K)	590	602

(R)FPDLEVLSFGEIADSK(S)	662	677

>sp|P41786|PRGK_SALTY Lipoprotein prgK OS=Salmonella typhimurium

Unique Peptides: 24
Sequence Coverage: **78%**

Sequence	Start	Stop
(K)GLDQEQANEVIAVLQMHNIEANK(I)	26	48
(K)GLDQEQANEVIAVLQMHNIEANKIDSGK(L)	26	53
(K)LGYSITVAEPDFTAAVYWIK(T)	54	73
(K)LGYSITVAEPDFTAAVYWIKTYQLPPRPR(V)	54	82
(K)TYQLPPRPR(V)	74	82
(R)VEIAQmFPADSLVSSPR(A)	83	99
(R)VEIAQmFPADSLVSSPRAEK(A)	83	102
(R)VEIAQMFPADSLVSSPRAEKAR(L)	83	104
(R)LYSAIEQR(L)	105	112
(R)LYSAIEQRLEQSLQTMEGVLSAR(V)	105	127
(R)LEQSLQTMEGVLSAR(V)	113	127
(R)GSPLAHQISDIK(R)	157	168
(R)GSPLAHQISDIKR(F)	157	169
(R)FLKNSFADVDYDNISVVLSER(S)	170	190
(K)NSFADVDYDNISVVLSER(S)	173	190
(R)SDAQLQAPGTPVK(R)	191	203
(R)SDAQLQAPGTPVKR(N)	191	204
(R)SDAQLQAPGTPVKRNSFATSWIVLIILLSVMSAGFGVWYYKNHYAR(N)	191	236
(R)NSFATSWIVLIILLSVMSAGFGVWYYKNHYAR(N)	205	236
(R)NKKGITADDK(A)	237	246
(R)NKKGITADDKAK(S)	237	248
(K)KGITADDKAK(S)	239	248
(K)KGITADDKAKSSNE(-)	239	252
(K)GITADDKAKSSNE(-)	240	252

>sp|P35672|INVG_SALTY Protein invG OS=Salmonella typhimurium

Unique Peptides: 38
Sequence Coverage: **64%**

Sequence	Start	Stop
(K)IPVTGSGFVAK(D)	28	38
(K)IPVTGSGFVAKDDSLR(T)	28	43
(K)DDSLRTFFDAMALQLKEPVIVSK(M)	39	61
(R)TFFDAMALQLK(E)	44	54
(R)TFFDAmALQLKEPVIVSK(M)	44	61
(R)KKITGNFEFHDPNALLEK(L)	66	83
(K)KITGNFEFHDPNALLEK(L)	67	83
(K)ITGNFEFHDPNALLEK(L)	68	83
(K)LSLQLGLIWYFDGQAIYIYDASEMR(N)	84	108
(R)NAVVSLR(N)	109	115
(R)NVSLNEFNNFLK(R)	116	127
(R)NVSLNEFNNFLKR(S)	116	128
(K)RSGLYNK(N)	128	134
(R)SGLYNKNYPLR(G)	129	139
(R)KGTFYVSGPPVYVDMVVNAATMMDK(Q)	144	168
(R)KGTFYVSGPPVYVDMVVNAATMMDKQNDGIELGR(Q)	144	177
(R)KGTFYVSGPPVYVDMVVNAATmMDKQNDGIELGRQK(I)	144	179
(K)QNDGIELGR(Q)	169	177
(K)qNDGIELGRQK(I)	169	179
(K)IGVMRLNNTFVGDR(T)	180	193
(R)LNNTFVGDR(T)	185	193
(R)LNNTFVGDRTYNLR(D)	185	198
(R)LNNTFVGDRTYNLRDQK(M)	185	201
(K)mVIPGIATAIER(L)	202	213
(K)AANYAGGMSLQEALK(Q)	245	259
(K)AANYAGGMSLQEALKQNAAAGNIK(I)	245	268
(K)IVAYPDTNSLLVK(G)	269	281
(K)LGVSLNQSSISTLDGSR(F)	335	351
(R)FIAAVNALEEKK(Q)	352	363
(K)KQATVVSRPVLLTQENVPAIFDNNR(T)	363	387
(R)NVALEHVTYGTMIR(V)	398	411
(R)TLISTIAR(V)	453	460

(K)SLLVGGYTR(D)	466	474
(R)DANTDTVQSIPFLGK(L)	475	489
(K)LPLIGSLFR(Y)	490	498
(R)VFMIEPK(E)	510	516
(K)EIVDPLTPDASESVNNILK(Q)	517	535
(R)VYLDRGQEAIK(-)	552	562

>sp|P41784|PRGI_SALTY Protein prgI OS=Salmonella typhimurium

not identified

spaP224aa

Unique Peptides: 11
Sequence Coverage: **24%**

Sequence	Start	Stop
(K)HVDEGLDGYR(D)	91	100
(K)HVDEGLDGYRDYLIK(Y)	91	105
(K)YSDRELVQFFENAQLK(R)	106	121
(K)YSDRELVQFFENAQLKR(Q)	106	122
(R)ELVQFFENAQLK(R)	110	121
(R)ELVQFFENAQLKR(Q)	110	122
(K)RQYGEETETVK(R)	122	132
(K)RQYGEETETVKR(D)	122	133
(R)QYGEETETVK(R)	123	132
(R)qYGEETETVKR(D)	123	133
(K)GLILQYMDIAT(-)	214	224

>sp|P41785|PRGJ_SALTY Protein prgJ OS=Salmonella typhimurium

not identified

spaQ86aa

not identified

spaS356aa

Unique Peptides: 1
Sequence Coverage: **2%**

Sequence	Start	Stop
(K)VGVPVIVDIK(L)	297	306

12.5. Publication

PNAS PNAS PNAS PNAS

Organization and coordinated assembly of the type III secretion export apparatus

Samuel Wagner[a], Lisa Königsmaier[b,c], María Lara-Tejero[a], Matthew Lefebre[a], Thomas C. Marlovits[b,c,1], and Jorge E. Galán[a,1]

[a]Section of Microbial Pathogenesis, Yale University School of Medicine, New Haven, CT 06536; [b]Research Institute of Molecular Pathology, A-1030 Vienna, Austria; and [c]Institute of Molecular Biotechnology, Austrian Academy of Sciences, A-1030 Vienna, Austria

Edited by Thomas J. Silhavy, Princeton University, Princeton, NJ, and approved September 7, 2010 (received for review June 8, 2010)

Type III protein secretion systems are unique bacterial nanomachines with the capacity to deliver bacterial effector proteins into eukaryotic cells. These systems are critical to the biology of many pathogenic or symbiotic bacteria for insects, plants, animals, and humans. Essential components of these systems are multiprotein envelope-associated organelles known as the needle complex and a group of membrane proteins that compose the so-called export apparatus. Here, we show that components of the export apparatus associate intimately with the needle complex, forming a structure that can be visualized by cryo-electron microscopy. We also show that formation of the needle complex base is initiated at the export apparatus and that, in the absence of export apparatus components, there is a significant reduction in the levels of needle complex base assembly. Our results show a substantial coordination in the assembly of the two central elements of type III secretion machines.

bacterial pathogenesis | cryo-electron microscopy | membrane proteins | organelle assembly | protein secretion

Widespread among bacteria pathogenic for plants, animals, or humans, type III secretion systems (T3SS) are essential for the establishment of intimate bacteria/host cell interactions (1, 2). Evolutionary and structurally related to flagella (3), these systems are among the most complex protein secretion systems known. *Salmonella enterica* serovar Typhimurium (*S.* Typhimurium) encodes one of these systems within its pathogenicity island 1 (SPI-1) (4), which is essential for this pathogen's ability to invade and replicate within mammalian host cells (5). Central components of type III secretion machines are the bacterial envelope-associated needle complex (NC) and the export apparatus, which makes the NC competent for secretion. The NC is composed of a multiring base (made up in the *S.* Typhimurium SPI-1 T3SS by the InvG, PrgH, and PrgK proteins), a central inner rod (made up by PrgJ), and a protruding needle-like structure (made up by PrgI), which is traversed by ~28 Å-wide channel that serves as a conduit for passage of the secreted proteins through the bacterial envelope (6, 7). The recent availability of the crystal structures of soluble domains of some of the components of the NC (8–10), combined with their docking onto the NC protein density map generated by cryo-electron microscopy (7, 11), is beginning to provide a high-resolution view of this organelle (12). Previous studies have shown that assembly of the needle complex occurs in an orderly manner, in which the base substructure is assembled first, followed by the assembly of the inner rod and needle substructure (13, 14). The assembly of the last two substructures requires the base to be rendered secretion-competent by the export apparatus, thus gaining the ability to secrete the needle and inner rod subunits. After the needle complex is fully assembled, the secretion machine switches substrate specificity, becoming competent for the secretion of translocases and effector proteins. Much less is known about the arrangement of the export apparatus, which is composed of a collection of highly conserved membrane proteins (InvA, SpaP, SpaQ, SpaR, and SpaS in the *S.* Typhimurium SPI-1–encoded T3SS) (1–3). Although all of the components of the export apparatus are essential for type III secretion, it is unknown whether these membrane proteins exert a common function or even if they exist as a single complex within the bacterial envelope. Furthermore, their functional and topological relationship to the NC is unknown. In this paper, we have investigated in *S.* Typhimurium the localization of the membrane proteins that make up the export apparatus and examined their role in the assembly of the NC. We found that membrane protein components of the export apparatus are intimately associated with the base substructure of the NC, forming a defined structure that can be visualized by cryo-electron microscopy. In addition, we found that formation of the NC base is initiated at the export apparatus and that the presence of export apparatus components is required for the assembly of a functional NC. These findings revealed a substantial coordination in the assembly of the export apparatus and NC components of the T3SS.

Results

Export Apparatus Is Intimately Associated with the NC. It has been previously shown that at least some components of the export apparatus are associated or cofractionate with the NC or the hook–basal body complex (a functional equivalent of the NC in flagella) (15, 16). Therefore, we investigated whether the components of the export apparatus of the *S.* Typhimurium SPI-1–encoded T3SS could be isolated in association with the NC. Because previously reported stringent NC isolation protocols may affect the identification of associated components (6), we developed a protocol to examine NC under milder conditions (*SI Materials and Methods* and Fig. S1). We first analyzed NC and associated proteins using 2D blue native PAGE (BN-PAGE). The NC and associated proteins migrated as a distinct band with a mobility that is consistent with that of a complex larger than 1,200 kDa (Fig. 1*A* and Fig. S2). Proteins making up this complex were identified by liquid chromatography followed by tandem MS (LC-MS/MS) and/or Western immunoblotting. In addition to the structural components of the inner and outer rings of the NC (PrgH, PrgK, and InvG) (6) and the needle and inner rod proteins (PrgI and PrgJ) (17, 18), we detected the export apparatus components InvA (19), SpaP, and SpaS (20) (Table S1). To validate the interaction of the export apparatus components with the NC base, we immunoprecipitated the complex from a strain carrying a carboxy terminal FLAG-epitope tagged allele of SpaS ($SpaS^{N258A}$), which carries a mutation in its catalytic, autoprocessing site, thus preventing the cleavage of its carboxyl terminus (21, 22). Proteins affinity purified with an anti-FLAG antibody were separated by BN-PAGE, and the band corresponding to the NC was analyzed by LC-MS/MS. This

Author contributions: S.W., L.K., M.L.-T., T.C.M., and J.E.G. designed research; S.W., L.K., M.L.-T., and M.L. performed research; S.W., L.K., M.L.-T., T.C.M., and J.E.G. analyzed data; and S.W. and J.E.G. wrote the paper.

The authors declare no conflict of interest.

This article is a PNAS Direct Submission.

Data deposition: The mass spectrometry data have been deposited on http://yped.med.yale.edu/repository (accession: Samuel Wagner).

[1]To whom correspondence may be addressed. E-mail: marlovits@imp.ac.at or jorge.galan@yale.edu.

This article contains supporting information online at www.pnas.org/lookup/suppl/doi:10.1073/pnas.1008053107/-/DCSupplemental.

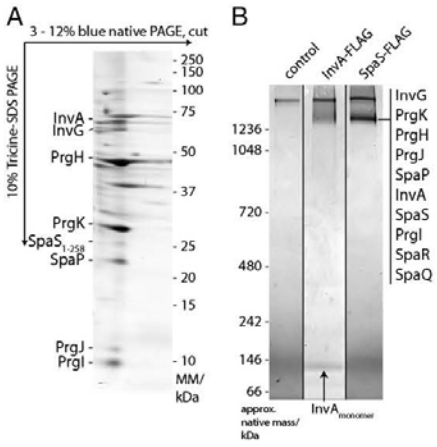

Fig. 1. The export apparatus is intimately associated with the NC. (*A*) Export apparatus components cofractionate with the NC. Protein complexes of purified *S.* Typhimurium inner membrane fractions were solubilized with n-dodecyl-β-D-maltopyranoside (DDM) and separated by 2D BN-PAGE. Indicated proteins were identified by LC-MS/MS or Western blotting. (*B*) The export apparatus interacts with the needle complex. DDM-solubilized inner membrane fraction proteins interacting with C-terminally FLAG-tagged InvA or SpaS^{N258A} were immunoprecipitated, separated by BN-PAGE, and identified by LC-MS/MS.

band contained all needle complex and export apparatus membrane protein components, including SpaR and SpaQ (Fig. 1*B*, Fig. S3, and Table S1). Similar results were obtained when the complex was immunoprecipitated from a strain expressing a functional FLAG-epitope tagged allele of InvA (Fig. 1*B*). Unlike SpaS, however, a significant amount of free InvA was also detected, suggesting a somewhat weaker association of InvA to the NC. Taken together, these results indicate that the export apparatus is intimately associated with the NC.

Export Apparatus Components Associate with One Another in the Absence of the NC. We investigated whether the components of the export apparatus themselves could form a complex in the absence of the NC. To this end, we constructed strains of *S.* Typhimurium expressing functional FLAG-tagged InvA, SpaP, SpaR, and SpaS (SpaQ could not be tagged in a manner that would retain function) in the context of the NC-defective Δ*prgHIJK* mutant. We purified inner membrane fractions from these strains and identified interacting proteins by immunoprecipitation combined with 2D BN-PAGE and LC-MS/MS analysis. We found that, in the absence of the NC, SpaP and SpaR could form a complex (Fig. 2*A*). In contrast, InvA and SpaS were not seen associated to any member of the export apparatus under the isolation conditions used in this assay (Fig. 2*A*). It is often the case that the stability of members of a multiprotein complex is compromised in the absence of other components of the complex (23). Therefore, we tested whether the stability of individual export apparatus components was compromised by the absence of other export apparatus components. Deletion of *spaP* resulted in reduced levels of SpaR (and vice versa) (Fig. 2*B*), presumably because of their reduced stability in the absence of their interacting partners. Furthermore, levels of SpaS^{N258A} were reduced in the absence of SpaP, SpaQ, and SpaR. In contrast, the levels of InvA were not affected by the removal of any of the other export apparatus components (Fig. 2*B*). These results indicate that a subset of the export apparatus components can assemble into a stable complex in the absence of the NC and that the members of this complex require each other for stability.

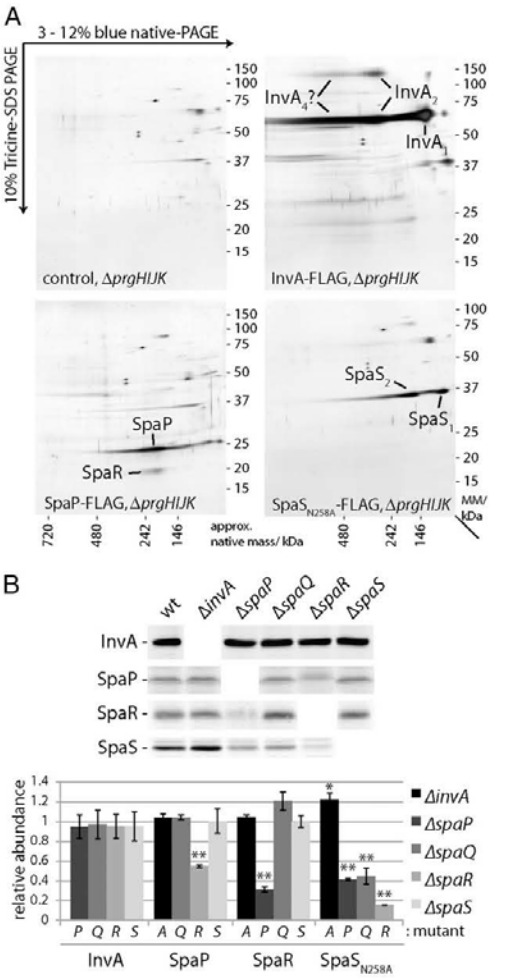

Fig. 2. Export apparatus components associate with one another in the absence of the needle complex. (*A*) The export apparatus components SpaP and SpaR form a complex in the absence of the NC. DDM-solubilized inner membrane fraction proteins of a *S.* Typhimurium Δ*prgH* Δ*prgI* Δ*prgJ* Δ*prgK* mutant strain expressing FLAG-epitope tagged SpaP, InvA, or SpaS^{N258A} (as indicated) were immunoprecipitated with an anti-FLAG antibody. Precipitated proteins were separated by 2D BN-PAGE, and indicated proteins were identified by LC-MS/MS. (*B*) The levels of SpaP, SpaR, and SpaS (but not InvA) are significantly reduced in the absence of some export apparatus components. Purified inner membrane fractions from wild-type *S.* Typhimurium (wt) or the Δ*spaP*, Δ*spaQ*, Δ*spaR*, Δ*spaS*, or Δ*invA* mutants expressing FLAG-epitope tagged InvA, SpaP, SpaR, or SpaS^{N258A} (as indicated) were analyzed by Western blotting (*Upper*). The intensity of the bands was quantified using the Odyssey imaging system (Li-Cor), and values represent the mean ± SD of three independent experiments (*Lower*). Values were standardized relative to a loading control (PrgH) and across different samples relative to wild type, which was assigned an arbitrary value of 1.

Hierarchy in the Recruitment of Export Apparatus Components to the NC. We analyzed the effect of removal of individual components of the export apparatus on the recruitment of the remaining export apparatus components to the NC using BN-PAGE combined with Western blotting and 2D BN-PAGE (Fig. 3 and

Fig. S4). Deletion of *invA* or *spaS* did not significantly affect the recruitment of any of the other components of the export apparatus to the NC base. In contrast, deletion of *spaP*, *spaQ*, or *spaR* resulted in the abrogation of the recruitment of all components of the export apparatus to the NC base. Taken together, these results indicate that there is a hierarchy in the recruitment of export apparatus components to the NC and that SpaP, SpaQ, and SpaR act first, playing a central role in the assembly process.

Export Apparatus Is Required for Efficient NC Base Assembly. The observation that the export apparatus is assembled in a coordinated fashion with the NC prompted us to examine the effect of the absence of export apparatus components on the assembly of the NC base. We have previously shown that NC base substructures can be detected in the absence of export apparatus components (13). However, using a quantitative assay, we found that deletion of *spaP*, *spaQ*, or *spaR* resulted in a drastic (~80%) reduction in the levels of NC bases, although the absence of the export apparatus did not affect the total levels of the NC individual components such as PrgH, PrgK, and InvG (Fig. 4 *A* and *B*). Consequently, the absence of SpaP, SpaQ, and SpaR also resulted in an accumulation of free NC protomers (Fig. 4*D*). In contrast, deletion of *invA* had no effect on the levels of assembled NC bases (or the accumulation of free protomers), whereas deletion of *spaS* had an intermediate phenotype (Fig. 4 *A* and *B*). Taken together, these results indicate that components of the export apparatus play an important role in the assembly and/or stability of the NC base.

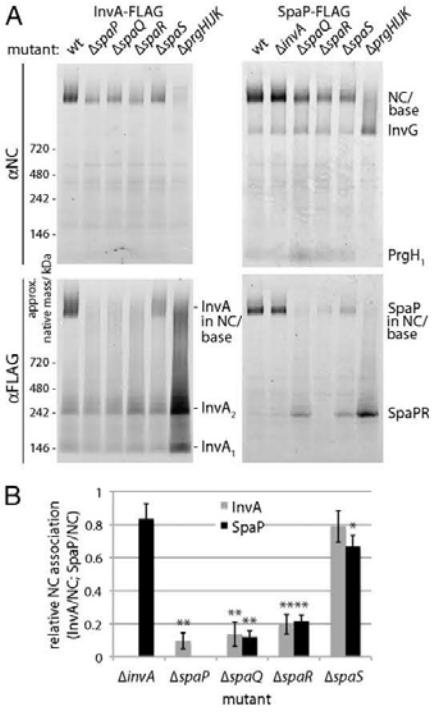

Fig. 3. Hierarchy in the recruitment to the needle complex of export apparatus components. Protein complexes of purified inner membrane fractions of wild type (wt) and the indicated mutants of *S.* Typhimurium expressing FLAG-epitope tagged InvA or SpaP were solubilized with DDM, separated by BN-PAGE, and analyzed by Western blotting using antibodies directed to the NC base or FLAG (to detect either SpaP or InvA; *A*). The intensity of the bands corresponding to SpaP or InvA associated with the NC was quantified as above (*B*), and values represent the mean ± SD of three independent experiments. Values were standardized relative to the levels of the NC and across different samples relative to wild type, which was assigned an arbitrary value of 1. The total levels of SpaP-FLAG and InvA-FLAG in the different mutants are shown in Fig. 2*B*.

To distinguish whether components of the export apparatus have an effect on the assembly or the stability of the NC base, we assayed to find out whether SpaP, SpaQ, SpaR, and SpaS were able to induce assembly of bases from presynthesized, free NC protomers. To this end, we constructed a strain in which expression of the NC components is controlled by an arabinose-inducible p^{araBAD} promoter (24) through the expression of HilA, the master transcriptional regulator of the SPI-1 T3SS (25). In addition, *invA* and *spaPQRS* were deleted from this strain and expressed from a low copy plasmid under the control of the rhamnose-inducible p^{rhaBAD} promoter (26). These strains and the growth conditions used (Fig. 4*C* and *Materials and Methods*) allowed the sequential expression of NC base and export apparatus components. As shown above, in the absence of the export apparatus components SpaP, SpaQ, SpaR, and SpaS, NC base assembly occurred inefficiently and led to the accumulation of free protomers (Fig. 4 *D* and *E*). However, immediately after *spaPQRS* expression, free protomers were efficiently incorporated into the de novo assembled bases. This resulted in a net increase in the total levels of NC bases without a corresponding increase in the total levels of its individual subunits PrgH, PrgK, or InvG (Fig. 4 *D* and *E*). The de novo assembled bases showed a substantially higher native mass (detectable by BN-PAGE, shown in Fig. 4*D*) than the preassembled bases, most likely because of the incorporation of the needle and inner rod proteins, which can only occur on the recruitment of the export apparatus. The levels of the preassembled fraction of NC bases remained largely constant, and its mobility was not shifted (Fig. 4*F*), suggesting that SpaP, SpaQ, and SpaR may not be able to be recruited into these preassembled structures (*Discussion*). In contrast to what was observed with *spaPQRS* expression, induction of *invA* expression had no effect on the levels of NC bases (Fig. 4 *D* and *E* and Fig. S5), which is consistent with the observation that, in the absence of InvA, NC assembly occurs normally without accumulation of free NC base protomers (Fig. 4 *D* and *E*). Nearly all NC bases were shifted into higher mobility on expression of InvA, presumably because of the incorporation of the needle and inner rod proteins (Fig. 4*F*), suggesting that, in contrast to SpaP, SpaQ, and SpaR, InvA may be incorporated into preassembled NC bases. Taken together, these results indicate that the export apparatus, particularly, SpaP, SpaQ, and SpaR, can promote NC base assembly rather than increase its stability. This conclusion is also consistent with the observation that, after assembled, the stability of the NC bases isolated from the Δ*spaPQRS* mutant is indistinguishable from that of wild type (Fig. S6).

To further explore the role of export apparatus components on NC base assembly, we compared the efficiency of incorporation of export apparatus components into de novo synthesized or preexisting NC bases. As shown above, we found that SpaP could not be incorporated into preexisting NC bases. We also found that incorporation of InvA into de novo synthesized NC structures was more efficient than its incorporation into preexisting NC bases (Fig. 5). The recruitment of InvA to the NC required the presence of SpaP, SpaQ, SpaR, and SpaS. However, InvA was not necessary for the recruitment of SpaP (and presumably, SpaQ and SpaR) into NC bases (Fig. S5). Taken together, these results indicate that NC assembly requires prior deployment of some components of the export apparatus and that at least those components (e.g., SpaP, SpaQ, and SpaR) must be housed at a location that is inaccessible after the assembly of the NC base is complete.

Components of the Export Apparatus Form a Defined Structure Within the NC Base. The intimate relationship between the assembly of the export apparatus and the NC base prompted us to

MICROBIOLOGY

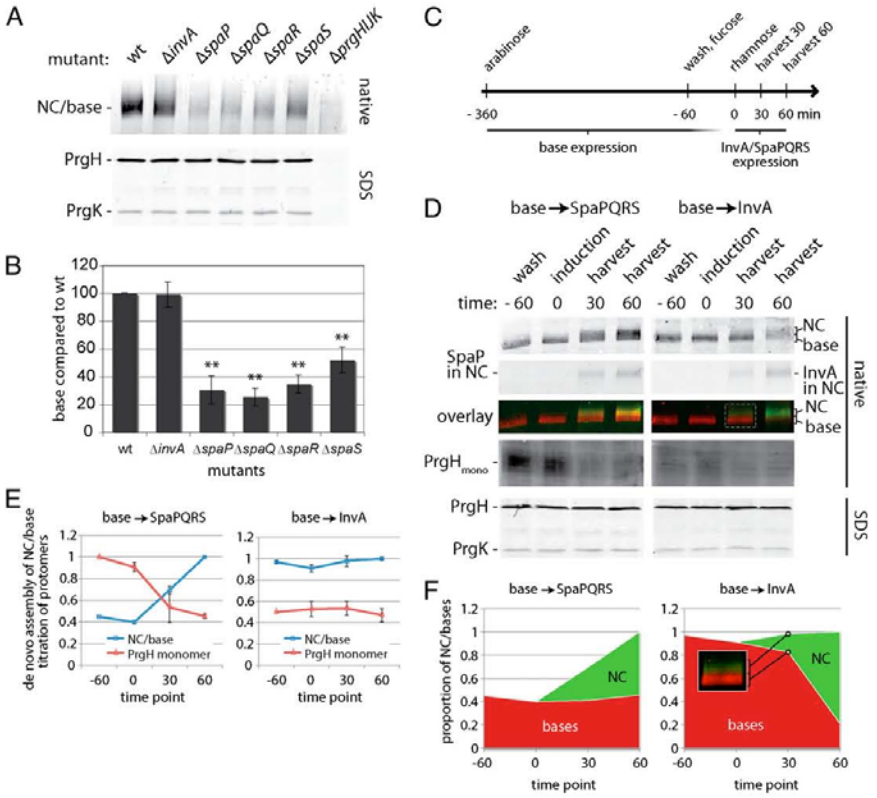

Fig. 4. The export apparatus is required for efficient NC base assembly. (*A* and *B*) Efficient NC base assembly requires SpaP, SpaQ, SpaR, and SpaS but not InvA. DDM-solubilized protein complexes of purified inner membrane fractions of wild type (wt) and the indicated mutants of *S.* Typhimurium were separated by BN-PAGE and analyzed by Western blotting (*A*). The total levels of PrgH and PrgK in the different mutants are shown in *A Lower*. The quantification of the relative levels of NC in the different mutants is shown (*B*). The intensity of the bands was quantified as above, and values represent the mean ± SD of three independent experiments. Values were standardized across different samples relative to wild type, which was considered 100%. (*C*–*E*). The export apparatus components SpaP, SpaQ, SpaR, and SpaS promote NC base assembly. (*C*) The experimental setup for these experiments involved the use of engineered strains of *S.* Typhimurim in which expression of the base components is under the control of an arabinose-inducible promoter, whereas the expression of either *spaPQRS* or *invA* is under the control of a rhamnose-inducible promoter (details in *Material and Methods*). Base expression was induced by the addition of arabinose. The inducer was washed away, and expression of the base components was blocked by the addition of the repressor fucose. Sixty minutes later (indicated as time 0 in the legend), expression of export apparatus components (either $SpaP^{FLAG}QRS$ or $InvA^{FLAG}$) was induced by the addition of rhamnose. Samples were harvested 30 min and 60 min thereafter, and DDM-solubilized proteins of whole-cell lysates were separated by BN-PAGE and analyzed by Western blotting with antibodies directed to NC base components (PrgH and PrgK) or FLAG (to detect SpaP or InvA, as indicated). SDS/PAGE of whole-cell lysates shows the absolute levels of the base components PrgH and PrgK, which remained constant throughout the experiment. *D Left* shows results in which expression of the base was followed by expression of SpaPQRS, whereas *D Right* shows results in which expression of the base was followed by expression of InvA. To minimize variation when comparing NC-associated proteins and PrgH monomers, we divided the same sample after solubilization and addition of Coomassie and loaded them onto two different gels (*D*). The total levels of PrgH and PrgK in different samples are shown in the bottom row (*D*). Quantification of these results is shown in *E* and *F*. The intensity of the bands was quantified as above, and values represent the mean ± SD of three independent experiments. The maximal values for bases/NC and PrgH protomers, respectively, were assigned an arbitrary value of 1. The proportion of bases and assembled NCs of the total base/NC signal (*D*) is shown in *F*. As an example, *Inset* in *F* shows, for a time point (*D*), the region corresponding to NC (green) or bases (red) in the BN-PAGE analysis.

examine the effect of removal of the export apparatus on the structure of the NC base. We have shown that NC base substructures can be obtained in the absence of the export apparatus, although in significantly lower amounts (*Results*). We, therefore, took advantage of this finding; we isolated NC base structures from a strain that does not express any components of the export apparatus and examined them by cryo-electron microscopy and single particle analysis (Fig. S7). Subtraction of the 2D class averages of NC bases obtained from the Δ*invA* Δ*spaP* Δ*spaQ* Δ*spaR* Δ*spaS* multiple mutant strain from class averages of NC bases obtained from wild type revealed significant differences. More specifically, structures obtained from the mutant strain lacked a significant amount of density at the center of the basal side of the NC base, including the cup and socket substructures (Fig. 6 *A*–*C*). We also analyzed NC bases obtained from a Δ*spaP* mutant strain, which looked indistinguishable from structures obtained from the mutant lacking all of the membrane components of the export apparatus (Fig. 6 *A*–*C*). Biochemical analysis of the NC preparations used for cryo-electron microscopy isolated with a stringent isolation protocol (*Material and Methods*) revealed the presence of SpaP and SpaR but not InvA or SpaS (Fig. 6 *D* and *E*). Because part of the socket substructure is missing from a mutant unable to secrete the regulatory protein InvJ protein (18) (which would not be secreted in the mutant strains used in this analysis), not all of the density absent from these mutant strains can be unambiguously assigned to these membrane proteins. Rather, it is likely that just the cup substructure, which is present even in the absence of InvJ (18), is formed by SpaP, SpaQ, and SpaR. Taken together, these results indicate that a subset of the export apparatus components form a defined substructure on the basal face of the NC and may account for yet unassigned density in the NC protein density map (12). Additional studies will be required to localize InvA and SpaS, which are lost from NC preparations generated with the stringent isolation protocol that is required to obtain particles suitable for cryo-electron microscopy.

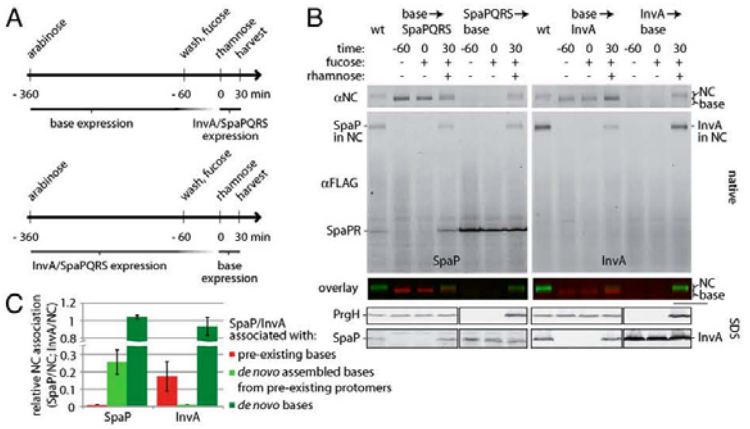

Fig. 5. NC base assembly requires the predeployment of the export apparatus. (*A*) Outline of the experimental setup to ensure that expression of the base components preceded expression of the export components (indicated as base > $SpaP^{FLAG}QRS$ or base > $InvA^{FLAG}$ in *B*) or vice versa (indicated as $SpaP^{FLAG}QRS$ > base or $InvA^{FLAG}$ > base in *B*). (*B* and *C*) Export apparatus components do not efficiently incorporate into preassembled bases. The incorporation of SpaP (*B Left*) or InvA (*B Right*) into preformed NC bases was examined by BN-PAGE of DDM-solubilized proteins of whole-cell lysates followed by Western blotting analysis with specific antibodies and an Odyssey (Li-Cor) infrared imaging system to simultaneously detect the indicated proteins. The merger of the two detection channels is shown in color [red, bases/NC (PrgH/PrgK); green, InvA or SpaP]. The total levels of PrgH and SpaP/InvA in the different samples are shown in *Lower* (*B*). (*C*) Quantification of the results shown in *B*. The intensity of the bands was quantified as above, and values represent the mean ± SD of three independent experiments. Incorporation of InvA or SpaP into preexisting bases, de novo assembled bases from free preexisting protomers, or de novo assembled bases from de novo synthesized protomers was determined as indicated in *SI Materials and Methods*. Values were standardized relative to the NC and across different samples relative to wild type, which was assigned an arbitrary value of 1.

Discussion

The assembly of complex protein machines often requires the coordinated deployment of its components, both in time and space. We have shown here that two central components of T3SS machines, the NC and the export apparatus, are assembled through a coordinated process that results in the incorporation of these two

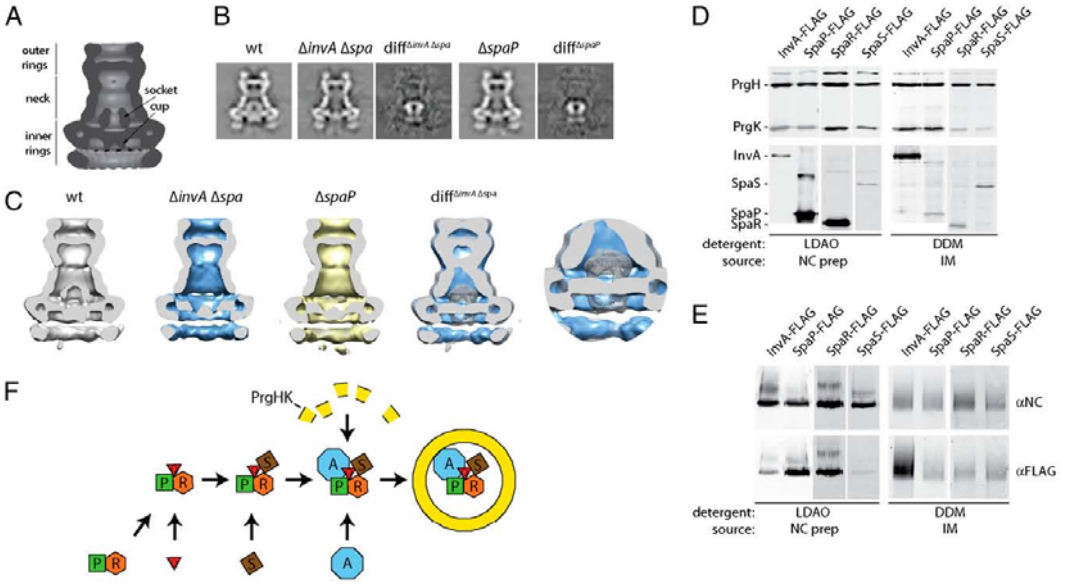

Fig. 6. Components of the export apparatus form a defined substructure in the NC base. (*A*) Diagram of the *S.* Typhimurium NC base depicting the different substructures. (*B*) Total class averages of single particle analysis of cryo-electron microscopy images and density differences between the averaged images of wild-type NCs and the indicated mutant strains. (*C*) Longitudinal sections through the center of base complexes from wild type or the indicated mutant strains lacking SpaP, SpaQ, SpaR, SpaS, and InvA or only SpaP reveal the absence of the cup and socket substructures observed in the NC base obtained from wild type. The difference images of sections from either of the mutant strains and wild type are very similar, indicating that removal of SpaP alone is sufficient to generate this structural phenotype. The cutaway view and blow-up view of an overlay of wild-type complexes (gray/mesh) and complexes from the Δ*spaPQRS* Δ*invA* mutant strain at a distance that allows the visualization of the entire cup and socket substructures in 3D emphasizes the difference between the complexes analyzed. (*D* and *E*) Highly purified NC bases contain SpaP and SpaR but no InvA or SpaS. NC bases either prepared in an identical manner to those used in cryo-electron microscopy studies or from purified inner membrane fractions were analyzed by SDS/PAGE (*D*) or BN-PAGE (*E*) followed by Western blotting with antibodies to detect the indicated proteins. (*F*) Model for the coordinated assembly of the T3SS export apparatus and NC base. SpaP forms a stable complex with SpaQ and SpaR, which is likely to be the nucleation point for PrgH/PrgK NC base ring assembly. The presence of SpaS further enhances the assembly of the PrgH/PrgK ring, although it does not seem to be essential. The presence of InvA is not required for efficient NC base formation or for the stability and/or recruitment of any of the other export apparatus components. These results suggest that InvA is the last component recruited to the export apparatus. However, InvA is not efficiently recruited into preassembled bases.

subcomplexes into a single structure. It was previously assumed that the assembly of the NC is initiated by the assembly of the inner and/or outer ring substructures (13, 14). However, we found that the assembly process is initiated by the deployment of a subset of the conserved inner membrane protein components of the export apparatus, which presumably provides a platform onto which subsequent elements of the NC can assemble (Fig. 6*F*). The organization of this inner membrane protein complex itself must also occur in an organized and coordinated fashion, because we have shown that there is a hierarchy in its formation; in this hierarchy, SpaP, SpaQ, SpaR, and to a lesser extent, SpaS play a central role, whereas InvA seems to be less critical for this process. We have also shown that some export apparatus components are not incorporated into preassembled NC bases, indicating that they must be placed at a location that is not accessible after the NC assembly is finished. We have shown that at least a subset of these inner membrane proteins, SpaP, SpaQ, and SpaR, forms a defined substructure within the NC, where they are well-positioned to receive the T3SS substrates and presumably, facilitate their passage through the inner membrane. Our findings, therefore, indicate that the NC and at least some components of the so-called export apparatus form an indivisible holostructure, which should be considered as a single functional entity. These studies have revealed unique insight into the assembly and organization of the T3SS organelle. Given the conservation of this system among pathogenic bacteria, this information could serve as the bases for the development of broadly applicable anti-infective strategies.

Materials and Methods

General Techniques. Detailed information about strains, plasmids, and culture conditions used can be found in *SI Materials and Methods* and Table S2. Western blotting was carried out using infrared fluorescent secondary antibodies (emission 680 or 800 nm). Bands were quantified using the Odyssey imaging system (Li-Cor). Cell fractionation was carried out as described before (27) with some modifications. BN-PAGE was carried out as described previously (28, 29). Identification of T3SS components by MS was carried out at the Keck Biotechnology Resource Laboratory (Yale University, New Haven, CT) according to its standardized protocol. Detailed techniques can be found in *SI Materials and Methods*.

Immunoprecipitation of Export Apparatus Components. FLAG-tagged export apparatus components were immunoprecipitated from purified inner membranes using the anti-FLAG M2 affinity gel according to the recommendations of the manufacturer. Precipitated complexes were eluted and subsequently analyzed by 1D or 2D BN-PAGE and transmission electron microscopy (*SI Materials and Methods*).

Coordinated Expression of T3SS Components. The coordinated expression of T3SS components was carried out by using bacterial strains in which expression of examined components was uncoupled by using two different compatible promoter/inducer systems (arabinose vs. rhamnose). Briefly, expression of HilA, which is the master regulator of the SPI-1 T3SS, was put under control of an arabinose-inducible promoter. The other components of interest were deleted from the chromosome and complemented *in trans* under control of a rhamnose-inducible promoter. Complex assembly was assessed by BN-PAGE and Western blotting. Details can be found in *SI Materials and Methods* and Fig. S8.

Stability of T3SS Bases. The stability of needle complexes/bases was assessed by using a modified BN-PAGE/Western blotting protocol. In brief, complexes were destabilized by increasing amounts of SDS (details in *SI Materials and Methods*).

NC Expression, Purification, Electron Microscopy, and Image Analysis. Electron microscopic analysis of needle complexes was carried out as described previously (7). More detailed methods are provided in *SI Materials and Methods*.

ACKNOWLEDGMENTS. We thank Tukiet Lam for his help with the LS-MS/MS analysis and members of the Galán laboratory for critical reading of this manuscript. This work was supported by postdoctoral fellowships from the Swedish Research Council (Vetenskapsrådet), the European Molecular Biology Organization (EMBO), and the Human Frontiers Science Program (to S.W.); Zentrum für Innovation und Technology Vienna (ZIT), Center of Molecular and Cellular Nanostructure Vienna (CMCN), and Raiffeisen Landesbank Oberösterreich grants (to T.C.M.); and National Institutes of Health Grant AI30492 (to J.E.G.).

1. Galán JE, Wolf-Watz H (2006) Protein delivery into eukaryotic cells by type III secretion machines. *Nature* 444:567–573.
2. Cornelis GR (2006) The type III secretion injectisome. *Nat Rev Microbiol* 4:811–825.
3. Minamino T, Imada K, Namba K (2008) Mechanisms of type III protein export for bacterial flagellar assembly. *Mol Biosyst* 4:1105–1115.
4. Galán JE, Curtiss R, 3rd (1989) Cloning and molecular characterization of genes whose products allow *Salmonella typhimurium* to penetrate tissue culture cells. *Proc Natl Acad Sci USA* 86:6383–6387.
5. Galán JE (2001) Salmonella interactions with host cells: Type III secretion at work. *Annu Rev Cell Dev Biol* 17:53–86.
6. Kubori T, et al. (1998) Supramolecular structure of the *Salmonella typhimurium* type III protein secretion system. *Science* 280:602–605.
7. Marlovits TC, et al. (2004) Structural insights into the assembly of the type III secretion needle complex. *Science* 306:1040–1042.
8. Crepin VF, et al. (2005) Structural and functional studies of the enteropathogenic Escherichia coli type III needle complex protein EscJ. *Mol Microbiol* 55:1658–1670.
9. Yip CK, et al. (2005) Structural characterization of the molecular platform for type III secretion system assembly. *Nature* 435:702–707.
10. Spreter T, et al. (2009) A conserved structural motif mediates formation of the periplasmic rings in the type III secretion system. *Nat Struct Mol Biol* 16:468–476.
11. Hodgkinson JL, et al. (2009) Three-dimensional reconstruction of the Shigella T3SS transmembrane regions reveals 12-fold symmetry and novel features throughout. *Nat Struct Mol Biol* 16:477–485.
12. Schraidt O, et al. (2010) Topology and organization of the Salmonella typhimurium type III secretion needle complex components. *PLoS Pathog* 6:e1000824.
13. Sukhan A, Kubori T, Wilson J, Galán JE (2001) Genetic analysis of assembly of the Salmonella enterica serovar Typhimurium type III secretion-associated needle complex. *J Bacteriol* 183:1159–1167.
14. Diepold A, et al. (2010) Deciphering the assembly of the Yersinia type III secretion injectisome. *EMBO J* 29:1928–1940.
15. Fan F, Ohnishi K, Francis NR, Macnab RM (1997) The FliP and FliR proteins of Salmonella typhimurium, putative components of the type III flagellar export apparatus, are located in the flagellar basal body. *Mol Microbiol* 26:1035–1046.
16. Zenk SF, et al. (2007) Identification of minor inner-membrane components of the Shigella type III secretion system 'needle complex'. *Microbiology* 153:2405–2415.
17. Kubori T, Sukhan A, Aizawa SI, Galán JE (2000) Molecular characterization and assembly of the needle complex of the Salmonella typhimurium type III protein secretion system. *Proc Natl Acad Sci USA* 97:10225–10230.
18. Marlovits TC, et al. (2006) Assembly of the inner rod determines needle length in the type III secretion injectisome. *Nature* 441:637–640.
19. Galán JE, Ginocchio C, Costeas P (1992) Molecular and functional characterization of the *Salmonella typhimurium* invasion gene *invA*: Homology of InvA to members of a new protein family. *J Bacteriol* 174:4338–4349.
20. Groisman EA, Ochman H (1993) Cognate gene clusters govern invasion of host epithelial cells by *Salmonella typhimurium* and *Shigella flexneri*. *EMBO J* 12:3779–3787.
21. Ferris HU, et al. (2005) FlhB regulates ordered export of flagellar components via autocleavage mechanism. *J Biol Chem* 280:41236–41242.
22. Lavander M, et al. (2002) Proteolytic cleavage of the FlhB homologue YscU of Yersinia pseudotuberculosis is essential for bacterial survival but not for type III secretion. *J Bacteriol* 184:4500–4509.
23. Akiyama Y, Kihara A, Tokuda H, Ito K (1996) FtsH (HflB) is an ATP-dependent protease selectively acting on SecY and some other membrane proteins. *J Biol Chem* 271:31196–31201.
24. Guzman LM, Belin D, Carson MJ, Beckwith J (1995) Tight regulation, modulation, and high-level expression by vectors containing the arabinose PBAD promoter. *J Bacteriol* 177:4121–4130.
25. Bajaj V, Hwang C, Lee CA (1995) hilA is a novel ompR/toxR family member that activates the expression of Salmonella typhimurium invasion genes. *Mol Microbiol* 18:715–727.
26. Haldimann A, Daniels LL, Wanner BL (1998) Use of new methods for construction of tightly regulated arabinose and rhamnose promoter fusions in studies of the Escherichia coli phosphate regulon. *J Bacteriol* 180:1277–1286.
27. Wagner S, et al. (2007) Consequences of membrane protein overexpression in Escherichia coli. *Mol Cell Proteomics* 6:1527–1550.
28. Schägger H, von Jagow G (1991) Blue native electrophoresis for isolation of membrane protein complexes in enzymatically active form. *Anal Biochem* 199:223–231.
29. Klepsch M, et al. (2008) Immobilization of the first dimension in 2D blue native/SDS-PAGE allows the relative quantification of membrane proteomes. *Methods* 46:48–53.